ENVIRONMENTAL EFFECTS ON TURFGRASS GROWTH AND WATER USE

by

KENTON W. PETERSON

B.S., University of Nebraska – Lincoln, 2007
M.S., University of Nebraska – Lincoln, 2009

AN ABSTRACT OF A DISSERTATION

submitted in partial fulfillment of the requirements for the degree

DOCTOR OF PHILOSOPHY

Department of Horticulture, Forestry and Recreation Resources
College of Agriculture

KANSAS STATE UNIVERSITY
Manhattan, Kansas

2013

Abstract

Researchers and practitioners can use numerous techniques to measure or estimate evapotranspiration (ET) from turfgrass but little is known about how they compare to ET using standard lysimeters. An investigation was conducted to compare measurements of ET from lysimeters (LYS_{ET}) with ET estimates from the FAO56 Penman-Monteith (PM_{ET}) and Priestley-Taylor (PT_{ET}) empirical models, atmometers (AT_{ET}), eddy covariance (EC_{ET}), and a canopy stomatal conductance model that estimates transpiration ($COND_T$). Methods were compared at the same site during the 2010, 2011, and 2012 growing seasons. Overall, PT_{ET} and EC_{ET} were not different from LYS_{ET}, whereas PM_{ET}, AT_{ET}, and $COND_T$, increasingly underestimated LYS_{ET}. Differences exist among ET measurement techniques and one should employ the technique that best fits their situation.

An atmometer is an inexpensive tool that can be used to measure turfgrass ET within microclimates, such as those typically found in an urban home lawn. An investigation was conducted to compare AT_{ET} estimates with PM_{ET} estimates within a number of lawn microclimates. Home lawns in Manhattan and Wichita, KS, were selected for study during the growing seasons of 2010 and 2011. Open sward AT_{ET} was 4.73 mm d^{-1}, whereas PM_{ET} was 5.48 mm d^{-1}. Within microclimates, AT_{ET} was 3.94 mm d^{-1} and PM_{ET} 3.23 mm d^{-1}. Atmometers can provide practitioners with reliable estimates of PM_{ET} within microclimates.

Zoysiagrass (*Zoysia* spp.) is a common turfgrass used on home lawns and golf courses. However, poor shade tolerance and cold hardiness have limited its use in the transition zone. A study was conducted to determine changes and differences in growth and physiology among selected *Zoysia* over a three-year period (2010-2012) in the transition zone. The genotypes were 'Emerald' [*Z. japonica* × *Z. pacifica*], 'Zorro' [*Z. matrella*], 'Meyer' and Chinese Common [*Z. japonica*], and experimental progeny Exp1 [*Z. matrella* × *Z. japonica*], and Exp2 and Exp3 [(*Z. japonica* × *Z. pacifica*) × *Z. japonica*]. 'Zorro' and 'Emerald' experienced winter injury. 'Meyer', Chinese Common, and Exp1 showed poor performance over the three-years. The Exp2 and Exp3 progeny, maintained high percent cover, visual quality, and tiller density, and may provide practitioners more shade-tolerant cultivar choices in the transition zone.

ENVIRONMENTAL EFFECTS ON TURFGRASS GROWTH AND WATER USE

by

KENTON W. PETERSON

B.S., University of Nebraska – Lincoln, 2007
M.S., University of Nebraska – Lincoln, 2009

A DISSERTATION

submitted in partial fulfillment of the requirements for the degree

DOCTOR OF PHILOSOPHY

Department of Horticulture, Forestry and Recreation Resources
College of Agriculture

KANSAS STATE UNIVERSITY
Manhattan, Kansas

2013

Approved by:

Co-Major Professor
Dale J. Bremer

Approved by:

Co-Major Professor
Jack D. Fry

Copyright

Abstract

Researchers and practitioners can use numerous techniques to measure or estimate evapotranspiration (ET) from turfgrass but little is known about how they compare to ET using standard lysimeters. An investigation was conducted to compare measurements of ET from lysimeters (LYS_{ET}) with ET estimates from the FAO56 Penman-Monteith (PM_{ET}) and Priestley-Taylor (PT_{ET}) empirical models, atmometers (AT_{ET}), eddy covariance (EC_{ET}), and a canopy stomatal conductance model that estimates transpiration ($COND_T$). Methods were compared at the same site during the 2010, 2011, and 2012 growing seasons. Overall, PT_{ET} and EC_{ET} were not different from LYS_{ET}, whereas PM_{ET}, AT_{ET}, and $COND_T$, increasingly underestimated LYS_{ET}. Differences exist among ET measurement techniques and one should employ the technique that best fits their situation.

An atmometer is an inexpensive tool that can be used to measure turfgrass ET within microclimates, such as those typically found in an urban home lawn. An investigation was conducted to compare AT_{ET} estimates with PM_{ET} estimates within a number of lawn microclimates. Home lawns in Manhattan and Wichita, KS, were selected for study during the growing seasons of 2010 and 2011. Open sward AT_{ET} was 4.73 mm d^{-1}, whereas PM_{ET} was 5.48 mm d^{-1}. Within microclimates, AT_{ET} was 3.94 mm d^{-1} and PM_{ET} 3.23 mm d^{-1}. Atmometers can provide practitioners with reliable estimates of PM_{ET} within microclimates.

Zoysiagrass (*Zoysia* spp.) is a common turfgrass used on home lawns and golf courses. However, poor shade tolerance and cold hardiness have limited its use in the transition zone. A study was conducted to determine changes and differences in growth and physiology among selected *Zoysia* over a three-year period (2010-2012) in the transition zone. The genotypes were 'Emerald' [*Z. japonica* × *Z. pacifica*], 'Zorro' [*Z. matrella*], 'Meyer' and Chinese Common [*Z. japonica*], and experimental progeny Exp1 [*Z. matrella* × *Z. japonica*], and Exp2 and Exp3 [(*Z. japonica* × *Z. pacifica*) × *Z. japonica*]. 'Zorro' and 'Emerald' experienced winter injury. 'Meyer', Chinese Common, and Exp1 showed poor performance over the three-years. The Exp2 and Exp3 progeny, maintained high percent cover, visual quality, and tiller density, and may provide practitioners more shade-tolerant cultivar choices in the transition zone.

Table of Contents

List of Figures ... viii
List of Tables ... ix
Acknowledgements ... x
Dedication ... xi
Chapter 1 - Turfgrass Evapotranspiration Measurement: a Comparison of Techniques ... 1
Abstract ... 2
Introduction ... 3
Lysimeters ... 3
Empirical models ... 4
Eddy covariance ... 6
Atmometers ... 7
Infrared Thermometry ... 8
Objective ... 9
Materials and Methods ... 10
Lysimeters ... 10
Empirical Models and Atmometers ... 11
Infrared Thermometry ... 12
Eddy Covariance ... 13
Statistical Analysis ... 15
Results and Discussion ... 17
Empirical Models ... 17
Eddy Covariance ... 19
Atmometers ... 20
Infrared Thermometry ... 21
Conclusion ... 22
References ... 24
Chapter 2 - Evaluation of Atmometers within Urban Home Lawn Microclimates ... 35
Abstract ... 36

Introduction 37
Objective 38
Materials and Methods 40
Statistical Analysis 41
Results and Discussion 43
Conclusions 46
References 48
Chapter 3 - Growth and Physiological Responses of *Zoysia* spp. Under Tree Shade 59
Abstract 60
Introduction 61
Objective 62
Materials and Methods 63
Statistical Analysis 65
Results and Discussion 67
Turfgrass Quality 67
Tiller Density 68
Leaf Extension Rate 69
Leaf Width 70
Percentage Green Cover 71
Fall Color 72
Spring Color 73
Carbon Dioxide Exchange Rate 73
Conclusions. 74
References 76
Appendix A - Using Infrared Thermometry to Calculate Canopy Stomatal Conductance to Water Vapor from Tall Fescue (*Festuca arundinacea* Schreb.) Turfgrass 88
Appendix B - Summary of Environmental Variables 108
Appendix C - Summary of Daily Evapotranspiration Values 110

List of Figures

Figure 1.1. Depiction of lysimeter vegetation overlap (a) and dimensions of lysimeter including lysimeter wall and lysimeter wall to soil gap (b). 33
Figure 1.2. Comparison of evapotranspiration techniques to lysimeter measured evapotranspiration. Bolded line represents the linear regression... 34
Figure 2.1. Comparison of daily estimated evapotranspiration from the atmometer (AT_{ET}) to the FAO56-Penman-Monteith model (PM_{ET}) at the open sward and microclimate locations, combined. Bolded line shows the modeled linear regression equation. 56
Figure 2.2. Comparison of daily estimated evapotranspiration from the atmometer (AT_{ET}) to the FAO56-Penman-Monteith model (PM_{ET}) at the open sward location, only. Bolded line shows the modeled linear regression equation.. 57
Figure 2.3. Comparison of daily estimated evapotranspiration from the atmometer (AT_{ET}) to the FAO56-Penman-Monteith model (PM_{ET}) at the microclimate locations, only. Bolded line shows the modeled linear regression equation... 58
Figure 3.1. Monthly mean, maximum, and minimum air temperatures at the study site from June 2010 through October 2012. Circles represent the mean monthly air temperature. Bars represent the maximum and minimum temperatures for each month.................................. 87
Figure A.1. Hourly canopy stomatal conductance, air temperature, canopy temperature, wind speed, and vapor pressure deficit of canopy temperature on 28 June 2012. 106
Figure A.2. Hourly canopy stomatal conductance, air temperature, canopy temperature, wind speed, and vapor pressure deficit of canopy temperature on 5 September 2012. 107

List of Tables

Table 1.1. Summary of instruments used by the weather station and eddy covariance system. .. 30
Table 1.2. Evapotranspiration measurement technique means and statistical analysis as compared to lysimeter measured evapotranspiration. 31
Table 1.3. Pearson correlation coefficients for average daytime (Rn > 0) net radiation, vapor pressure deficit, air temperature, and wind speed comparisons to ET difference (ET technique – Lysimeter ET). 32
Table 2.1. Evapotranspiration measurement dates for microclimate study locations at Manhattan, KS in 2010-2011and Wichita, KS in 2011. 51
Table 2.2. Mean atmometer and FAO56-PM evapotranspiration and statistical analysis of AT_{ET} to PM_{ET} comparison. 52
Table 2.3. Analysis of atmometer and FAO56-PM evapotranspiration by wind speed classification. 53
Table 2.4. Analysis of atmometer and FAO56-PM evapotranspiration by vapor pressure deficit (VPD) classification. 54
Table 2.5. Analysis of atmometer and FAO56-PM evapotranspiration by net radiation. 55
Table 3.1. Mean turfgrass quality ratings of zoysiagrass genotypes for 2010, 2011, and 2012. .. 79
Table 3.2. Tiller density percentage of June 2010 for zoysiagrass genotypes in 2010, 2011, and 2012. 80
Table 3.3. Leaf extension rates for zoysiagrass genotypes in 2010, 2011, and 2012. 81
Table 3.4. Leaf width for zoysiagrass genotypes in 2010, 2011, and 2012. 82
Table 3.5. Percentage green cover for zoysiagrass genotypes in 2011 and 2012. 83
Table 3.6. Fall color for zoysiagrass genotypes in 2011, and 2012. 84
Table 3.7. Spring green-up for zoysiagrass genotypes in 2011, and 2012. 85
Table 3.8. Carbon dioxide flux measurements conducted in July of 2010, 2011, and 2012. 86
Table B.1. Average Daytime (R_n > 0) Net Radiation, Air Temperature, Wind Speed, Relative Humidity, and Vapor Pressure Deficit from Evapotranspiration Comparison Study 108
Table C.1. Summary of Daily Evapotranspiration Values from Evapotranspiration Comparison Study 110

Acknowledgements

I would like to thank the Department of Horticulture, Forestry & Recreation Resources at Kansas State University. I would also like to thank the Kansas Turfgrass Foundation, Heart of America Golf Course Superintendents Association, USDA National Integrated Water Quality Program, and SodShop of Wichita for their support. A special thank you is in order for my advisors, Dr. Dale Bremer and Dr. Jack Fry. Their guidance over the last few years will not be forgotten. Also, committee members, Dr. Steve Keeley and Dr. Mary Kirkham provided excellent support and feedback on my projects. A great deal of gratitude is due to Ms. Kira Shonkwiler who helped me with equipment and taught me much about micrometeorology. A thank you is due to Mark Blonquist Jr. for helping me with the conductance model. In addition, the graduate students that I worked with made the time very enjoyable. So to you guys, Dr. Cody Domenghini, Cole Thompson, Dr. Jason Lewis, Josh Chabon, Josh Pool, Ross Braun, Dr. Tony Goldsby, Zane Raudenbush, thank you. Also, thank you to Dr. Cathie Lavis and Dr. Richard Mattson for whom I was a graduate teaching assistant.

Finally, but certainly not least, I want to thank my family. I have been a career college student for a great portion of my life. Without their support along the way this would not have been possible. Erin you supported me more than I could ever have hoped. Kyler, maybe someday you will read this, but the joy you bring to my life made every day brighter. Lastly, my parents, brothers, in-laws, and friends for never questioning and always supporting my academic career. Thank you.

Dedication

To My Family

Erin and Kyler

Chapter 1 - Turfgrass Evapotranspiration Measurement: a Comparison of Techniques

Abstract

Evapotranspiration (ET) can be measured directly using lysimeters or eddy covariance, estimated using empirical models, or simulated using an atmometer. These techniques are widely used by researchers and practitioners but little is known about how they compare to each other. An investigation was conducted to compare measurements of ET from lysimeters (LYS_{ET}) with ET estimates from the FAO56 Penman-Monteith (PM_{ET}) and Priestley-Taylor (PT_{ET}) empirical models, atmometers (AT_{ET}), eddy covariance (EC_{ET}), and transpiration from a canopy stomatal conductance model ($COND_T$), all at the same site. The investigation was conducted at the Rocky Ford Turfgrass Research Center at Manhattan, KS, within a sward of tall fescue (*Festuca arundinacea* Schreb.) turfgrass. Evapotranspiration data were collected on precipitation free days during the growing season in 2010 through 2012. Data were analyzed using root mean square error (RMSE), mean bias error (MBE), percent error (%E), index of agreement (d), paired *t*-test, and regression analysis. Overall mean ET from the techniques were, from greatest to least, LYS_{ET} (5.58 mm d^{-1}), PT_{ET} (5.44 mm d^{-1}), EC_{ET} (5.32 mm d^{-1}), PM_{ET} (5.17 mm d^{-1}), AT_{ET} (4.61 mm d^{-1}), and $COND_T$ (4.14 mm d^{-1}). Priestley-Taylor ET and EC_{ET} were not different from LYS_{ET}, based on paired *t*-test, and had the lowest MBE. The PM_{ET} and PT_{ET} models had the lowest RMSE and highest d. Atmometer ET and $COND_T$ underestimated LYS_{ET} the greatest, %E = -15.0 and -29.6%, respectively. Practitioners and researchers should be aware of differences among ET measurement techniques and employ the technique that best fits their situation.

Introduction

Turfgrasses in the United States are estimated to cover 16 to 20 million hectares, an area three times larger than any irrigated crop (Morris, 2003; Milesi et al., 2005). The total turfgrass area in the United States is likely to increase greatly as urbanization continues to expand (Alig et al., 2004). Irrigation of turfgrasses in urban areas is a common practice, creating an increasing demand for water in expanding urban areas. However, many homeowners do not understand how to manage the irrigation for their lawn (Bremer et al., 2012; Bremer et al., 2013). A better understanding of turfgrass irrigation requirements (i.e. ET) would help homeowners manage their irrigation more efficiently, reducing the demand for water.

Accurate measurement or estimation of ET is very important for irrigation management and scientific research. A number of techniques are available to measure or estimate ET. Practitioners and researchers will often select a single method of ET estimation for determining irrigation requirements. Each method has its positive and negative attributes (Allen et al., 2011). Selection of one method over another could lead to inaccurate or biased ET information, resulting in incorrect irrigation recommendations or an incorrect interpretation of results.

Lysimeters

Lysimeters are perhaps the oldest ET measurement technology. Feldhake et al. (1983) used lysimeters to determine factors influencing ET in urban microclimates. Using lysimeters in full sun and varying degrees of shade, they found that ET increased linearly with solar radiation. They also observed that Kentucky bluegrass [*Poa pratensis* (L.)] mowed at 5 cm used 13% more water than when mowed at 2 cm.

Lysimeters are often used as the standard for developing and determining the accuracy of other ET measurement techniques, especially empirical models (Allen, 1986; Allen et al., 1989;

Fry et al., 1997; López-Urrea et al., 2006; Chávez et al., 2009; Trajkovic, 2010). However, lysimeters may not always provide correct measurement of actual ET. A common error in lysimeter ET calculation is the definition of the effective evaporative surface area of the lysimeter (Allen et al., 1991; Allen et al., 2011). Overlap of vegetation from within to outside of the lysimeter combined with lysimeter wall thickness and the gap between the lysimeter and surrounding soil should be considered when defining effective lysimeter surface area (Fig. 1.1; Allen et al., 1991; Allen et al., 2011). Improper filling of the lysimeter container with soil could lead to different soil physical properties than the surrounding soil, resulting in different plant growth characteristics (Hershey, 1990). Turfgrass research often utilizes microlysimeters that are small enough for an individual to handle and can be replicated for determination of varietal differences in ET. Bremer (2003) investigated water content and plant growth from several common microlysimeter designs. Leaf area index and biomass were altered by microlysimeter design, which affected ET, and differences in soil fill contributed to differences in ET. Hence, lysimeter design choice is crucial to accurately measure ET.

Empirical models

Empirical models are used for estimating potential ET (ET_p) or reference ET (ET_o). Potential ET is the maximum ET possible under non water-limiting conditions whereas reference ET is the ET possible for a vegetated surface. In 1948, Penman published his paper "Natural evaporation from open water, bare soil and grass", which was the first attempt to incorporate atmospheric and plant physics into estimates of ET_p (Penman, 1948, 1956, 1963). Monteith (1965) utilized the work by Penman to derive an improved evaporation equation incorporating physiological characteristics of stomata into the equation. This new combination approach presented by Monteith (1965) is:

$$\lambda ET = \frac{\Delta(R_n - G) + \rho C_p \frac{e_s - e_a}{r_a}}{\Delta + \gamma\left(1 + \frac{r_s}{r_a}\right)} \quad [1]$$

where Δ is the slope of the saturation vapor pressure curve (kPa K^{-1}), R_n is net radiation (W m^{-2}), G is soil heat flux (W m^{-2}), r_a is aerodynamic resistance (s m^{-1}), r_s is surface resistance (s m^{-1}), ρ is air density (kg m^{-3}), C_p is specific heat of air (J kg^{-1} K^{-1}), e_s is saturation vapor pressure (kPa), e_a is actual vapor pressure of the air (kPa), γ is the psychometric constant (kPa K^{-1}), and λ is latent heat of vaporization (J kg^{-1}), which provides ET_o and not ET_p, allowing for model use under water-limiting conditions. The Food and Agriculture Organization (FAO56-PM, Allen et al., 1998) along with the American Society of Civil Engineers (ASCE-EWRI, 2005) have published standardized versions of the Penman-Monteith equation that are widely used. Allen et al. (1998, 2006) defined the grass reference surface as a cool-season grass that is clipped to 0.12 m, has a surface resistance of 70 s m^{-1}, and an albedo of 0.23. Recently, ASCE-EWRI (2005) and Allen et al. (2006) showed that using a surface resistance of 50 s m^{-1} during daytime and 200 s m^{-1} during nighttime improved ET_o accuracy, this recommendation is supported by other research as well (Trajkovic, 2010).

The Penman-Monteith ET_o equation's measurement reliability and accuracy has been compared to other equations (Itenfisu et al., 2003; López-Urrea et al., 2006) and lysimeters (Howell et al., 2000; Bakhtiari et al., 2011). López-Urrea et al. (2006) determined that the FAO56-PM equation was the most precise of the seven models used in their study compared to lysimeter ET. Howell et al. (2000) found the FAO56-PM equation to overestimate in the spring and fall (i.e. when ET rates are low) while underestimating during the summer (i.e. when ET rates are high), compared to lysimeter measurements. In Iran, the FAO56-PM equation did not perform as well as the FAO-24 radiation equation under dry and advective conditions (Bakhtiari et al., 2011).

Priestley and Taylor (1972) proposed an ET_p equation requiring only net or solar radiation and air temperature measurements. Their equation is:

$$ET_p = \alpha \frac{\Delta(R_n - G)}{\lambda(\Delta + \gamma)} \quad [2]$$

where α is a coefficient commonly set at 1.26, and all other variables were previously defined in the Penman-Monteith model (Eq. 1). This equation can be viewed as a simplified version of the Penman equation, working best under humid conditions (Rosenberg et al., 1983). However, unlike the Penman-Monteith equation, the Priestley-Taylor (PT) approach is an estimate of ET for use under non-advective or non-water-limiting conditions (Rosenberg et al., 1983). Suleiman and Hoogenboom (2007), however, observed PT to overestimate ET during the summer in Georgia, a humid climate, and that the Penman-Monteith equation would improve irrigation efficiency. Stannard (1993) found that the Penman-Monteith equation did not perform well when vegetation was not fully closed, but that the PT equation did perform very well under such conditions.

Eddy covariance

The eddy covariance (EC) technique is a method for measuring carbon dioxide and water fluxes. Swinbank (1951) proposed a technique to measure vertical flux of water vapor in the atmosphere that is:

$$E = \frac{\varepsilon}{P} \rho_a \overline{w' e_a'} \quad [3]$$

where E is water vapor flux, ε is the ratio of molecular weights of water vapor and dry air, P is atmospheric pressure, ρa is the density of moist air, w' is the instantaneous departure from the mean of the vertical wind velocity, ea' is the instantaneous departure from the mean of the vapor pressure, and the overbar indicates that the variables are an average. The two main components of an EC system are the infrared gas analyzer, to measure CO_2 and H_2O concentration, and an ultrasonic anemometer to measure wind direction and velocity. These measurements are often taken at frequencies as great as 10-20 Hz (10-20 times a second). The instruments require frequent maintenance, are expensive, and the data require extensive post-processing (Rosenberg et al., 1983; Meyers and Baldocchi, 2005; Foken, 2008b; Allen et al., 2011; Leuning et al., 2012). The EC technique can provide a measure of actual ET if a number of criteria are met (Baldocchi, 1988; Foken, 2008b). However, much concern with this technique has centered on the inability to close the energy balance equation (Foken, 2008a). The energy balance equation is:

$$R_n - G = H + \lambda E \qquad [4]$$

where R_n is net radiation, G is soil heat flux, H is sensible heat flux, and λE is latent heat flux. The lack of closure has been attributed to $H + \lambda E$ being underestimated as compared to R_n - G by as much as 30% (Twine et al., 2000; Wilson et al., 2002; Foken, 2008a; Leuning et al., 2012). Typically, when there is a lack of energy balance closure, the Bowen ratio (Bowen, 1926) is used to force closure of the energy balance (Twine et al., 2000). Kochendorfer et al. (2012) found that the type of sonic anemometer used to measure wind velocities could explain the lack of energy balance closure from EC measurements. When wind velocity is corrected, they found that CO_2, sensible heat, and latent heat fluxes were increased by approximately 11%.

Atmometers

An atmometer is a simple tool that may provide accurate ET_o data at a fraction of the cost of most other techniques. The porous Bellani plate atmometer described by Livingston (1915) was modified by Altenhofen (1985) to cover the ceramic plate with a green canvas having an albedo similar to alfalfa and resistance to water diffusion similar to stomata. Several researchers have reported that corrections to atmometer ET_o are necessary, using the Penman-Monteith ET_o equation as the standard, under humid/rainy (Irmak et al., 2005; Chen and Robinson, 2009) and semi-arid (Alam and Trooien, 2001) climates. In contrast, good agreement was found between the atmometer and Penman-Monteith ET_o in a semi-arid environment, and no corrections were necessary (Magliulo et al., 2003; Gavilan and Castillo-Llanque, 2009).

Infrared Thermometry

Leaf or plant canopy temperature can be an indicator of plant water status. The process of transpiration, or evaporation of water from the surface of leaves, lowers the temperature of the canopy. Stomata are the main mechanisms that control the conductance of water vapor from the leaf interior to the atmosphere. Specifically, as water inside the leaf evaporates it must exit through stomata, which open and close to regulate the rate of water vapor flux. In water-stressed plants, stomata begin to close and evaporative, or transpirational cooling, is reduced resulting in greater canopy temperatures.

Measuring the temperature of a leaf or canopy surface can help researchers understand and quantify the transport of energy from leaf to atmosphere. The temperature of the canopy, or leaf, can be measured with thermocouples. However, this technique requires the thermocouple to be in direct contact with the leaf and does not provide an accurate representation of the entire leaf or canopy (Tanner, 1963). An infrared thermometer (IRT) can remotely measure the integrated temperature of multiple leaves in a plant canopy, eliminating the problems associated with thermocouple measurements. Infrared thermometers measure the canopy temperature based upon received thermal radiation in the 8 to 14 μm range (Jackson et al., 1980).

Infrared thermometers can be used to measure the plants temperature accurately, and with additional meteorological data (such as wind speed, air temperature, relative humidity, and solar radiation), plant responses, such as stomatal conductance, can be calculated. This technique may allow for the decoupling of ET (i.e., transpiration versus evaporation from the soil surface) as transpiration can be calculated by knowing stomatal and boundary layer conductance to water vapor.

Objective

Allen et al. (2011) discussed a number of methods used for obtaining ET data and the potential biases in each. However, to our knowledge, no research exists in the literature that compares ET data obtained from these techniques simultaneously and side-by-side. Such a comparison would be invaluable in demonstrating their performance relative to each other when placed in the same environment. Therefore, the objective of this investigation was to compare measurements of ET from lysimeters with ET estimates from a number of techniques including the FAO56-PM and PT empirical models, atmometers, EC, and transpiration from a canopy stomatal conductance model, all at the same site.

Materials and Methods

This investigation was initiated in July 2010 at the Rocky Ford Turfgrass Research Center at Manhattan, KS, and continued during the growing seasons of 2011 and 2012. The study was conducted within a sward of tall fescue turfgrass. Soil type was a Chase silt loam (fine, montmorillonitic, mesic, Aquic, Argiudoll). The turfgrass was maintained at 10 cm mowing height. Irrigation was applied to prevent stress and to ensure that measurements were made under non water-limiting conditions. Evapotranspiration comparisons were conducted on precipitation free days and were continued on consecutive days until irrigation was necessary to maintain a plentiful supply of water to the turfgrass.

Lysimeters

Three lysimeters were constructed from polyvinylchloride (Fig. 1.1). Intact cores of tall fescue were obtained at the study site and placed in each lysimeter. Wall thickness of the lysimeters was 1.03 cm, the gap between lysimeter and soil was 1.03 cm, the inside diameter was 30.2 cm, and the depth was 22 cm (Fig. 1.1). Effective evaporating area of the lysimeter was 0.0817 m^2. A hole was drilled in the center of the bottom of each lysimeter to allow for free water drainage. The hole was plugged using a rubber stopper during measurement periods. At the beginning of each measurement period, water was added to the lysimeters to bring them above container capacity. Lysimeters were then allowed to drain freely overnight (~12-14 hrs). The following morning, lysimeters were weighed and that value was used as the initial lysimeter mass for the measurement period. On successive mornings during the measurement period, lysimeters were weighed (24 h mass) and water added to bring them back to the initial lysimeter mass. Lysimeter ET was calculated as:

$$\text{LYS}_{\text{ET}} = \frac{\text{Initial Mass} - \text{24h Mass}}{\text{Effective Evaporating Area}} \quad [5]$$

where LYS_{ET} is in mm d^{-1}, initial and 24 h mass in kg, and effective evaporating area in m^2.

Empirical Models and Atmometers

Three atmometers (ETgage Model E, ETgage Company, Loveland, CO) were placed within 0.5 m of a weather station at the study site. Atmometers were installed according to manufacturer instructions so that the top of the ceramic Bellani plate on the atmometer was 1 m above the ground. Grass reference evapotranspiration was obtained by covering the Bellani plate with the manufacturer supplied number 30 green canvas cover. Data from the atmometers were recorded with a datalogger (CR1000, Campbell Scientific, Logan, UT) and summed at 30-minute intervals. Atmometer ET was summed each day during measurement periods and the average of the three atmometers was used for comparison with LYS_{ET}.

The weather station at the site recorded meteorological variables necessary to calculate ET from empirical models (Table 1.1). Weather station data were recorded at 1 Hz on the same datalogger used to record atmometer data; data were averaged and stored at 30-minute intervals.

Data collected from the portable weather station were used to calculate ET_o using the FAO56-PM empirical model and the PT radiation based empirical ET model. The FAO56-PM model is:

$$PM_{ET} = \frac{0.408\Delta(R_n - G) + \gamma \frac{C_n}{T + 273} u_2 (e_s - e_a)}{\Delta + \gamma(1 + C_d u_2)} \quad [6]$$

where PM_{ET} is grass reference evapotranspiration (mm 30 min^{-1}), u is the wind speed (m s^{-1}) at 2 m, C_n is the numerator constant for the 30-minute time step, C_d is the denominator constant for aerodynamic and surface resistances, and all other variables have been previously defined. Allen et al. (2006) suggested that the FAO56-PM ET_o method use variable resistance for daytime and nighttime periods. The resulting denominator constant, C_d, for hourly FAO56-PM ET_o calculation is 0.24 during daytime (i.e. $R_n > 0$) and 0.96 during nighttime periods.

Evapotranspiration from the Priestley-Taylor (Priestley and Taylor, 1972) empirical model was calculated from Eq. 2, all variables are as described for the FAO56-PM model. Thirty-minute ET values from FAO56-PM and PT were summed each day during the measurement periods.

Infrared Thermometry

Four infrared radiometers (SI-111, Apogee Instruments, Inc., Logan, UT) were used to measure canopy temperature. Radiometers were installed at 1.5 m height, aimed in the compass directions, east, west, and south, with a view angle of 50° from nadir. The fourth radiometer was installed with a view angle of 0° from nadir. Canopy temperature was calculated as:

$$T_c = \sqrt[4]{\frac{T_{IRT}^4 - (1-\varepsilon)T_{sky}^4}{\varepsilon}} \qquad [7]$$

where T_c, T_{IRT}, and T_{sky} are canopy, IRT, and sky temperature, respectively, all in K. Emissivity of the grass canopy was assumed to be 0.97. Sky temperature was calculated from the model used by Blonquist et al. (2009) (personal communication). Meteorological data from the weather station were used along with the canopy temperature to calculate canopy stomatal conductance. Canopy stomatal conductance was calculated according to the model proposed by Blonquist et al. (2009):

$$g_c = \frac{g_v P_B\left[(R_{nc} - A_n) - g_h C_p (T_c - T_a)\right]}{g_v \lambda (e_{sc} - e_a) - P_B\left[(R_{nc} - A_n) - g_h C_p (T_c - T_a)\right]} \qquad [8]$$

where g_v is boundary layer water vapor conductance (mol m^{-2} s^{-1}), g_h is boundary layer heat conductance (mol m^{-2} s^{-1}), C_p is the heat capacity of air (29.17 J mol^{-1} C^{-1}), T_c is canopy temperature (°C), T_a is air temperature (°C), P is atmospheric pressure (kPa), e_a is vapor pressure (kPa), e_{sc} is saturation vapor pressure at T_c (kPa), A_n is net assimilation (W m^{-2}), the energy used in photosynthesis), R_{nc} is net radiation divergence in the canopy (W m^{-2}), and λ is latent heat of vaporization (J mol^{-1}). For a full explanation of the model and variable calculations, see Appendix A.

Transpiration water loss, $COND_T$, can be calculated using g_c and g_v to calculate g_t, total water vapor conductance. The $COND_T$ for a 30-minute interval can be calculated as:

$$g_t = \frac{1}{\left(\frac{1}{g_v}\right) + \left(\frac{1}{g_c}\right)} \text{, and} \qquad [9]$$

$$COND_T = a1800 g_t \left(\frac{e_{sc} - e}{P}\right) \qquad [10]$$

where a is 0.018 kg H_2O mol^{-1} H_2O.

Eddy Covariance

An EC system was installed at the study site (Table 1.1). A 3-D sonic anemometer was oriented at 210° magnetic. The infrared gas analyzer was tilted 15° toward the footprint and separation distance from the sonic anemometer was 0.14 m. Eddy covariance data were recorded at 20 Hz and stored on a CR3000 (Campbell Scientific, Inc.) datalogger. Meteorological data were sampled at 10 s intervals and then averaged and stored at 30-minute intervals. Data were processed using EddyPro (version 4.1, Li-Cor, Inc., Lincoln, NE; Infrastructure for Measurements of the European Carbon Cycle Consortium). Axis rotation for tilt was corrected using the double rotation method. Detrending of turbulent fluctuations was conducted using the block average technique. Compensation of density fluctuations was conducted according to

Webb et al. (1980). Fast fourier transform using the Hamming window was conducted (Kaimal and Kristensen, 1991). Spectral corrections in the low frequency range were conducted according to Montcrieff et al. (2004) and in the high frequency range according to Montcrieff et al. (1997). Random uncertainty of flux estimation due to sampling errors was conducted according to Finkelstein and Sims (2001). Quality flags were used to determine the quality of data (Mauder and Foken, 2006).

Gap-filling of EC sensible and latent heat fluxes was conducted using an online gap-filling program (http://www.bgc-jena.mpg.de/~MDIwork/eddyproc/, Max Planck Institute for Biogeochemistry, Jena, Germany). The gap-filling method is similar to Falge et al. (2001a,b) "but that consider both the covariation of fluxes with meteorological variables and the temporal auto-correlation of the fluxes" (Reichstein et al., 2005). Missing flux values and flux values that were flagged with a value of "2" using the method described by Mauder and Foken (2006) were replaced with gap-filled values.

Energy balance closure was forced using the Bowen ratio, B = H / LE, (Twine et al., 2000; Chávez et al., 2005; Chávez et al., 2009) obtained from the sonic anemometer. This method assumes that the sonic anemometer correctly estimated B. Energy balance closure is forced by finding the quantity of energy needed to add to the gap-filled fluxes:

$$D = Rn - G - H - LE, \quad [11]$$

$$\Delta LE = D / (1 + B), \quad [12]$$

$$\Delta H = D - \Delta LE, \quad [13]$$

$$LE = LE + \Delta LE, \text{ and} \quad [14]$$

$$H = H + \Delta H, \quad [15]$$

where D is the energy balance residual, ΔH and ΔLE represent the lacking energy to close the energy balance.

Latent heat fluxes (W m^{-2}) were converted to ET using the equation:

$$EC_{ET} = \frac{C \times LE}{\lambda \times \rho_w} \times M \qquad [16]$$

where EC_{ET} is eddy covariance measured ET (mm 30 min^{-1}), C is a time conversion (1800 for 30 min. intervals), LE is measured from the EC system (W m^{-2}), λ is the latent heat of vaporization (MJ kg^{-1}), ρ_w is the density of water (1000 kg m^{-3}), and M is a conversion factor to convert ET to mm (0.001).

Statistical Analysis

Evapotranspiration values were compared to the corresponding mean LYS_{ET} value each day. Regression analysis ($ET_x = mLYS_{ET} + b$) was conducted using the REG procedure of SAS (SAS Institute, Inc., Cary, NC) at $P < 0.05$, where "m" is the slope and "b" the dependent variable (ET_x technique) intercept. Linear association between LYS_{ET} and the other ET measurement techniques was determined using the coefficient of determination (r^2). Paired *t*-tests were conducted to determine differences between LYS_{ET} and the other ET measurement techniques using the TTEST procedure (SAS Institute, Inc., Cary, NC) at $P < 0.05$. The null hypothesis for the *t*-test was that the difference between techniques was zero. Root mean square error (RMSE), mean bias error (MBE), and mean percent error (%E) between LYS_{ET} and the other ET measurement techniques were calculated as:

$$RMSE = \sqrt{\frac{1}{n}\sum_{i=1}^{n}\left(ET_{x_i} - LYS_{ET_i}\right)^2}, \qquad [17]$$

$$MBE = \frac{1}{n}\sum_{i=1}^{n}\left(ET_{x_i} - LYS_{ET_i}\right), \text{ and} \qquad [18]$$

$$\%E = \sum \left(\frac{ET_{x_i} - LYS_{ET_i}}{LYS_{ET_i}} \right) \times 100, \quad [19]$$

where n = number of observations, ET_{x_i} = evapotranspiration measurement technique, and LYS_{ET_i} = lysimeter measured ET.

An index of agreement (d) was used as a measure of association to overcome problems associated with RMSE and r^2, such as the presence of any outlying data, (Willmott, 1981; Legates and McCabe, 1999). Like the coefficient of determination, the index of agreement produces a value between 0 and 1, with values closer to 1 indicating better agreement between LYS_{ET} and the other ET measurement techniques. The index of agreement was calculated as:

$$d = 1 - \left[\frac{\sum_{i=1}^{n} \left(ET_{x_i} - LYS_{ET_i} \right)^2}{\sum_{i=1}^{n} \left[\left| ET_{x_i} - \overline{LYS_{ET}} \right| + \left| LYS_{ET_i} - \overline{LYS_{ET}} \right| \right]^2} \right], \quad [20]$$

where the overbar indicates overall mean ET, all other variables have been previously defined.

Differences between LYS_{ET} and the other ET measurement techniques (ET technique – LYS_{ET}) may not be similar under all climatic conditions. Therefore, ET difference (ET technique – LYS_{ET}) was correlated with meteorological variables (net radiation, air temperature, vapor pressure deficit, and wind speed) during the daytime, where $R_n > 0$. Pearson correlation coefficients and statistical significance are reported to determine relationships among the variables with observed ET differences.

Results and Discussion

Three lysimeters were used in this study to obtain a better estimate of actual ET. Data indicated there was good agreement among the three lysimeters. Standard error of lysimeter measurements ranged from 0.01 to 0.88 mm d^{-1} with an average standard error of 0.25 mm d^{-1}. Similarly, among the three atmometers used in this study, standard error for ET ranged from 0.00 to 0.68 mm d^{-1} with an average standard error of 0.11 mm d^{-1}.

Empirical Models

The two empirical models, FAO56-PM and PT had the highest index of agreement, 0.93 and 0.92, respectively, and lowest RMSE, 1.00 and 1.08 mm d^{-1}, respectively, when compared to LYS_{ET} (Table 1.2). However, the models did not perform equally with the lysimeters. According to the *t*-tests, PT_{ET} was similar to LYS_{ET} while PM_{ET} was different from LYS_{ET}. The PM_{ET} %E was -4.4%, while PT_{ET} %E was 1.9%. The MBE of PT_{ET} was -0.13 mm d^{-1} and PM_{ET} MBE was -0.40 mm d^{-1}. This indicates that less variability was observed between PT_{ET} comparisons to LYS_{ET} than PM_{ET}. However, regression analysis indicates a better fit for PM_{ET} than PT_{ET} to LYS_{ET} (Fig. 1.2). The difference between the two techniques is expected because the two models are vastly different. The PT model is a potential ET calculation based heavily on net radiation and should perform best under non water-limiting conditions (Rosenberg et al., 1983). The FAO56-PM model is a combination approach that should generally produce a value closer to actual ET.

The differences between PM_{ET} and LYS_{ET} were not significantly correlated with any individual meteorological variable (i.e. differences in ET between PM_{ET} and LYS_{ET} were similar at all values of each variable) (Table 1.3). However, differences between PT_{ET} and LYS_{ET} were significantly correlated with vapor pressure deficit and wind speed (Table 1.3). These correlations illustrate the limitations of using the standard PT_{ET} in non-humid and strongly advective conditions. Conversely, two variables that are included in the PT model, air temperature and net radiation, were not significantly correlated with differences in ET between PT_{ET} and LYS_{ET}. This indicates that PT consistently and, presumably, accurately modeled the effects of air temperature and net radiation on ET.

The FAO56-PM ET has been found to underestimate ET, especially during hot and dry conditions. Bakhtiari et al. (2011) observed ET_o from six different models to underestimate LYS_{ET} in Iran. In their study, RMSE for PM_{ET} was 2.17 mm d^{-1} during periods of high evaporative demand and 1.70 mm d^{-1} during periods of low evaporative demand. Those values are much greater than those observed in this study. Similarly, Howell et al. (2000) found PM_{ET} to underestimate LYS_{ET} in the summer, especially when ET was greater than 8 mm d^{-1}. Conversely, López-Urrea et al. (2006) found that PM_{ET} performance was better under high demand (summer) than during low demand periods (spring and autumn) compared to LYS_{ET} using tall fescue within a semiarid climate in Spain. The climate in which the ET measurements are conducted is likely an important factor influencing differences between PM_{ET} and LYS_{ET}.

Fry et al. (1997) compared several empirical models to LYS_{ET} values (at the same location as our study site) from bermudagrass [*Cynodon dactylon* (L.) Pers. x *C. transvaalensis* Burtt-Davy], buffalograss [*Buchloe dactyloides* (Nutt.) Engelm.], zoysiagrass [*Zoysia japonica* Steud.], tall fescue, and perennial ryegrass [*Lolium perenne* L.]. They found the coefficients of determination to vary greatly with the model used, turfgrass species, cultivar, and mowing height. Their best coefficient of determination for the PT and Penman-Monteith models in tall fescue were 0.540 and 0.547, respectively. The coefficients of determination in this study were 0.72 and 0.80, for PT_{ET} and PM_{ET}, respectively (Fig. 1.2). Qian et al. (1996) reported slopes of

0.91 and 1.02 from lysimeter-measured tall fescue ET compared to Penman-Montieth ET for their two study years, at the same location as our study site. However, their coefficients of determination were only 0.53 and 0.60 for the two study years.

Eddy Covariance

Eddy covariance mean ET, 5.32 mm d^{-1}, was 3% less than LYS_{ET} (LYS_{ET} during EC_{ET} measurements was 5.48 mm d^{-1}) after closure was forced (Table 1.2). The RMSE, 1.25 mm d^{-1}, index of agreement, d = 0.87, and coefficient of determination, r^2 = 0.61 (Fig. 1.2), indicate that EC_{ET} may not compare as well with LYS_{ET} as did PM_{ET} and PT_{ET}. However, MBE, -0.16 mm d^{-1} and %E was 4.1%, were relatively small, and the *t*-test showed no difference between EC_{ET} and LYS_{ET}. The latter statement suggests that EC_{ET} is similar to LYS_{ET}. Regression analysis of EC_{ET} compared to LYS_{ET} indicates that EC_{ET} overestimates LYS_{ET} on low ET days (i.e., less than ~5 mm d^{-1}) and underestimates LYS_{ET} on high ET days (Fig. 1.2). This may not necessarily be an indication of poor performance of the EC system. Although, the lysimeter is the best approach to measure actual ET, heating of the lysimeter soil core and potentially greater leaf area index of the lysimeter (Bremer, 2003) could result in greater water loss from the lysimeter than from the surrounding turf.

Few studies have measured ET from turfgrass using EC. In Florida, on bahiagrass (*Paspalum notatum* Flugge), EC_{ET} averaged 32% less than ET_o (Jia et al., 2009). Our reference crop ET using the FAO56-PM (PM_{ET} during EC_{ET} measurements was 4.96 mm d^{-1}) was 7% less than EC measured ET. The climate in Florida is much more humid than our study site in Kansas, which likely led to greater EC_{ET} due to greater drying power of the air at our study site.

The underestimation of EC_{ET} compared to LYS_{ET} is well documented, even after closure is forced. Chávez et al. (2009), studying cotton in the Texas High Plains, found EC_{ET} to underestimate LYS_{ET} 0.10 to 0.12 mm h^{-1} before closure was forced using B. After forcing closure, EC_{ET} underestimates were only 0.05 to 0.08 mm h^{-1} and MBE was -0.03 mm h^{-1}. Ding et al. (2010), studying maize in arid China, observed EC_{ET} to underestimate LYS_{ET} by 21.8% before closure and 4.8% after closure. This is similar to our finding of 5% EC_{ET} underestimation of LYS_{ET} after closure was forced. Castellvi and Snyder (2010) found a poor relationship between EC_{ET} and LYS_{ET} during stable atmospheric conditions when $R_n – G$ was negative, e.g. nighttime. Nighttime ET is often relatively small compared to total daily ET. However, stomatal closure during nighttime should not be assumed as nighttime transpiration can be 5-15% of total daily ET (Caird et al., 2007; Irmak, 2011).

Differences in ET between EC and the lysimeters were significantly correlated with wind speed, air temperature, and vapor pressure deficit (Table 1.3). Eddy covariance ET is an actual ET measurement, like LYS_{ET}. However, the response of the two techniques to these variables is not similar. This could be due to the problems associated with lysimeter design or an inability of the EC system to accurately measure ET under certain conditions, such as periods when gap-filling models are required.

Atmometers

Atmometers underestimated LYS_{ET} more than any of the other ET methods (Table 1.2). Mean AT_{ET} was 4.61 mm d^{-1}, which was 17% less than LYS_{ET}. The RMSE, 1.47 mm d^{-1} and MBE, -0.97 mm d^{-1}, were the highest among the measurement techniques. Regression analysis of AT_{ET} indicates that underestimation of ET will become greater with increasing LYS_{ET} (Fig. 1.2). Differences between AT_{ET} and LYS_{ET} were significantly correlated with wind speed (Table 1.3). Increasing underestimates in AT_{ET} with increasing wind speed may be due to the inability of the atmometer to wick water into the atmosphere effectively at high wind speeds. Magliulo et al.

(2003) found AT_{ET} to have a 1 to 1 slope and y-axis intercept not different from zero when regressed versus LYS_{ET} using perennial ryegrass. Qian et al. (1996), using a black Bellani plate, observed a good agreement between AT_{ET} and LYS_{ET}, $r^2 = 0.67 - 0.82$, in tall fescue turfgrass, however, the slope of their regression line (slope = 0.45 to 0.57) was much less than what was observed in this study (slope = 0.74).

Among the techniques used in this study, the atmometer is perhaps the easiest to use and the lowest cost to purchase and maintain. Even though the atmometer performance in this study was poorer compared to the other techniques, one should not necessarily be deterred from its use. The overall error from the atmometer is relatively small compared to LYS_{ET} (%E = -0.15) and can provide practitioners reliable ET_o for irrigation management. Atmometers can provide relatively accurate measurements of ET compared with PM_{ET} (Chapter 2) and have proved very useful for irrigation scheduling (Ervin and Koski, 1997; Knox et al., 2011).

Infrared Thermometry

The transpiration calculated using the canopy stomatal conductance model, $COND_T$, underestimated LYS_{ET} 29.6%, which was more than any ET technique (Table 1.2). The MBE was -1.71 mm d^{-1}, and %E was -29.6% (Table 1.2). Regression analysis of $COND_T$ versus LYS_{ET} resulted in a slope of 0.78 and y-axis intercept of -0.41 (Fig. 1.2). The y-axis intercept was closer to zero than any other technique and the slope similar to the other techniques.

The transpiration from a fully closed-canopy crop, such as turfgrass, can be 80 - 90% of ET (Allen et al., 1998). According to the $COND_T$ data in this study, on average, 29% of ET was from evaporation and 71% of ET from transpiration (LYS_{ET} during $COND_T$ measurements was 5.85 mm d^{-1}). Thus, soil evaporation apparently accounted for more of the ET than expected. This may be a result of collecting measurements over a well-watered turfgrass where plentiful soil water may have attributed to a greater than expected evaporative contribution to ET. Nighttime transpiration is often considered about 5 to 15% of total daily ET (Caird et al., 2007; Irmak, 2011). Assuming 10% transpiration during nighttime, total transpiration would then be 4.72 mm d^{-1}, which is 81% of LYS_{ET}.

Difference between $COND_T$ and LYS_{ET} was significantly correlated with wind speed (Table 1.3). Increasing wind speed over the turfgrass increases evaporation of water from the canopy, thus increasing transpirational cooling of the canopy. The modeled stomatal conductance response to wind speed and $COND_T$ estimates may be underestimated compared to LYS_{ET} as wind speed increases because the actual transpiration from the lysimeter may be more sensitive to wind speed than the canopy stomatal conductance model.

This model relies heavily upon accurate measurement of canopy temperature and iteration for boundary layer conductance. This is a complex approach and much research is necessary to validate and improve the model.

Conclusion

Evapotranspiration measurements with lysimeters were compared with ET measured with several other techniques in tall fescue turfgrass. Eddy covariance ET and PT_{ET} produced ET values closest to LYS_{ET}, based on mean ET, MBE, *t*-tests, and %E. The PM_{ET} and PT_{ET} models had the best index of agreement with LYS_{ET}. The PT_{ET} and EC_{ET} techniques underestimated LYS_{ET} 0.14 and 0.16 mm d^{-1}, respectively. The stomatal conductance model, $COND_T$, and AT_{ET} underestimated LYS_{ET} 1.71 and 0.97 mm d^{-1}, respectively. The PM_{ET} was intermediate, underestimating LYS_{ET} by 0.41 mm d^{-1}. Further investigation of ET differences among these techniques is warranted under various climatic conditions that are different from this study. The differences in ET among techniques in this study do not attempt to diminish the importance of any one technique. Each technique has its advantages and disadvantages in any given situation. Differences among these ET measurement techniques should be expected and practitioners and researchers should select the technique that best fits their situation.

References

Alam, M. and T.P. Trooien. 2001. Estimating reference evapotranspiration with an atmometer. Appl. Eng. Agric. 17(2):153-158.

Alig, R.J., J.D. Kline, and M. Lichtenstein. 2004. Urbanization on the US landscape: looking ahead in the 21st century. Landsc. Urban Plan. 69:219-234.

Allen, R.G. 1986. A Penman for all seasons. J. Irrig. Drain. Eng. 112(4):348-368.

Allen, R.G., M.E. Jensen, J.L. Wright, and R.D. Burman. 1989. Operational estimates of reference evapotranspiration. Agron. J. 81(4):650-662.

Allen, R.G., L.S. Pereira, D. Ross, and M. Smith. 1998. Crop evapotranspiration – guidelines for computing crop water requirements – FAO irrigation and drainage paper 56. Food and Agriculture Organization of the United Nations, Rome.

Allen, R.G., L.S. Pereira, T.A. Howell, and M.E. Jensen. 2011. Evapotranspiration information reporting: I. Factors governing measurement accuracy. Agric. Water Manage. 98:899-920.

Allen, R.G., W.O. Pruitt, and M.E. Jensen. 1991. Environmental requirements of lysimeters. p.170-181. *In.* Lysimeters for evapotranspiration and environmental measurements. Proc. Intl. Symp. Lysimetry, Honolulu, HI, 23-25 July, Am. Soc. Civil Eng. New York, NY.

Allen, R.G., W.O. Pruitt, J.L. Wright, T.A. Howell, F. Ventura, R. Snyder, D. Itenfisu, P. Steduto, J Berengena, J.B. Yrisarry, M. Smith, L.S. Pereira, D. Raes, A. Perrier, I. Alves, I. Walter, and R. Elliott. 2006. A recommendation on standardized surface resistance for hourly calculation of reference ET_o by the FAO56 Penman-Monteith method. Agric. Water Manage. 81:1-22.

Altenhofen, J. 1985. A modified atmometer for on-farm ET determination.p.177-184. *In.* Advances in evapotranspiration. Proc. Natl. Conf. Adv. Evapotranspiration, Chicago, IL, 16-17 Dec., Am. Soc. Agric. Eng. St. Joseph, MI.

ASCE-EWRI. 2005. The ASCE Standardized Reference Evapotranspiration Equation. Environmental and Water Resources Institute (EWRI) of ASCE, Standardization of Reference Evapotranspiration Task Committee Final Rep. http://www.kimberly.uidaho.edu/water/asceewri/ascestzdetmain2005.pdf.

Bakhtiari, B., N. Ghahreman, A.M. Liaghat, and G. Hoogenboom. 2011. Evaluation of reference evapotranspiration models for a semiarid environment using lysimeter measurements. J. Agr. Sci. Tech. 13:223-237.

Baldocchi, D.D., B.B. Hincks, and T.P. Meyers. 1988. Measuring biosphere-atmosphere exchanges of biologically related gases with micrometeorological methods. Ecology. 69(5):1331-1340.

Blonquist Jr., J.M., J.M. Norman, and B. Bugbee. 2009. Automated measurement of canopy stomatal conductance based on infrared temperature. Agric. Forest Meteorol. 149:1931-1945.

Bowen, I.S. 1926. The ratio of heat losses by conduction and by evaporation from any water surface. Physical Review. 27:779-787.

Bremer, D.J. 2003. Evaluation of microlysimeters used in turfgrass evapotranspiration studies using the dual-probe heat-pulse technique. Agron. J. 95(6):1625-1632.

Bremer, D.J., S.J. Keeley, A. Jager, and J.D. Fry. 2013. Lawn-watering perceptions and behaviors of residential homeowners in three Kansas (USA) cities: implications for water quality and quantity. Int. Turfgrass Soc. Res. J. 12:23-29.

Bremer, D.J., S.J. Keeley, A. Jager, J.D. Fry, and C. Lavis. 2012. In-ground irrigation systems affect lawn-watering behaviors of residential homeowners. HortTech. 22(5):651-658.

Caird, M.A., J.H. Richards, L.A. Donovan. 2007. Nighttime stomatal conductance and transpiration in C3 and C4 plants. Plant Physiol. 143:4-10.

Castellvi, F. and R.L. Snyder. 2010. A comparison between latent heat fluxes over grass using a weighing lysimeter and surface renewal analysis. J. Hydrol. 381:213-220.

Chávez, J.L. C.M.U. Neale, L.E. Hipps, J.H. Prueger, and W.P. Kustas. 2005. Comparing aircraft-based remotely sensed energy balance fluxes with eddy covariance tower data using heat flux source area functions. J. Hydromet. 6(6):923-940.

Chávez, J.L., T.A. Howell, and K.S. Copeland. 2009. Evaluating eddy covariance cotton ET measurements in an advective environment with large weighting lysimeters. Irrig. Sci. 28:35-50.

Chen, F. and P.J. Robinson. 2009. Estimating reference crop evapotranspiration with ETgages. J. Irrig. Drain. Eng. 135(3):335-342.

Ding, R., S. Kang, F. Li, Y. Zhang, L. Tong, and Q. Sun. 2010. Evaluating eddy covariance method by large-scale weighting lysimeter in a maize field of northwest China. Agric. Water Manage. 98:87-95.

Ervin, E.H. and A.J. Koski. 1997. A comparison of modified atmometer estimates of turfgrass evapotranspiration with Kimberly-Penman alfalfa reference evapotranspiration. Int. Turfgrass Soc. Res. J. 8:663-670.

Falge, E., D. Baldocchi, R. Olson, et al. 2001a. Gap filling strategies for long term energy flux data sets. Agric. Forest Meteorol. 107:71-77.

Falge, E., D. Baldocchi, R. Olson, et al. 2001b. Gap filling strategies for defensible annual sums of net ecosystem exchange. Agric. Forest Meteorol. 107:43-69.

Feldhake, C.M., R.E. Danielson, and J.D. Butler. 1983. Turfgrass evapotranspiration. I. Factors influencing rate in urban environments. Agron. J. 75:824-830.

Finkelstein, P.L. and P.F. Sims. 2001. Sampling error in eddy correlation flux measurements. J. Geophys. Res. 106:3503-3509.

Fry, J., S. Wiest, Y. Qian, and W. Upham. 1997. Evaluation of empirical models for estimating turfgrass water use. Intl. Turfgrass Soc. Res. J. 8:1268-1273.

Foken, T. 2008a. The energy balance closure problem: an overview. Ecological Applications. 18(6):1351-1367.

Foken, T. 2008b. Micrometeorology. Springer-Verlag. Berlin. 306p.

Gavilan, P. and F. Castillo-Llanque. 2009. Estimating reference evapotranspiration with atmometers in a semiarid environment. Agric. Water Manage. 96:465-472.

Hershey, D.R. 1990. Container-soil physics and plant growth. BioScience. 40:685-686.

Howell, T.A., S.R. Evett, A.D. Schneider, D.A. Dusek, and K.S. Copeland. 2000. Irrigated fescue grass ET compared with calculated reference grass ET. p.228-242. In. Proc., 4th National Irrig. Symp., ASAE, Phoenix, AZ.

Irmak, S. 2011. Dynamics of nocturnal, daytime, and sum-of-hourly evapotranspiration and other surface energy fluxes over nonstressed maize canopy. J. Irrig. Drain. Eng. 137(8):475-490.

Irmak, S., M.D. Dukes, and M.J. Jacobs. 2005. Using modified Bellani plate evapotranspiration gauges to estimate short canopy reference evapotranspiration. J. Irrig. Drain. Eng. 131(2):164-175.

Itenfisu, D., R.L. Elliott, R.G. Allen, and I.A. Walter. 2003. Comparison of reference evapotranspiration calculations as part of the ASCE standardization effort. J. Irrig. Drain. Eng. 129(6):440-448.

Jackson, R.D., P.J. Pinter, Jr., R.J. Reginato, and S.B. Idso. 1980. Hand-held radiometry. Agric. Rev. Manuals, ARM-W-19, United States Department of Agriculture, Science and Education Administration, Western Region, Oakland, CA.

Jia, X., M.D. Dukes, and J.M. Jacobs. 2009. Bahiagrass crop coefficients from eddy correlation measurements in central Florida. Irrig. Sci. 28(1):5-15.

Kaimal, J.C. and L. Kristensen. 1991. Time series tapering for short data samples. Boundary-Layer Meteorol. 57:187-194.

Knox, J.W., J.A. Rodriguez-Diaz, and T.M. Hess. 2011. Estimating evapotranspiration by using atmometers for irrigation scheduling in a humid environment. J. Irrig. Drain. Eng. 137(11):685-691.

Kochendorfer, J., T.P. Meyers, J. Frank, W.J. Massman, and M.W. Heuer. 2012. How well can we measure the vertical wind speed? Implications for fluxes of energy and mass. Boundary-Layer Meteorol. 145(2):383-398.

Legates, D.R. and G.J. McCabe Jr., 1999. Evaluating the use of "goodness-of-fit" measures in hydrologic and hydroclimatic model validation. Water Resour. Res. 35(1):233-241.

Leuning, R., E. van Gorsel, W.J. Massman, and P.R. Isaac. 2012. Reflections on the surface energy imbalance problem. Agric. Forest Meteorol. 156:65-74.

Livingston, B.E. 1915. A modification of the Bellani porous plate atmometer. Science. 41(1067):872-874.

López-Urrea, R., F. Martín de Santa Olalla, C. Fabeiro, and A. Moratalla. 2006. Testing evapotranspiration equations using lysimeter observations in a semiarid climate. Agric. Water Manage. 85:15-26.

Magliulo, V., R. d'Andria, and G. Rana. 2003. Use of the modified atmometer to estimate reference evapotranspiration in Mediterranean environments. Agric. Water Manage. 62:1-14.

Mauder, M. and T. Foken. 2006. Impact of post-field data processing on eddy covariance flux estimates and energy balance closure. Meteorologische Zeitschrift. 15:597-609.

Meyers, T.P. and D.D. Baldocchi. 2005. Current micrometeorological flux methodologies with applications in agriculture. p. 381-396. *In:* J.L. Hatfield and J.M. Baker (eds) Micrometeorology in Agricultural Systems, Agronomy Monograph no. 47. ASA/CSSA/SSSA, Madison, WI.

Milesi, C., S.W. Running, C.D. Elvidge, J.B. Dietz, B.T. Tuttle, and R.R. Nemani. 2005. Mapping and modeling the biogeochemical cycling of turf grasses in the United States. Environ. Mgt. 36(3):426-438.

Montcrieff, J.B., J.M Massheder, H. de Bruin, J. Ebers, T. Friborg, B. Heusinkveld, P. Kabat, S. Scott, H. Soegaard, and A. Verhoef. 1997. A system to measure surface fluxes of momentum, sensible heat, water vapor and carbon dioxide. J. Hydrol. 188-189:589-611.

Montcrieff, J.B., R. Clement, J. Finnigan, and T. Meyers. 2004. Averaging, detrending and filtering of eddy covariance time series. p. 7-31. *In.* X. Lee, W.J. Massman, and B.E. Law (eds.) Handbook of micrometeorology: a guide for surface flux measurements. Kluwer Academic.

Monteith, J.L. 1965. Evaporation and environment. p.205-234. *In.* The state and movement of water in living organisms, Symp. Soc. Exp. Biol. Vol. 19. Cambridge University Press, Cambridge, UK.

Morris, K. 2003. The national turfgrass research initiative. National Turfgrass Federation and National Turfgrass Evaluation Program, Beltsville, MD. 2 Aug. 2013. <http://www.turfresearch.org/pdf/turfinitiative.pdf>.

Penman, H.L. 1948. Natural evaporation from open water, bare soil and grass. Proc. Royal Soc. London (A). 193(1032):120-145.

Penman, H.L. 1956. Evaporation-an introductory survey. Neth. J. Agric. Sci. 4:9-29.

Penman, H.L. 1963. Vegetation and hydrology. Tech. Comm. No. 53, Commonwealth Bureau of Soils, Harpenden, England. 125 p.

Priestley, C.H.B. and R.J. Taylor. 1972. On the assessment of surface heat flux and evaporation using large-scale parameters. Mon. Weather Rev. 100(2):81-92.

Qian, Y.L., J.D. Fry, S.C. Wiest, and W.S. Upham. 1996. Estimating turfgrass evapotranspiration using atmometers and the Penman-Monteith model. Crop Sci. 36(3):699-704.

Reichstein, M., E. Falge, D. Baldocchi, et al. 2005. On the separation of net ecosystem exchange into assimilation and ecosystem respiration: review and improved algorithm. Global Change Biology. 11:1424-1439.

Rosenberg, N.J., B.L. Blad, and S.B. Verma. 1983. Microclimate: the biological environment. John Wiley & Sons, Inc. New York, NY.

Stannard, D.I. 1993. Comparison of Penman-Monteith, Shuttleworth-Wallace, and modified Priestley-Taylor evapotranspiration models for wildland vegetation in semiarid rangeland. Water Resour. Res. 29(5):1379-1392.

Suleiman, A.A. and G. Hoogenboom. 2007. Comparison of Priestley-Taylor and FAO-56 Penman-Monteith for daily reference evapotranspiration in Georgia. 133(2):175-182.

Swinbank, W.C. 1951. The measurement of vertical transfer of heat and water vapor by eddies in the lower atmosphere. J. Meteorol. 8(3):135-145.

Tanner, C.B. 1963. Plant temperatures. Agron. J. 55:210-211.

Trajkovic, S. 2010. Testing hourly reference evapotranspiration approaches using lysimeter measurements in a semiarid climate. Hydrol. Res. 41(1):38-49.

Twine, T.E., W.P. Kustas, J.M. Norman, D.R. Cook, P.R. Houser, T.P. Meyers, J.H. Prueger, P.J. Starks, and M.L. Wesely. 2000. Correcting eddy-covariance flux underestimates over a grassland. Agric. Forest Meteorol. 103:279-300.

Webb, E.K., G.I. Pearman, and R. Leuning. 1980. Correction of flux measurements for density effects due to heat and water vapor transfer. Q. J. Royal Meteorol. Soc. 106:85-100.

Willmott, C.J. 1981. On the validation of models. Phys. Geogr. 2(2):184-194.

Wilson, K., A. Goldstein, E. Fagle, M. Aubinet, D. Baldocchi, P. Berbigier, C. Bernhofer, R. Ceulemans, H. Dolman, C. Field, A. Grelle, A. Ibrom, B.E. Law, A Kowalski, T. Meyers, J. Moncrieff, R. Monson, W. Oechel, J. Tenhunen, R. Valentini, and S. Verma. 2002. Energy balance closure at FLUXNET sites. Agric. Forest Meteorol. 113:223-243.

Table 1.1. Summary of instruments used by the weather station and eddy covariance system.

Instrument	Model	Manufacturer	Height
			-- m --
Weather Station			
Temperature and Relative Humidity	HMP50	Vaisala, Inc., Helsinki, Finland	2.0
2-D Sonic Anemometer	Windsonic1	Gill Instruments Ltd., Hampshire, England	2.0
Net Radiometer	NR-Lite	Kipp & Zonen, Inc., The Netherlands	1.5
Eddy Covariance System			
Net Radiometer	CNR-1	Kipp & Zonen, Inc., The Netherlands	1.5
Temperature and Relative Humidity	HMP45C	Vaisala, Inc., Helsinki, Finland	1.5
3-D Sonic Anemometer	CSAT3	Campbell Scientific, Inc., Logan, UT, USA	1.5
Infrared Gas Analyzer	LI-7500	Li-Cor, Inc., Lincoln, NE, USA	1.5
Soil Heat Flux (2)	HFP01	Huskeflux Thermal Sensors B.V., The Netherlands	-0.07
Soil Water Content (2)	10HS	Decagon Devices, Inc., Pullman, WA, USA	-0.035
Soil Temperature (2)	TCAV	Campbell Scientific, Inc., Logan, UT, USA	-0.02, -0.05

Table 1.2. Evapotranspiration measurement technique means and statistical analysis as compared to lysimeter measured evapotranspiration.

Measurement Technique	n	Mean ET	RMSE†	MBE‡	%E§	d¶	p††
		------------- mm d^{-1} --------------					
Lysimeter‡‡	78	5.58					
FAO56-PM	78	5.17	1.00	-0.40	-4.4	0.93	***
Priestley-Taylor	78	5.44	1.08	-0.13	1.9	0.92	NS
Eddy Covariance	70	5.32	1.32	-0.16	4.1	0.87	NS
Atmometer	78	4.61	1.47	-0.97	-15.0	0.87	***
Conductance Model	42	4.14	1.89	-1.71	-29.6	0.72	***

†RMSE is the root mean square error calculated as: $\text{RMSE} = \sqrt{\frac{1}{n}\sum_{i=1}^{n}\left(ET_{x_i} - LYS_{ET_i}\right)^2}$.

‡MBE is the mean bias error calculated as: $\text{MBE} = \frac{1}{n}\sum_{i=1}^{n}\left(ET_{x_i} - LYS_{ET_i}\right)$.

§%E is the mean percent error calculated as: $\%E = \sum\left(\frac{ET_{x_i} - LYS_{ET_i}}{LYS_{ET_i}}\right)\times 100$.

¶d is the index of agreement calculated, $d = 1 - \left[\frac{\sum_{i=1}^{n}\left(ET_{x_i} - LYS_{ET_i}\right)^2}{\sum_{i=1}^{n}\left[\left|ET_{x_i} - \overline{LYS_{ET}}\right| + \left|LYS_{ET_i} - \overline{LYS_{ET}}\right|\right]^2}\right]$.

††Probability that ET_x and Lysimeter ET are significantly different from each other based on paired *t*-test at $P < 0.05$.

‡‡Mean lysimeter ET was 5.48 and 5.85 mm d^{-1} during eddy covariance and conductance model measurement periods, respectively.

*** indicates significant difference at $P < 0.001$.

Table 1.3. Pearson correlation coefficients for average daytime (Rn > 0) net radiation, vapor pressure deficit, air temperature, and wind speed comparisons to ET difference (ET technique – Lysimeter ET).

	Atmometer	FAO56-PM	Priestley-Taylor	Eddy Covariance	Conductance Model
Net Radiation	-0.20	-0.02	0.05	-0.10	-0.26
Vapor Pressure Deficit	0.07	0.02	-0.25*	-0.48***	-0.23
Air Temperature	0.05	-0.00	-0.11	-0.31**	-0.10
Wind Speed	-0.34**	-0.04	-0.53***	-0.53***	-0.38*

*, **, and *** indicate significance at P < 0.05, 0.01, and 0.001, respectively.

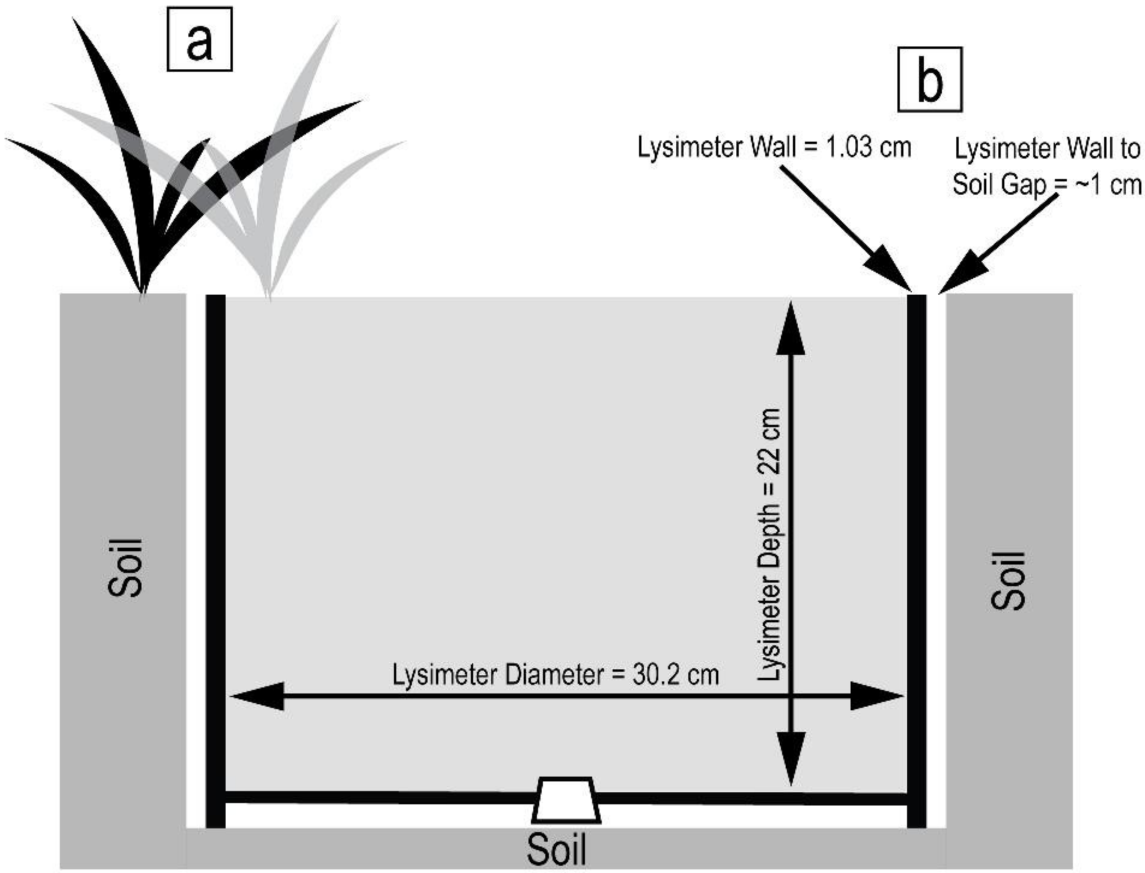

Figure 1.1. Depiction of lysimeter vegetation overlap (a) and dimensions of lysimeter including lysimeter wall and lysimeter wall to soil gap (b).

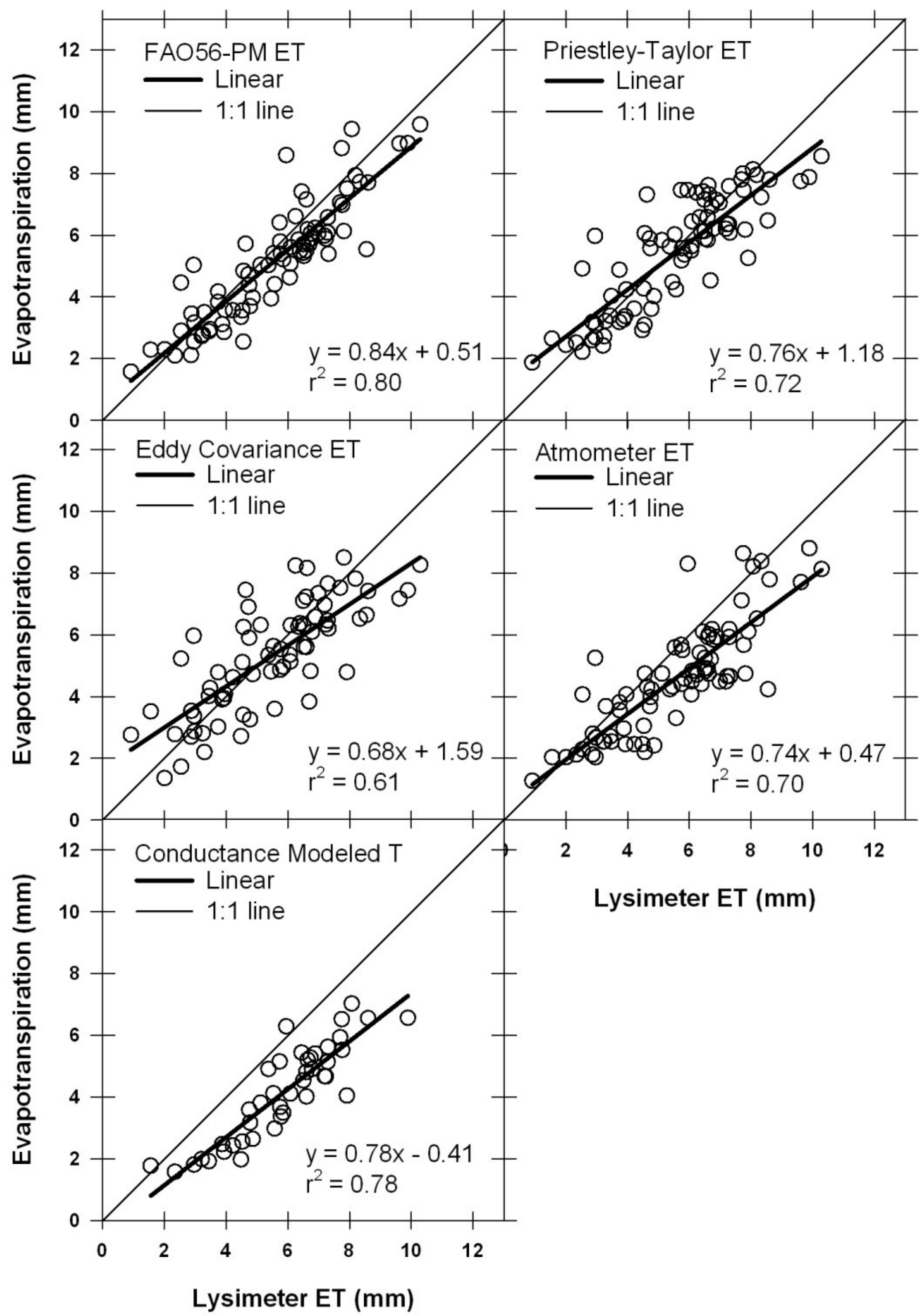

Figure 1.2. Comparison of evapotranspiration techniques to lysimeter measured evapotranspiration. Bolded line represents the linear regression.

Chapter 2 - Evaluation of Atmometers within Urban Home Lawn Microclimates

Abstract

An atmometer is an inexpensive tool used to measure evapotranspiration (ET) *in situ*. The effects of microclimates, such as those typically associated with an urban lawn, on the performance of atmometers are not well documented. The objective of this study was to compare ET estimates from atmometers with ET estimates from the FAO-56 Penman-Monteith equation (PM_{ET}, FAO56-PM), including within a number of lawn microclimates. The study was conducted in six home lawns in 2010 and one in 2011 in Manhattan, KS, and four home lawns in Wichita, KS in 2011. A weather station and atmometer were positioned in an open sward of turfgrass near each city during each measurement period in Manhattan and Wichita, KS. A commercially available Bellani plate atmometer (ET_{gage}®), using the #30 green canvas cover for grass reference ET (AT_{ET}), was placed next to a portable weather station in two contrasting microclimates within each lawn. Weather stations recorded temperature, net radiation, relative humidity, and wind speed data used to calculate PM_{ET}. Open sward AT_{ET} (4.73 mm d^{-1}) averaged 14% less than PM_{ET} (5.48 mm d^{-1}). However, within the microclimates, AT_{ET} (3.94mm d^{-1}) averaged 22% greater than PM_{ET} (3.23 mm d^{-1}). The differences in ET estimates between measurement techniques varied with wind speed, net radiation, and vapor pressure deficit. The best relationships between AT_{ET} and PM_{ET}, at the open sward and within microclimates, were observed when wind speed was greater than 1 m s^{-1}, vapor pressure deficit was greater than 2 kPa, and net radiation was greater than 5 MJ m^{-2} d^{-1}. Overall, atmometers can provide reliable estimates of PM_{ET} and should provide practitioners a means to manage irrigation within microclimates.

Introduction

Turfgrasses in the United States are estimated to cover 16 to 20 million hectares, an area three times larger than any irrigated crop (Morris, 2003; Milesi et al., 2005). The total turfgrass area in the United States is likely to increase greatly as urbanization continues to expand (Alig et al., 2004). Irrigation of turfgrasses in urban areas is a common practice creating an increasing demand for water in expanding urban areas. However, many homeowners do not understand how to manage the irrigation for their lawn (Bremer et al., 2012; Bremer et al., 2013). A better understanding of turfgrass irrigation requirements (i.e. ET) would help homeowners manage their irrigation more efficiently, reducing the demand for water.

Turfgrass irrigation requirements are often determined by ET estimates. Typically, ET estimates are obtained from either on-site or off-site weather stations that collect weather data to calculate ET using an empirical model. However, a weather station can be expensive to set up and maintain. Siting of the weather station can also create a bias resulting in inaccurate ET estimation (Ley et al., 1996). This is problematic for practitioners who utilize ET-based irrigation scheduling.

In addition to weather-monitoring equipment, the presence of microclimates within a home lawn or golf course can result in variability in ET across microclimates (Jiang et al., 1988). This is caused by alterations of environmental conditions within each microclimate, such as solar radiation, wind speed, humidity, and air temperature (Rosenberg et al., 1983; Jiang et al., 1988; Skaggs and Irmak, 2012). Feldhake et al. (1983) used lysimeters to determine factors influencing ET in urban microclimates. Using lysimeters in full sun and varying degrees of shade, they found that ET increased linearly with solar radiation. Accurate estimation of on-site ET, including microclimates, may lead to improved irrigation efficiency, reduced demand for water resources, and fewer potential environmental impacts of water applied to a site.

An atmometer is a simple tool that can provide practitioners with accurate on-site ET data. The porous Bellani plate atmometer described by Livingston (1915) was modified by Altenhofen (1985) to cover the ceramic Bellani plate with a green canvas having an albedo similar to alfalfa and resistance to water diffusion similar to stomata. Prior to this modification, the ceramic Bellani plates were colored either black or white.

Several studies have investigated the performance of modified atmometers across environmental conditions and for irrigation scheduling. Broner and Law (1991) compared the modified atmometer to a Penman combination evapotranspiration equation (Jensen, 1983) and found that atmometer ET was only 3.9% greater than model predicted ET. However, over the past twenty years, the Penman-Monteith (Monteith, 1965) evapotranspiration equation has become a standard empirical model for estimating reference evapotranspiration. When comparing atmometer ET values to the Penman-Monteith equation, evidence suggests that corrections are necessary in humid, rainy (Irmak et al., 2005; Chen and Robinson, 2009) and semi-arid (Alam and Trooien, 2001) climates. In contrast to requiring corrections, good agreement has been reported between the atmometer and Penman-Monteith ET_o in semi-arid environments (Magliulo et al., 2003; Gavilan and Castillo-Llanque, 2009). Magliulo et al. (2003) also found good agreement between atmometer ET and a class A pan and lysimeters. However, daily ET values averaged over multiple days (i.e. 3 to 7 days) can increase the accuracy of AT_{ET} estimates (Irmak et al., 2005) and can improve irrigation efficiency (Knox et al., 2011).

Objective

Few studies have investigated the performance of atmometers in turfgrass settings. Qian et al. (1996), using a black Bellani plate, found their atmometer to provide better ET estimation than a class A pan and the Penman-Monteith model, when compared to lysimeter ET. Ervin and

Koski (1997) concluded that an atmometer, similar to the model used in this study, could be used for irrigation scheduling on cool-season turfgrass in semi-arid climates. The objective of this study was to compare ET estimates from atmometers with ET estimates from the FAO-56 Penman-Monteith (Allen et al., 1998) equation, including within a number of lawn microclimates.

Materials and Methods

This investigation was initiated in June 2010 at Manhattan, KS and was continued in 2011 at sites in Manhattan, KS and Wichita, KS (Table 2.1). Contrasting microclimates within each home lawn were selected for study. Based on visual observations of the home lawn, contrasting microclimates were selected by presence of trees or structures that may obstruct airflow, wind, or solar radiation.

A portable weather station and atmometer (ETgage Model E, ETgage Company, Loveland, CO) were positioned in two contrasting microclimates at each home site. An additional weather station and atmometer were placed in an open sward of turfgrass in each city. The atmometer was placed within 0.5 m of the corresponding portable weather station within each microclimate. Atmometers were installed according to manufacturer instructions so that the top of the ceramic Bellani plate on the atmometer was 1 m above the ground. Grass reference evapotranspiration was obtained by covering the Bellani plate with the manufacturer supplied number 30 green canvas cover. Evaporation data from the atmometer were summed and recorded at 30-minute intervals by a datalogger (CR1000, Campbell Scientific Inc., Logan, UT) that was attached to the corresponding portable weather station.

Portable weather stations recorded meteorological variables necessary to calculate grass reference ET. Air temperature and relative humidity were obtained using a platinum resistance thermometer and capacitive chip, respectively, (HMP50, Vaisala, Inc., Helsinki, Finland). Wind speed and direction were obtained with a two-dimensional sonic anemometer (WindSonic1, Gill Instruments Ltd., Hampshire, England). Net radiation, was measured using a net radiometer (NR-Lite, Kipp & Zonen, Inc., The Netherlands). All meteorological data were measured at 1 Hz and stored at 30-minute intervals, using the same datalogger described above for the atmometer.

Data collected from the portable weather stations were used to calculate grass reference evapotranspiration using the FAO56-PM empirical model (Allen et al., 1998), described as:

$$PM_{ET} = \frac{0.408\Delta(R_n - G) + \gamma \frac{C_n}{T + 273} u_2 (e_s - e_a)}{\Delta + \gamma(1 + C_d u_2)} \quad [1]$$

where PM_{ET} is grass reference ET (mm 30 min^{-1}), Δ is the slope of the saturation vapor pressure curve (kPa °C^{-1}), R_n is net radiation (MJ m^{-2} 30 min^{-1}), G is soil heat flux density (MJ m^{-2} 30 min^{-1}), γ is the psychrometric constant (kPa °C^{-1}), T is the mean 30-minute air temperature at 2 m (°C), e_s is the saturation vapor pressure at air temperature T (kPa), e_a is the actual vapor pressure at 2 m (kPa), u is the wind speed (m s^{-1}) at 2 m, C_n is the numerator constant for the 30-minute time step, and C_d is the denominator constant for aerodynamic and surface resistances. All calculations were conducted according to Allen et al. (1998). Thirty-minute evapotranspiration values from the FAO56-PM model (PM_{ET}) and atmometer (AT_{ET}) were summed for 24 h periods.

Statistical Analysis

Data were analyzed using several statistical procedures. The PM_{ET} values were used as the reference for comparison to AT_{ET}. Regression analysis ($AT_{ET} = mPM_{ET} + b$) was conducted using the REG procedure of SAS (SAS Institute, Inc., Cary, NC) at $P < 0.05$, where "m" is the slope and "b" the dependent variable (AT_{ET}) intercept. Linear association between PM_{ET} and AT_{ET} was determined using the coefficient of determination (r^2). Paired *t*-tests were conducted to determine differences between AT_{ET} and PM_{ET} using the TTEST procedure (SAS Institute, Inc., Cary, NC) at $P < 0.05$. The null hypothesis for the *t*-test was that the difference between AT_{ET} and PM_{ET} values was zero.

Measures of difference between AT_{ET} and PM_{ET} were calculated. Root mean square error (RMSE), mean bias error (MBE), and mean percent error (%E) between AT_{ET} and PM_{ET} were calculated as:

$$\mathrm{RMSE} = \sqrt{\frac{1}{n}\sum_{i=1}^{n}\left(AT_{ET_i} - PM_{ET_i}\right)^2}\,, \qquad [2]$$

$$\mathrm{MBE} = \frac{1}{n}\sum_{i=1}^{n}\left(AT_{ET_i} - PM_{ET_i}\right), \text{ and} \qquad [3]$$

$$\%E = \sum\left(\frac{AT_{ET_i} - PM_{ET_i}}{PM_{ET_i}}\right)\times 100, \qquad [4]$$

where AT_{ET_i} is atmometer ET, PM_{ET_i} is FAO56-PM ET, n is the number of observations, and i is the ith observation.

An index of agreement (d) was used as a measure of association to overcome problems associated with RMSE and r^2, such as the presence of any outlying data, (Willmott, 1981; Legates and McCabe, 1999). Like the coefficient of determination, the index of agreement produces a value between 0 and 1, with values closer to 1 indicating better agreement between the atmometer and FAO56-PM model. The index of agreement was calculated as:

$$d = 1 - \left[\frac{\sum_{i=1}^{n}\left(AT_{ET_i} - PM_{ET_i}\right)^2}{\sum_{i=1}^{n}\left[\left|AT_{ET_i} - \overline{PM}_{ET}\right| + \left|PM_{ET_i} - \overline{PM}_{ET}\right|\right]^2}\right], \qquad [5]$$

where the overbar indicates overall mean ET, and all other variables have been previously defined.

Results and Discussion

Combined microclimate and open sward ET values from the atmometer and FAO56-PM equation exhibited good agreement (Fig. 2.1). The coefficient of determination was high (76%) however, the slope of the line, 0.80, and its AT_{ET} intercept, 1.04 mm d^{-1}, indicate that AT_{ET} performance may differ with varying PM_{ET} values (Fig. 2.1). Based on this regression analysis, AT_{ET} overestimates PM_{ET} when PM_{ET} is less than 5.2 mm d^{-1} and underestimated PM_{ET} when PM_{ET} was greater than 5.2 mm d^{-1}. Jiang et al. (1998) noted that AT_{ET} was less than Penman modeled ET when ET was greater than 4 mm d^{-1}. However, Gavilan and Castillo-Llanque (2009) observed more accurate AT_{ET} when PM_{ET} was greater than 5 mm d^{-1}. Overall, among all locations, mean AT_{ET} was 6% greater than PM_{ET} (Table 2.2). However, the %E was 23%, indicating that large differences between AT_{ET} and PM_{ET} were sometimes observed.

Differences between AT_{ET} and PM_{ET} varied from the open sward to within microclimates (Table 2.2). Open sward AT_{ET} and PM_{ET} demonstrated how these measurement techniques compare under an ideal setting. The open sward placement of the portable weather station and accompanying atmometer provided a large footprint area with little or no influence due to vegetation differences or structures. The open sward comparison between AT_{ET} and PM_{ET} produced a coefficient of determination of 88% and slope and intercept of 0.86 and 0.01 mm d^{-1}, respectively, indicating that there was a good relationship between AT_{ET} and PM_{ET} in the open sward (Fig. 2.2). Root mean square error at the open sward was 1.11 mm d^{-1}. This value is consistent with other reported values for RMSE using the FAO56-PM (Irmak et al., 2005; Gavilan and Castillo-Llanque, 2009; Knox et al., 2011). Similarly, Chen and Robinson (2009), comparing AT_{ET} to alfalfa reference evapotranspiration reported RMSEs as high as 1.9 mm d^{-1} and as low as 0.76 mm d^{-1}. Open sward mean AT_{ET} was 14% less than PM_{ET} (Table 2.2). Percent error, %E, was also –14% indicating that there may be less discrepancy between paired observations of AT_{ET} and PM_{ET} than what was observed when open sward and microclimate data were combined. This would indicate that the greatest variability is within microclimates.

The 14% underestimation of PM_{ET} by AT_{ET} at the open sward is comparable to other studies. Gavilan and Castillo-Llanque (2009), using the FAO56-PM equation, observed AT_{ET} to underestimate PM_{ET} by 9%. Irmak et al. (2005) also observed AT_{ET} to underestimate PM_{ET}, %E of –12 to –27.5%, comparable to %E = –14% in our study at the open sward (Table 2.2). Chen and Robinson (2009) observed AT_{ET} to underestimate alfalfa reference ET by 21%.

Within the microclimates, there was a good relationship between AT_{ET} and PM_{ET} (r^2 = 78%, Table 2.2). The slope of the regression line for AT_{ET} versus PM_{ET} was closer to a 1 to 1 slope than the same comparison in the open sward (Fig. 2.3). However, mean AT_{ET} was 22% greater than PM_{ET} within the microclimates, and %E was 42%. Greater variability among measurements of AT_{ET} and PM_{ET} within the microclimates may be responsible for the greater differences in mean ET between methods. Greater variability in ET measurements could be due to differences between the environmental conditions immediately surrounding the atmometer and each of the various sensors on the accompanying weather station. For example, differences in wind speed, air temperatures, solar radiation, or relative humidity at the locales of the atmometer evaporative surface and individual weather station sensors within each microclimate could have affected ET estimates differently for each method.

Previous research on the sensitivity of the FAO56-PM equation to changes in environmental variables by Kwon and Choi (2011) shows sensitivity in order of vapor pressure > wind speed > radiation. In their study, a ±20% change in vapor pressure altered PM_{ET} by ±22 to 32%, while the same change in wind speed (±20%) altered PM_{ET} by only ±12%. Irmak et al. (2006), using the ASCE Penman-Monteith equation (ASCE-EWRI, 2005) for PM_{ET}, found that

PM_{ET} was most sensitive to vapor pressure deficit (VPD) followed by wind speed. These sensitivities could contribute to greater variability between AT_{ET} and PM_{ET} within nonstandard sites, such as within microclimates, where environmental conditions may vary significantly.

To evaluate the effects of the environmental variables of wind speed, VPD, and net radiation on differences between AT_{ET} to PM_{ET}, the environmental variables were divided arbitrarily into classifications. Wind speed was divided into three classes, less than 1 m s^{-1}, 1-2 m s^{-1}, and greater than 2 m s^{-1}. Detailed statistics of the wind speed analysis are presented in Table 2.3. When wind speed was 1-2 m s^{-1}, AT_{ET} and PM_{ET} showed the best agreement (smallest RMSE, MBE, and %E) at the open sward. Within the microclimates, wind speeds < 1 m s^{-1} resulted in poor agreement, %E = 61%, between AT_{ET} and PM_{ET}. However, agreement improved as wind speed increased. When wind speed was > 2 m s^{-1}, the paired *t*-test showed no difference between AT_{ET} and PM_{ET} within microclimates. Regression analysis does not indicate a superb fit, $r^2 = 0.64$, within microclimates; however, the MBE (0.17 mm d^{-1}) when wind speed was > 2 m s^{-1} is quite small compared to the other conditions (Table 2.3). Chen and Robinson (2009) found the AT_{ET} to alfalfa reference ET ratio to become smaller as wind speed increased, especially at wind speeds, > 3 m s^{-1}, similar to this study. They observed their best agreements at low wind speeds, ≤ 1 m s^{-1}, whereas we observed very poor agreement between AT_{ET} and PM_{ET} at low wind speeds.

Vapor pressure deficit was divided into three classifications, less than 1 kPa, 1-2 kPa, and greater than 2 kPa. Statistical analysis results are presented in Table 2.4. Both open sward and microclimate AT_{ET} to PM_{ET} comparisons were affected by VPD. Mean AT_{ET} at the open sward was less than PM_{ET} for all three VPD classifications. Within the microclimates, however, AT_{ET} was greater than PM_{ET} for all three VPD classifications. Chen and Robinson (2009) found greater AT_{ET} underestimations of alfalfa reference ET at VPD < 0.72 kPa than at classifications above 0.72 kPa. This disagrees with our findings where the MBE showed that AT_{ET} underestimations at the open sward increased with increasing VPD and overestimations of AT_{ET} to PM_{ET} increased with increasing VPD within microclimates.

Net radiation was divided into two classifications, less than 5 MJ m^{-2} d^{-1} and greater than 5 MJ m^{-2} d^{-1}. Statistical analysis results are presented in Table 2.5. The sample size at the open sward was small for net radiation less than 5 MJ m^{-2} d^{-1}, n=13, and regression analysis shows very poor agreement between AT_{ET} and PM_{ET}, $r^2 = 0.14$, and a slope of 0.38. Total net radiation of less than 5 MJ m^{-2} d^{-1} in an open area is very low and is likely associated with rainy, cloud-covered days. Poor performance of atmometers under rainy conditions is well documented (Irmak et al., 2005; Chen and Robinson, 2009). When net radiation was greater than 5 MJ m^{-2} d^{-1} agreement was good between AT_{ET} and PM_{ET} at the open sward (%E = –13%) and within microclimates (%E = 16%). However, similar to vapor pressure deficit and wind speed, MBE showed that AT_{ET} underestimated PM_{ET} at the open sward for both classifications. Chen and Robinson (2009) observed greater variance between AT_{ET} and alfalfa reference ET at solar radiation less than 14.2 MJ m^{-2} d^{-1}. Faber (2004) and Jiang et al. (1998) observed AT_{ET} to be less on the backside of a hill, the shaded side not facing the sun, than AT_{ET} on the hilltop. It is likely that radiation was less on the backside of the hill than the side facing direct solar radiation, causing AT_{ET} to be less on the backside of the hill.

Conclusions

Accurate measurement of ET within microclimates could result in increased overall irrigation efficiency to turfgrass. The performance of atmometers was evaluated against the FAO-56 Penman-Monteith equation within microclimates and at an open sward. The atmometer underestimated PM_{ET} at the open sward but overestimated PM_{ET} within microclimates. At all levels of wind speed, VPD, and net radiation, AT_{ET} underestimated PM_{ET} at the open sward and overestimated PM_{ET} within microclimates. The best relationships between AT_{ET} and PM_{ET}, based on %E, were observed at wind speeds greater than 1 m s^{-1}, VPD greater than 2 kPa, and net radiation greater than 5 MJ m^{-2} d^{-1} at the open sward and within microclimates. Based on these findings, atmometers can provide reliable PM_{ET} estimates, providing practitioners a means to manage irrigation within microclimates.

References

Alam, M. and T.P. Trooien. 2001. Estimating reference evapotranspiration with an atmometer. Appl. Eng. Agric. 17(2):153-158.

Alig, R.J., J.D. Kline, and M. Lichtenstein. 2004. Urbanization on the US landscape: looking ahead in the 21st century. Landsc. Urban Plan. 69:219-234.

Allen, R.G., L.S. Pereira, D. Ross, and M. Smith. 1998. Crop evapotranspiration – guidelines for computing crop water requirements – FAO irrigation and drainage paper 56. Food and Agriculture Organization of the United Nations, Rome.

Altenhofen, J. 1985. A modified atmometer for on-farm ET determination.p.177-184. *In.* Advances in evapotranspiration. Proc. Natl. Conf. Adv. Evapotranspiration, Chicago, IL, 16-17 Dec. Am. Soc. Agric. Eng. St. Joseph, MI.

ASCE-EWRI. 2005. The ASCE Standardized Reference Evapotranspiration Equation. Environmental and Water Resources Institute (EWRI) of ASCE, Standardization of Reference Evapotranspiration Task Committee Final Rep. http://www.kimberly.uidaho.edu/water/asceewri/ascestzdetmain2005.pdf.

Bremer, D.J. 2003. Evaluation of microlysimeters used in turfgrass evapotranspiration studies using the dual-probe heat-pulse technique. Agron. J. 95(6):1625-1632.

Bremer, D.J., S.J. Keeley, A. Jager, and J.D. Fry. 2013. Lawn-watering perceptions and behaviors of residential homeowners in three Kansas (USA) cities: implications for water quality and quantity. Int. Turfgrass Soc. Res. J. 12:23-29.

Bremer, D.J., S.J. Keeley, A. Jager, J.D. Fry, and C. Lavis. 2012. In-ground irrigation systems affect lawn-watering behaviors of residential homeowners. HortTech. 22(5):651-658.

Broner, I. and R.A.P. Law. 1991. Evaluation of a modified atmometer for estimating reference ET. Irrig. Sci. 12:21-26.

Chen, F. and P.J. Robinson. 2009. Estimating reference crop evapotranspiration with ETgages. J. Irrig. Drain. Eng. 135(3):335-342.

Ervin, E.H. and A.J. Koski. 1997. A comparison of modified atmometer estimates of turfgrass evapotranspiration with Kimberly-Penman alfalfa reference evapotranspiration. Int. Turfgrass Soc. Res. J. 8:663-670.

Faber, B.A. 2004. Slope and aspect effect on evaporation as measured by atmometer. p.213-216. *In.* ed. R.L. Snyder. IV Intl. Symp. Irrigation Hort. Crops. Davis, CA, 1-6 Sept. ISHS Acta Hort, 664.

Feldhake, C.M., R.E. Danielson, and J.D. Butler. 1983. Turfgrass evapotranspiration. I. Factors influencing rate in urban environments. Agron. J. 75:824-830.

Gavilan, P. and F. Castillo-Llanque. 2009. Estimating reference evapotranspiration with atmometers in a semiarid environment. Agric. Water Manage. 96:465-472.

Irmak, S., J.O. Payero, D.L. Martin, A. Irmak, T.A. Howell. 2006. Sensitivity analyses and sensitivity coefficients of standardized daily ASCE-Penman-Monteith equation. J. Irrig. Drain. Eng. 132(6):564-578.

Irmak, S., M.D. Dukes, and M.J. Jacobs. 2005. Using modified Bellani plate evapotranspiration gauges to estimate short canopy reference evapotranspiration. J. Irrig. Drain. Eng. 131(2):164-175.

Jensen, M.E. 1983. Design and operation of farm irrigation systems. Am. Soc. Agric. Eng., St. Joseph, MI.

Jiang, H., J.D. Fry. And S.C. Wiest. 1998. Variability in turfgrass water requirements on a golf course. HortScience. 33(4):689-691.

Knox, J.W., J.A. Rodriguez-Diaz, and T.M. Hess. 2011. Estimating evapotranspiration by using atmometers for irrigation scheduling in a humid environment. J. Irrig. Drain. Eng. 137(11):685-691.

Kwon, H. and M. Choi. 2011. Error assessment of climate variables for FAO-56 reference evapotranspiration. Meteorol. Atmos. Phys. 112:81-90.

Legates, D.R. and G.J. McCabe Jr., 1999. Evaluating the use of "goodness-of-fit" measures in hydrologic and hydroclimatic model validation. Water Resour. Res. 35(1):233-241.

Ley, T.W., R.G. Allen, and R.W. Hill. 1996. Weather station siting effects on reference evapotranspiration. p.727-734. *In*. Camp, et al. (Eds) Evapotranspiration and irrigation scheduling. Proc. Int. Conf., San Antonio, TX. 3-6 Nov. Am. Soc. Agric. Eng. St. Joseph, MI.

Livingston, B.E. 1915. A modification of the Bellani porous plate atmometer. Science. 41(1067):872-874.

Magliulo, V., R. d'Andria, and G. Rana. 2003. Use of the modified atmometer to estimate reference evapotranspiration in Mediterranean environments. Agric. Water Manage. 62:1-14.

Milesi, C., S.W. Running, C.D. Elvidge, J.B. Dietz, B.T. Tuttle, and R.R. Nemani. 2005. Mapping and modeling the biogeochemical cycling of turf grasses in the United States. Environ. Mgt. 36(3):426-438.

Monteith, J.L. 1965. Evaporation and environment. p.205-234. *In.* The state and movement of water in living organisms, Symp. Soc. Exp. Biol. Vol. 19. Cambridge University Press, Cambridge, UK.

Morris, K. 2003. The national turfgrass research initiative. National Turfgrass Federation and National Turfgrass Evaluation Program, Beltsville, MD. 2 Aug. 2013. <http://www.turfresearch.org/pdf/turfinitiative.pdf>.

Qian, Y.L., J.D. Fry, S.C. Wiest, and W.S. Upham. 1996. Estimating turfgrass evapotranspiration using atmometers and the Penman-Monteith model. Crop Sci. 36(3):699-704.

Rosenberg, N.J., B.L. Blad, and S.B. Verma. 1983. Microclimate: the biological environment. John Wiley & Sons, Inc. New York, NY.

Skaggs, K.E. and S. Irmak. 2012. Analysis of mircoclimate data measured over grass and soybean canopy and their impacts on Penman-Monteith grass and alfalfa reference evapotranspiration. J Irrig. Drain. Eng. 138(2):120-134.

Willmott, C.J. 1981. On the validation of models. Phys. Geogr. 2(2):184-194.

Table 2.1. Evapotranspiration measurement dates for microclimate study locations at Manhattan, KS in 2010-2011and Wichita, KS in 2011.

Lawn	Location	Number of Microclimate Observation Days†
1	Manhattan, KS	46
2	Manhattan, KS	52
3	Manhattan, KS	33
4	Manhattan, KS	26
5	Manhattan, KS	24
6	Manhattan, KS	11
7	Wichita, KS	15
8	Wichita, KS	26
9	Wichita, KS	24
10	Wichita, KS	12

†N=269

Table 2.2. Mean atmometer and FAO56-PM evapotranspiration and statistical analysis of AT_{ET} to PM_{ET} comparison.

Location	n	AT_{ET}	PM_{ET}	RMSE†	MBE‡	%E§	d¶	*t*-test††
		---------------- mm d^{-1} ----------------						
Open Sward	132	4.73	5.48	1.11	-0.75	-14	0.96	***
Microclimates	269	3.94	3.23	1.25	0.71	42	0.91	***
All Locations	401	4.20	3.97	1.21	0.23	23	0.93	***

†RMSE is the root mean square error calculated as $\mathrm{RMSE} = \sqrt{\frac{1}{n}\sum_{i=1}^{n}\left(AT_{ET_i} - PM_{ET_i}\right)^2}$, in mm d^{-1}.

‡MBE is the mean bias error calculated as $\mathrm{MBE} = \frac{1}{n}\sum_{i=1}^{n}\left(AT_{ET_i} - PM_{ET_i}\right)$, in mm d^{-1}.

§%E is the mean percent error calculated as: $\%E = \sum\left(\frac{AT_{ET_i} - PM_{ET_i}}{PM_{ET_i}}\right)\times 100$.

¶d is the index of agreement calculated as $d = 1 - \left[\frac{\sum_{i=1}^{n}\left(AT_{ET_i} - PM_{ET_i}\right)^2}{\sum_{i=1}^{n}\left[\left|AT_{ET_i} - \overline{PM_{ET}}\right| + \left|PM_{ET_i} - \overline{PM_{ET}}\right|\right]^2}\right]$.

††Probability that AT_{ET} and PM_{ET} are significantly different from each other based on paired t-test at $P < 0.05$.
*** indicates significant difference at $P < 0.001$.

Table 2.3. Analysis of atmometer and FAO56-PM evapotranspiration by wind speed classification.

Location	n	AT_{ET}	PM_{ET}	RMSE†	MBE‡	%E§	d¶	*t*-test ††	m‡‡	b‡‡	r^2
		---------------- mm d^{-1} ----------------									
Wind Speed < 1 m s^{-1}											
Open Sward§§	2	4.45	4.10								
Microclimates	158	2.93	2.08	1.16	0.85	61	0.85	***	0.95	0.96	0.73
All Locations	160	2.95	2.11	1.16	0.85	60	0.85	***	0.94	0.97	0.73
Wind Speed 1-2 m s^{-1}											
Open Sward	32	4.02	4.26	0.51	-0.24	-6	0.99	**	0.99	-0.20	0.88
Microclimates	75	5.06	4.39	1.32	0.67	20	0.96	***	0.99	0.73	0.68
All Locations	107	4.75	4.35	1.14	0.40	12	0.96	***	1.00	0.40	0.68
Wind Speed > 2 m s^{-1}											
Open Sward	98	4.97	5.91	1.25	-0.94	-17	0.98	***	0.87	-0.27	0.89
Microclimates	36	6.02	5.85	1.46	0.17	2	0.97	NS	1.10	-0.42	0.64
All Locations	134	5.25	5.89	1.31	-0.64	-12	0.98	***	0.92	-0.15	0.78

†RMSE is the root mean square error calculated as $RMSE = \sqrt{\frac{1}{n}\sum_{i=1}^{n}\left(AT_{ET_i} - PM_{ET_i}\right)^2}$, in mm d^{-1}.

‡MBE is the mean bias error calculated as $MBE = \frac{1}{n}\sum_{i=1}^{n}\left(AT_{ET_i} - PM_{ET_i}\right)$, in mm d^{-1}.

§%E is the mean percent error calculated as: $\%E = \sum\left(\frac{AT_{ET_i} - PM_{ET_i}}{PM_{ET_i}}\right)\times 100$.

¶d is the index of agreement calculated as $d = 1 - \left[\frac{\sum_{i=1}^{n}\left(AT_{ET_i} - PM_{ET_i}\right)^2}{\sum_{i=1}^{n}\left[\left|AT_{ET_i} - \overline{PM}_{ET}\right| + \left|PM_{ET_i} - \overline{PM}_{ET}\right|\right]^2}\right]$.

††Probability that AT_{ET} and PM_{ET} are significantly different from each other based on paired t-test at $P < 0.05$.
‡‡Regression analysis ($AT_{ET} = mPM_{ET} + b$) where "m" is the slope of the line and "b" the y-axis intercept.
§§Statistical analyses were not conducted for comparisons at the open sward as there were only two observations.
***, **, and NS indicates significant difference at $P < 0.001$, $P < 0.01$, and not significant, respectively.

Table 2.4. Analysis of atmometer and FAO56-PM evapotranspiration by vapor pressure deficit (VPD) classification.

Location	n	AT_{ET}	PM_{ET}	RMSE†	MBE‡	%E§	d¶	*t*-test ††	m‡‡	b‡‡	r^2
		---------------- mm d^{-1}	----------------								
VPD < 1 kPa											
Open Sward	44	2.52	3.08	0.94	-0.56	-18	0.91	***	0.74	0.22	0.57
Microclimates	75	1.93	1.63	0.69	0.31	41	0.88	***	0.77	0.68	0.68
All Locations	119	2.15	2.16	0.79	-0.01	19	0.88	NS	0.65	0.74	0.62
VPD 1-2 kPa											
Open Sward	61	4.88	5.70	1.10	-0.81	-13	0.98	***	0.49	2.12	0.42
Microclimates	140	3.81	3.18	1.15	0.63	44	0.94	***	0.60	1.89	0.70
All Locations	201	4.14	3.94	1.13	0.19	27	0.94	*	0.53	2.05	0.70
VPD > 2 kPa											
Open Sward	27	7.98	8.89	1.36	-0.92	-9	0.99	***	0.55	3.10	0.48
Microclimates	54	7.06	5.58	1.93	1.48	36	0.96	***	0.72	3.06	0.57
All Locations	81	7.36	6.68	1.76	0.68	21	0.97	***	0.49	4.07	0.50

†RMSE is the root mean square error calculated as $\mathrm{RMSE} = \sqrt{\frac{1}{n}\sum_{i=1}^{n}\left(AT_{ET_i} - PM_{ET_i}\right)^2}$, in mm d^{-1}.

‡MBE is the mean bias error calculated as $\mathrm{MBE} = \frac{1}{n}\sum_{i=1}^{n}\left(AT_{ET_i} - PM_{ET_i}\right)$, in mm d^{-1}.

§%E is the mean percent error calculated as: $\%E = \sum\left(\frac{AT_{ET_i} - PM_{ET_i}}{PM_{ET_i}}\right)\times 100$.

¶d is the index of agreement calculated as $d = 1 - \left[\frac{\sum_{i=1}^{n}\left(AT_{ET_i} - PM_{ET_i}\right)^2}{\sum_{i=1}^{n}\left[\left|AT_{ET_i} - \overline{PM}_{ET}\right| + \left|PM_{ET_i} - \overline{PM}_{ET}\right|\right]^2}\right]$.

††Probability that AT_{ET} and PM_{ET} are significantly different from each other based on paired t-test at $P < 0.05$.
‡‡Regression analysis ($AT_{ET} = mPM_{ET} + b$) where "m" is the slope of the line and "b" the y-axis intercept.
***,*, and NS indicates significant difference at $P < 0.001$, $P < 0.05$, and not significant, respectively.

Table 2.5. Analysis of atmometer and FAO56-PM evapotranspiration by net radiation.

Location	n	ATET	PMET	RMSE†	MBE‡	%E§	d¶	*t*-test ††	m‡‡	b‡‡	r^2
		---------------- mm d^{-1} ----------------									
Rn < 5 MJ m-2 d^{-1}											
Open Sward	13	1.54	2.05	1.07	-0.51	-22	0.70	NS	0.38	0.77	0.14
Microclimates	104	2.16	1.24	1.16	0.92	81	0.63	***	1.43	0.40	0.63
All Locations	117	2.09	1.33	1.15	0.76	70	0.61	***	0.93	0.85	0.35
Rn > 5 MJ m-2 d^{-1}											
Open Sward	119	5.08	5.85	1.12	-0.78	-13	0.99	***	0.85	0.12	0.86
Microclimates	165	5.06	4.48	1.30	0.58	16	0.97	***	0.93	0.87	0.64
All Locations	284	5.07	5.06	1.23	0.01	4	0.98	NS	0.79	1.09	0.65

†RMSE is the root mean square error calculated as $\mathrm{RMSE} = \sqrt{\frac{1}{n}\sum_{i=1}^{n}\left(AT_{ET_i} - PM_{ET_i}\right)^2}$, in mm d^{-1}.

‡MBE is the mean bias error calculated as $\mathrm{MBE} = \frac{1}{n}\sum_{i=1}^{n}\left(AT_{ET_i} - PM_{ET_i}\right)$, in mm d^{-1}.

§%E is the mean percent error calculated as: $\%E = \sum\left(\frac{AT_{ET_i} - PM_{ET_i}}{PM_{ET_i}}\right)\times 100$.

¶d is the index of agreement calculated as $d = 1 - \left[\frac{\sum_{i=1}^{n}\left(AT_{ET_i} - PM_{ET_i}\right)^2}{\sum_{i=1}^{n}\left[\left|AT_{ET_i} - \overline{PM_{ET}}\right| + \left|PM_{ET_i} - \overline{PM_{ET}}\right|\right]^2}\right]$.

††Probability that AT_{ET} and PM_{ET} are significantly different from each other based on paired t-test at $P < 0.05$.
‡‡Regression analysis ($AT_{ET} = mPM_{ET} + b$) where "m" is the slope of the line and "b" the y-axis intercept.
*** and NS indicates significant difference at $P < 0.001$ and not significant, respectively.

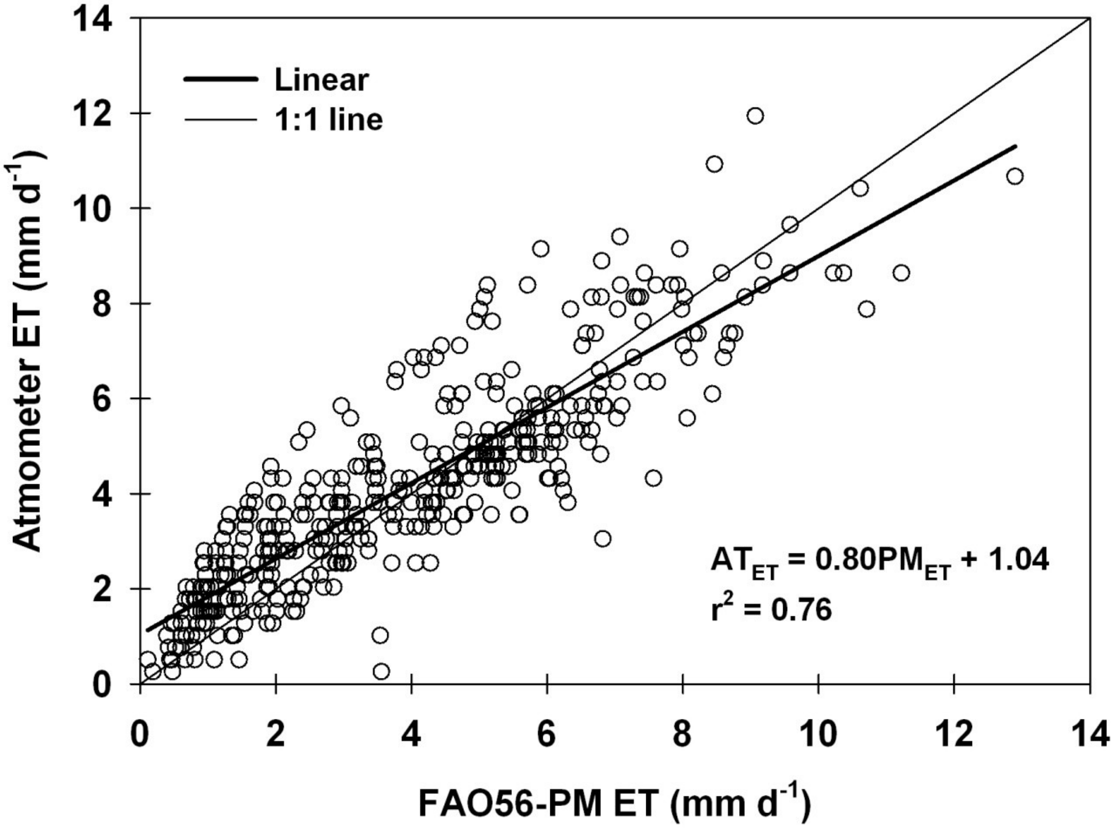

Figure 2.1. Comparison of daily estimated evapotranspiration from the atmometer (AT_{ET}) to the FAO56-Penman-Monteith model (PM_{ET}) at the open sward and microclimate locations, combined. Bolded line shows the modeled linear regression equation.

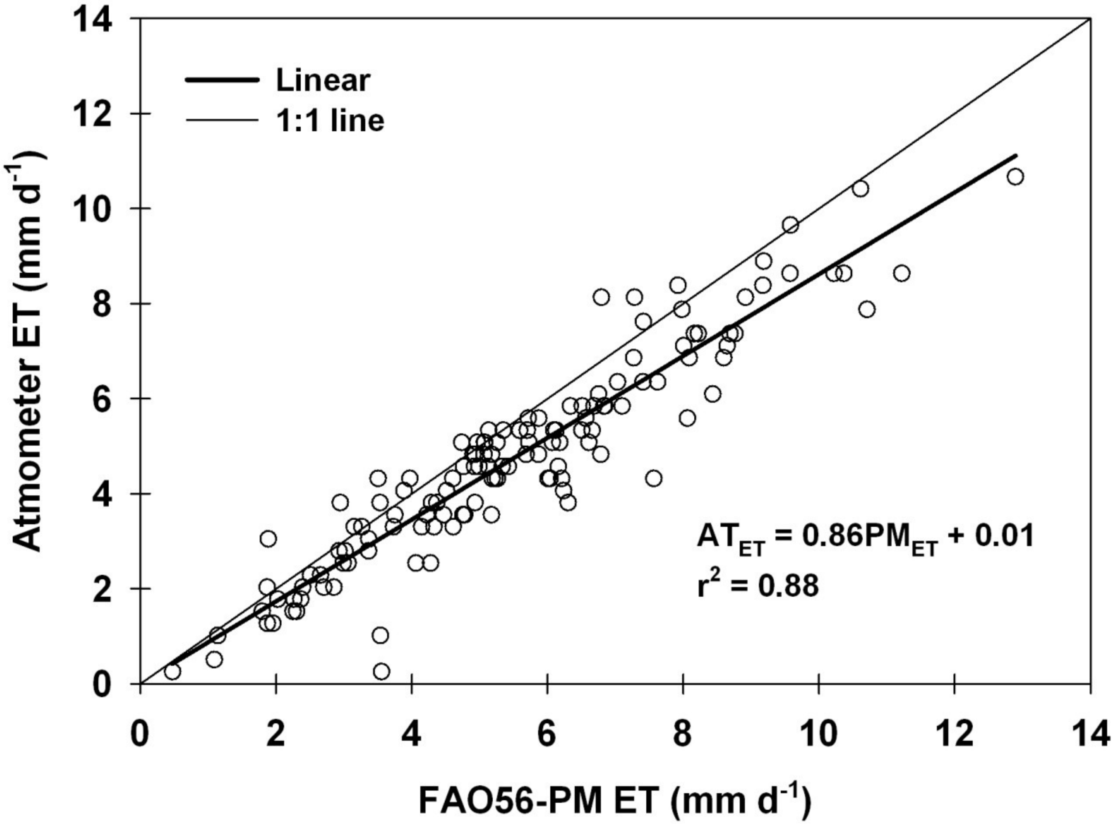

Figure 2.2. Comparison of daily estimated evapotranspiration from the atmometer (AT_{ET}) to the FAO56-Penman-Monteith model (PM_{ET}) at the open sward location, only. Bolded line shows the modeled linear regression equation.

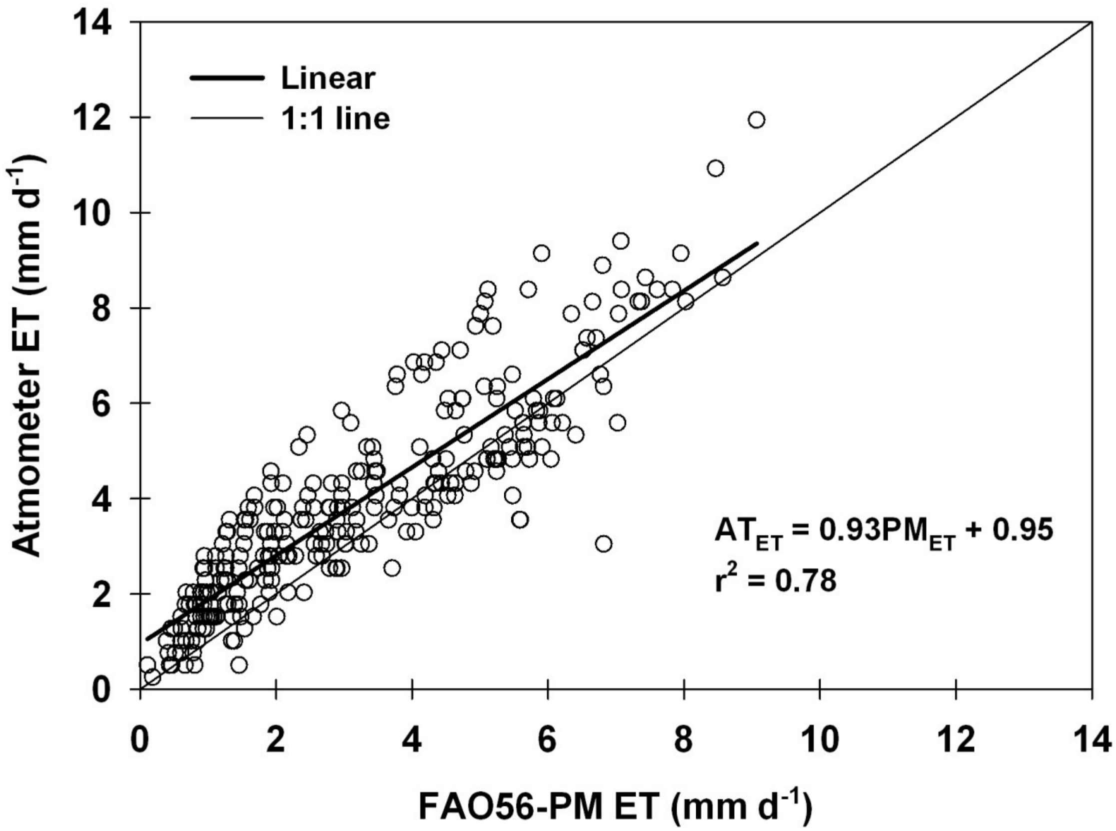

Figure 2.3. Comparison of daily estimated evapotranspiration from the atmometer (AT_{ET}) to the FAO56-Penman-Monteith model (PM_{ET}) at the microclimate locations, only. Bolded line shows the modeled linear regression equation.

Chapter 3 - Growth and Physiological Responses of *Zoysia* spp. Under Tree Shade

Abstract

'Meyer' zoysiagrass (*Zoysia japonica* Steudel) is commonly planted on home lawns and golf courses in the transition zone; however, poor shade tolerance limits its widespread use. This study was conducted to determine changes and differences in growth and physiology among selected *Zoysia* cultivars and progeny over a three-year period in the transition zone. The study was initiated in June 2010 at the Rocky Ford Turfgrass Research Center in Manhattan, KS. Soil type was a Chase silt loam. *Zoysia* genotypes were sodded in 0.37 m^2 plots and arranged in a randomized complete block with five replications under silver maple (*Acer saccharinum* L.) shade. Genotypes included 'Zorro' [*Z. matrella* (L.) Merrill.], 'Emerald' [*Z. japonica* × *Z. pacifica* (Goudswaard) Hotta & Kuroki], 'Meyer', Chinese Common (*Z. japonica*), and experimental progeny Exp1 (*Z. matrella* × *Z. japonica*), Exp2 and Exp3 [(*Z. japonica* × *Z. pacifica*) × *Z. japonica*]. 'Zorro' and 'Emerald' experienced winter injury, which negatively affected their performance. Tiller numbers decreased 50% in 'Meyer' from June 2010 to June 2012, but declines in [(*Z. japonica* × *Z. pacifica*) × *Z. japonica*] progeny were only 4% for Exp2 and 28% for Exp3. The progeny, Exp2 and Exp3, maintained high percent green cover throughout the study. In general, by the third year of evaluation, progeny of [(*Z. japonica* × *Z. pacifica*) × *Z. japonica*] had higher quality ratings and greater tiller numbers than 'Meyer', and may one day provide more shade-tolerant cultivar choices for transition zone turf managers.

Introduction

Shade stress is a major problem affecting the quality of an estimated 20 to 25% of all turfs (Beard, 1973; Dudeck and Peacock, 1992). Shading reduces incident solar radiation and alters the microclimate in which the turf grows (Beard, 1997). Turfgrass grown under shade suffers from reduced photosynthesis (Dudeck and Peacock, 1992; Qian et al., 1998), lower carbohydrate reserves (Burton et al., 1959; Qian et al., 1998; Bell and Danneberger, 1999; Atkinson et al., 2012), and reduced tillering (Qian et al., 1998; Ervin et al., 2002; Okeyo et al., 2011a). As a result, turfgrass grown under shade often declines in quality. Few turfgrass species have genotypes that are well adapted to shaded environments. Species with good to excellent shade tolerance are the fine fescues [*Festuca* spp.], rough bluegrass [*Poa trivialis* (L.)], St. Augustinegrass [*Stenotaphrum secundatum* (Walt.) O. Kuntze], and zoysiagrass [*Zoysia* spp. (Willdenow)] (Beard, 1973; Turgeon, 2005).

Zoysiagrass is a sod-forming warm-season perennial turfgrass indigenous to the Pacific Rim (Anderson, 2000). There are eleven species in the *Zoysia* genus, of which three are used as a turfgrass: *Z. japonica*, *Z. matrella*, and *Z. pacifica* (Engelke and Anderson, 2003). In the United States, zoysiagrass is used extensively on golf courses and home lawns throughout the transition zone. The lower input requirements of zoysiagrass compared with other available turfgrasses make it a desirable choice for use as a turfgrass in this region.

Zoysiagrasses vary in shade tolerance. In general, *Z. matrella* cultivars and 'Emerald' (*Z. japonica* x *Z. pacifica*) are considered more shade tolerant than *Z. japonica* cultivars (Fry and Huang, 2004; Sladek et al., 2009; Okeyo et al., 2011a; Wherley et al., 2011). 'Meyer' Z*oysia* has been the primary zoysiagrass used in the transition zone since its release in 1951, mainly due to its excellent cold hardiness (Grau and Radko, 1951). However, 'Meyer' performs poorly under moderate to dense shade (Riffel et al., 1995; Ervin et al., 2002; Sladek et al., 2009). This is problematic on golf courses and home lawns with a considerable amount of shade. Often 'Meyer' is replaced with *Z. matrella* cultivars or 'Emerald', which suffer winter injury and can only be used in the southernmost part of the transition zone.

Since 2004, researchers at Kansas State University (Manhattan, KS) and Texas A&M University (Texas AgriLife Research and Extension Center at Dallas, TX) have collaborated to develop zoysiagrass cultivars with excellent quality and freeze tolerance. In an effort to produce improved zoysiagrasses, researchers crossed lines of (*Z. japonica* × *Z. pacifica*) and *Z. matrella* with *Z. japonica* lines. Their goal was to develop cultivars with excellent density and a fine leaf texture like that of *Z. matrella*, but with freezing tolerance equal to or better than that of 'Meyer'. Over 600 progeny from the aforementioned crosses have been evaluated for quality and winter survival at the Rocky Ford Turfgrass Research Center at Manhattan, KS (Fry et al., 2008; Okeyo et al., 2011b). Evaluation of several of these grasses indicates that progeny from [*Z. matrella* × *Z. japonica*] or [(*Z. japonica* × *Z. pacifica*) × *Z. japonica*] exhibited superior stolon production under natural shade compared to 'Meyer' (Okeyo et al., 2011a) and have a freezing tolerance equal to that of 'Meyer' (Okeyo et al., 2011b).

Objective

The long-term shade tolerance of these high performing progeny has not been evaluated. Identifying genotypes with improved shade tolerance compared to 'Meyer' and characteristics aiding survival under dense shade will help lead to improved zoysiagrasses for the transition zone. This study was conducted to determine changes and differences in growth and physiology among selected *Zoysia* cultivars and progeny grown under a natural shade environment over a three-year period in the transition zone.

Materials and Methods

This study was initiated in June 2010 at the Rocky Ford Turfgrass Research Center at Manhattan, KS. Soil type was a Chase silt loam (fine, montmorillonitic, mesic, Aquic, Argiudoll) with pH 5.7, 3.3% organic matter, 48 mg kg^{-1} P, and 295 mg kg^{-1} K determined prior to planting (Soil Testing Laboratory, Kansas State University, Manhattan, KS).

Zoysiagrass was planted as plugs in flats in the greenhouse to establish sod pieces measuring 61 by 30.5 cm. Sod was planted in the field as 0.37 m^2 plots on 10 June 2010. Plots were fertilized at planting with 5 g N m^{-2} using an 18N-20P-0K fertilizer, were maintained at a 7 cm mowing height, and received 5 g N m^{-2} 46N-0P-0K annually. Irrigation was applied to prevent severe drought stress.

Seven genotypes were selected for this study: the cultivars Zorro (*Z. matrella*), Emerald (*Z. japonica* × *Z. pacifica*), Meyer (*Z. japonica*), and Chinese Common (*Z. japonica*) and the experimental progeny Exp1 (*Z. matrella* × *Z. japonica*), Exp2 and Exp3 [(*Z. japonica* × *Z. pacifica*) × *Z. japonica*]. The experimental progeny have been previously evaluated and are considered to have excellent freeze tolerance at the study site.

Data collected during the growing season included leaf extension rate (mm d^{-1}), tiller density (tillers m^{-2}), leaf width (mm), visual quality, fall color retention, spring green-up, percentage green cover, and carbon dioxide flux rates. Visual turfgrass quality was rated on a 1 to 9 scale (1 = poor, 6 = minimally acceptable, 9 = superior). Fall color retention and spring green-up were also visually evaluated on 15 Nov. 2010, 23 May and 31 Oct. 2011, 2 April and 4 Nov. 2012, on a 1 to 9 scale (1 = straw brown, 6 = minimally acceptable color, and 9 = dark green).

Carbon dioxide exchange rates were measured during the growing season on a turf area basis using a custom photosynthesis chamber (Lewis, 2010). Net ecosystem exchange (NEE, P_g

– R_c – R_s) and dark respiration ($R_c + R_s$) measurements were obtained from the sunlit and shaded chamber measurements, respectively, where P_g is gross canopy photosynthesis, R_c is canopy respiration, and R_s is soil respiration (Bremer and Ham, 2005). In this paper, as in Bremer and Ham (2005), positive values are used for P_g, R_c, and R_s. However, unlike Bremer and Ham (2005), because we recorded the sunlit measurement as a negative value, P_g was calculated by taking the absolute value of the sunlit minus the shaded measurement (i.e. |sunlit – shaded|). The sunlit measurement includes CO_2 contributions from plant and soil respiration along with plant CO_2 uptake via photosynthesis, while the shaded measurement includes CO_2 contributions only from plant and soil respiration.

Measurement of carbon dioxide exchange rates under natural tree shade can be troublesome. The presence of respiring tree roots near the soil surface and sun flecks that spatially alter photosynthetic rates can contribute to considerable variability in CO_2 exchange rate measurements. Consequently, observations from the raw data indicated that outliers might be present. To check for the presence of outliers, CO_2 exchange rate values were subjected to quartile analysis. The upper boundary was defined as Q3 + k(Q3-Q1) and the lower boundary as Q1 – k(Q3-Q1), where Q3 and Q1 are the 75 and 25% quartiles, respectively, and k is a multiplication coefficient affecting the conservativeness of the test that is commonly set between 1 and 3 (Frigge et al., 1989). To ensure that only highly unusual data were removed, a value of k=3 was utilized for conservativeness. Outlying data were deleted from the dataset. The process of removing outliers resulted in the data becoming unbalanced. Therefore, means were calculated using the least squares means method.

Beginning in 2011, a lighted camera box was used to evaluate percentage green cover (Richardson et al., 2001). The lighted camera box contained four compact fluorescent light bulbs (model CF13EL/MICRO/C/865/BL2; Sylvania, Danvers, MA). Color temperature at the grass surface was found to be 5,200 K using a color temperature meter (model C-500, Sekonic Corporation, North White Plains, NY). Digital images were obtained with a Nikon D5000 (Nikon Corporation, Tokyo, Japan) digital camera mounted on the light box. Camera shutter speed was 1/400 s, aperture F4.5, and focal length 26 mm. Digital images were analyzed for percentage green cover using the "Turf Analysis" macro (Karcher and Richardson, 2005) for SigmaScan Pro 5.0 (SPSS, Inc., Chicago, IL) with hue and saturation thresholds of 50-107 and 0-100, respectively.

An on-site weather station, positioned in full sun within 100 m of the study area, recorded average air temperature, 2 m above the ground, at hourly intervals and maximum and minimum air temperatures daily. Photosynthetically active radiation was also collected at hourly intervals using a quantum sensor (LI-190, LiCor, Inc., Lincoln, NE).

Plots were arranged along the north side of a mature line of silver maple trees. Photosynthetically active radiation under the shade was measured hourly, for 24h periods, with an automated ceptometer (AccuPAR LP-80, Decagon Devices, Inc., Pullman, WA) at three locations within the study area on cloud-free days on 10, 13, and 19 August 2012. Photosynthetically active radiation was found to be reduced by 91% under the tree shade compared to full sun.

Statistical Analysis

Experimental design was a randomized complete block with 5 replications. Zoysiagrass genotype (Chinese Common, 'Emerald', 'Meyer', 'Zorro', Exp1, Exp2, and Exp3) was the single treatment factor. Data were subjected to analysis of variance ($P < 0.05$) using the PROC GLM procedure (SAS Institute Inc., Cary, NC). Where appropriate, means were separated using Fisher's protected LSD at $P < 0.05$.

Results and Discussion

Turfgrass Quality

Visual turfgrass quality was rated from June through September in each of the three study years, 2010-2012. Significant differences were observed among the genotypes on all rating dates (Table 3.1). In 2010, turfgrass quality was acceptable for all genotypes. 'Emerald', 'Zorro', and Exp2 exhibited the highest turfgrass quality on the last rating date, 30 September, in 2010.

In June 2011 'Emerald' and 'Zorro' had the lowest turfgrass quality ratings. 'Emerald' and 'Zorro' are considered southern adapted zoysiagrasses and are not winter hardy in Manhattan, KS. During the winter of 2010-2011, minimum air temperature was -13.4, -21.6, and -23.0°C during the months of December 2010, January 2011, and February 2011, respectively (Fig. 3.1). Though the experimental progeny had been evaluated for winter hardiness, Exp1 appeared to experience some winter injury. The stress of growing under the shade may not have allowed Exp1 to acclimate fully to cold temperatures, resulting in winter injury. During the summer of 2011, 'Emerald' and 'Zorro' did recover somewhat but quality ratings remained lower than most other genotypes. Exp1 recovered sufficiently to attain minimally acceptable quality by August 2011. Progeny Exp2 and Exp3, and 'Meyer' were the top performers in 2011 with Exp2 consistently having the highest rating.

The winter of 2011-2012 was particularly mild (Fig. 3.1) and no winter injury was observed. Progeny Exp2 and Exp3, and 'Emerald' maintained superior quality ratings throughout the summer of 2012. Chinese Common and 'Meyer' quality ratings continued to decline throughout the summer of 2012. In August 2012, turfgrass damage due the bluegrass billbug (*Sphenophorus parvulus* Gyllenhal) was observed. The damage was most notable on Exp2 and 'Meyer', causing their quality ratings to decline from July to August whereas the quality rating among the others stayed relatively the same or increased. However, by the end of the summer the progeny Exp2 and Exp3, and the cultivars 'Emerald' and 'Zorro', all had quality ratings greater than the minimally acceptable level of 6.0.

Few studies have investigated zoysiagrass quality under tree shade (Riffell et al., 1995; Wherley et al., 2011). Riffell et al. (1995) found 'Meyer' to be one of the poorest performers while 'Emerald' performed very well. In our study 'Emerald' showed an overall increase in visual quality during each of the three growing seasons, whereas the visual quality of 'Meyer' usually decreased. The resource utilization (such as carbohydrate use or photosynthetic capacity) of 'Emerald' may be superior to that of 'Meyer' allowing it to persist for longer periods under dense shade. Wherley et al. (2011) concluded that *Z. matrella* genotypes might be better adapted to heavy shade than *Z. japonica* types, like 'Meyer', under 89% reduced light natural tree shade. Both studies were conducted at Dallas, TX, a climate much different from our study site. The extended growing season and milder winters of the southern United States would likely result in differences in turf performance compared to Manhattan, KS.

Tiller Density

Tiller density was evaluated from June through September in all three study years, 2010-2012. Each month, tiller density was adjusted to represent the percentage of June 2010 tiller density. No differences were observed among genotypes for tiller density in 2010 (Table 3.2). The August 2010 tiller density change shows that no genotype declined more than 15% prior to the onset of autumn.

Tiller density change decreased markedly from September 2010 to June 2011 (Table 3.2). As discussed previously, the winter of 2010-2011 was very cold and winter injury was observed on 'Emerald', 'Zorro', and Exp1. The extreme cold temperatures and the shade stress may have created an interaction resulting in some of the genotypes being less acclimated to the cold temperatures than they would otherwise have been in full sun. Progeny Exp2 exhibited a decline in tiller density of 8% whereas that of all other genotypes declined 17 to 62%. However, tiller density increased in all genotypes, except Chinese Common, from June 2011 to August 2011. This shows that the zoysiagrasses in this study do have potential to recuperate during the summer months, even when PAR is reduced over 90%. Progeny Exp2 and 'Meyer' showed the greatest improvement and had tiller density of 90 and 76%, respectively, by August 2011.

The winter of 2011-2012 was milder and the spring warmer than the previous year (Fig. 3.1). Most genotypes exhibited their highest tiller counts of 2012 earlier in the summer than in 2011. The extended spring due to mild winter temperatures and warm spring temperatures (Fig. 3.1) may have allowed the zoysiagrasses to grow more rapidly in late spring and early summer. However, that may also have resulted in more plant tissue to maintain, and indirectly caused a decline in tiller density change earlier in 2012 than what was observed in 2011.

Leaf Extension Rate

Leaf extension rate was measured July through September 2010, June through September 2011, and June through August 2012. Significant differences were observed on five of the ten evaluation dates (Table 3.3). Overall, leaf extension rate reached its maximum during early to midsummer each year. Chinese Common consistently had the greatest leaf extension rate and exhibited the greatest decline in quality and tiller density throughout the season each year indicating that it may have used large amounts of its stored carbohydrates for leaf extension, resulting in decline of the turfgrass stand. The experimental progeny Exp2 and Exp3 maintained high leaf extension rates but also showed less quality and tiller density decline over the duration of the experiment than Chinese Common and Exp1. This indicates that Exp2 and Exp3 may use less energy for leaf extension or cell maintenance respiration resulting in better turfgrass quality and density.

Often under shade, an increased leaf length is observed (Qian et al., 1997; Qian et al., 1998; Wherley et al., 2011). In a shaded environment, energy stores are already decreased (Burton et al., 1959; Qian et al., 1998; Bell and Danneberger, 1999) therefore extra energy used for excessive leaf extension may prove detrimental to the turfgrass stand. Wherley et al. (2011) observed that the zoysiagrass cultivars that performed best under shade had the shortest leaf extension. This is in contrast to our study where Exp2 and Exp3 often had high leaf extension rates but were top performers. Leaf extension rate may also reflect the energy efficiency of the turfgrass and its ability to utilize stored energy for plant growth. Turfs that consistently use energy more efficiently for leaf extension purposes may persist under dense shade while those using energy less efficiently may exhibit turfgrass quality decline.

Leaf Width

Leaf width was measured July through September 2010, June through September 2011, and June through August 2012. Significant differences were observed on all measurement dates (Table 3.4). 'Zorro' and 'Emerald' consistently had the narrowest leaf blades while Chinese Common and 'Meyer' had the widest. For unknown reasons, leaf width increased 0.3 to 1.4 mm from September 2010 to June 2011. However, this was not observed from September 2011 to June 2012.

Leaf width is the defining characteristic of turfgrass texture. In general, *Z. japonica* genotypes have a coarser texture than the more desired finer texture of *Z. matrella* and *Z. pacifica* genotypes. Data from this study resulted in a similar conclusion as Chinese Common and 'Meyer' consistently had the greatest leaf width. The experimental progeny were often intermediate to the coarser *Z. japonica* types and finer 'Zorro' and 'Emerald'.

Leaf width has been reported to decrease in turfgrass grown under shade (Wilkinson and Beard, 1974; Winstead and Ward, 1974). This may be due to cell elongation preventing the widening of the leaf blade. In this study, the overall mean leaf width for each month did decline somewhat during each growing season. However, a decline was not observed for each genotype. Peacock and Dudeck (1993) and Winstead and Ward (1974) also reported a decline in leaf blade width. on St. Augustinegrass exposed to different light intensities. Tree shade filters most of the red portion of the spectrum out of the light penetrating the canopy (Bell et al., 2000) causing a smaller red to far-red light ratio than in full sun. This altered red to far-red light ratio could result in plant morphological changes such as decreased leaf width and increased leaf elongation.

Percentage Green Cover

Percentage green cover was evaluated monthly from June through September in 2011 and 2012, with additional measurements taken in May and October 2011, and April and November 2012. Significant differences among genotypes were observed on all dates (Table 3.5). Percentage green cover was greatest during late summer in 2011 and early summer in 2012. The difference may be due to the warmer spring temperatures in 2012 than in 2011. The earlier peak in green cover in 2012, which may have been due to warmer spring temperatures than in 2011, may have posed an energy problem for the turfgrass stand. More green tissue earlier in the season may result in greater stand loss because the turfgrass cannot maintain such quantities of phytomass in shade for a more extended time, as was seen in 2012 as opposed to 2011.

Chinese Common, 'Meyer', and Exp2 had the greatest green cover in May 2011, and 'Meyer' and Exp2 the greatest cover in April 2012. However, the southern adapted genotype

'Zorro' had the greatest green cover in October 2011, and 'Emerald' and 'Zorro' the greatest cover in November 2012. The superior adaptation to shade is seen with 'Emerald' and 'Zorro' as they performed very well when winter injury was not observed. However, progeny Exp2 and Exp3 both exhibited high percent coverage through much of the study indicating that they possess excellent shade tolerance characteristics.

Trappe et al. (2011) measured the green coverage of several zoysiagrass cultivars under 49% artificial shade in the field at Fayetteville, AR. They found green coverage of 'Meyer', 'Zorro', and 'Diamond' to be greater than 90% after 2 years of shading. In our study, only Exp2 exceeded 90% green coverage during the two years of green coverage evaluation. Greater shading intensity in our study may be responsible for the differences. Because tree leaves filter the photosynthetically important red and blue wavelengths before it reaches the turf, lower light quality may also have contributed to less green coverage in our study. 'Meyer', which is typically considered shade intolerant, may not have been affected by the 49% shading and green coverage may not decline unless shading intensity is increased. Trappe et al. (2011) also maintained their plots at a much lower cutting height (1.3 cm) than in our study (7 cm).

Fall Color

Fall color was rated on 15 November 2010, 31 October 2011, and 4 November 2012. Significant differences were observed for each rating date (Table 3.6). 'Emerald' and 'Zorro' had the highest color rating on each date. Both of these cultivars are southern adapted zoysiagrasses and are not considered winter hardy at the study site. Dunn et al. (1993), in central Missouri, observed increased winter injury on a southern adapted zoysiagrass genotypes when fall green color was enhanced by late fall fertilization. The cold tolerant 'Meyer' did not show any winter injury in their study. The extended green color of these two grasses may make them more vulnerable to winter injury. Extended fall color is a desirable characteristic as extended green color along with winter hardiness is preferred.

Spring Color

Spring color was rated on 23 May 2011 and 2 April 2012. Significant differences were observed among genotypes in both years. Chinese Common, 'Meyer', and Exp2 all exhibited the highest spring color rating in both years (Table 3.7). The rapid green-up of Exp2 may aid its tolerance to shade. Rapid green-up may result in the turf being vulnerable to injury from late spring freezes. However, early green-up may not be problematic for cold tolerant genotypes. Greening-up earlier than the other genotypes may allow the turf to utilize greater irradiance as the tree canopy may not be fully enclosed.

Carbon Dioxide Exchange Rate

Carbon dioxide exchange rate measurements were made on one day in mid-season of each year on 22, 14, and 27 July in 2010, 2011, and 2012, respectively. For unknown reasons, no significant differences were detected for NEE, dark respiration, or gross photosynthesis on any of the dates. Nevertheless, differences in CO_2 exchange rates among genotypes in this study may be biologically relevant and could indicate physiological differences among the genotypes in this study in relation to their shade tolerance.

The establishment year, 2010, provided the best opportunity to assess the performance of these turfgrasses, based on carbon dioxide exchange rate, because density or quality had not yet substantially declined, as they did in later years. Presumably, greater P_g during the establishment year may help indicate which genotypes will perform better long-term. During the establishment year, P_g was much lower for 'Meyer' and Exp1 than the other genotypes (Table 3.8). Both 'Meyer' and Exp1 had significantly lower mid-season (July) turfgrass quality ratings (Table 3.1) and tiller density (Table 3.2) in 2012. By the final year of the study, 2012, differences in P_g were small among the genotypes. However, notable differences were present for net ecosystem exchange and dark respiration over the three-years. The greatest NEE and dark respiration (e.g. July 2012, Table 3.8) was frequently observed on the genotypes with the greatest tiller density percentage (Table 3.2), such as 'Emerald', Exp2, and Exp3. Those genotypes with the greatest phytomass should be expected to have a greater dark respiration than those with less phytomass. Qian et al. (1998) made a similar observation on 'Diamond' zoysiagrass treated with trinexapac-ethyl. They observed greater dark respiration on trinexapac-ethyl plots than untreated plots in a greenhouse after 34 weeks under 88% shade. They attributed this response to increased living tissue (i.e. greater tiller density and phytomass) in the trinexapac-ethyl treated plots than in the untreated control.

The survival of these zoysiagrasses under heavy shade relies partially upon the use of sunflecks through the tree canopy to provide sufficient energy for plant growth and maintenance. Ögren and Sundin (1996) found differences in sunfleck use efficiency among several species. They found that this difference might be related to the ratio of electron transport capacity to carboxylation capacity or their rate of photosynthetic induction. It is possible there may be a similar response from the zoysiagrasses used in this study. Further research is needed to investigate this possibility.

Conclusions.

Zoysiagrass use throughout the transition zone has been limited by adaptation to cold temperatures and shade tolerance. The response to tree shade of four zoysiagrass cultivars and three experimental progeny over a three-year period were evaluated. The cold tolerant genotypes, 'Meyer' and Chinese Common, both exhibited declining turfgrass quality and density during the course of the study. The shade tolerant southern adapted cultivars,' Emerald' and 'Zorro', both performed well but exhibited much injury after a cold winter, such as 2010-2011. The experimental progeny Exp1 exhibited winter injury to a lesser degree but was unable to recover as well as the southern adapted types. Two of the [(*Z. japonica* × *Z. pacifica*) × *Z. japonica*] progeny, Exp2 and Exp3, both exhibited excellent tolerance to shade. Progeny Exp3 was a steady performer, and exhibited no decline in turfgrass quality over the three-year study. Progeny Exp2 was the top performer of this study. Its turfgrass quality ratings demonstrated little change over this three-year study and tiller density remained high in the final year of the study, prior to the billbug damage. Overall, turfgrass quality and tiller density did decline over time with variability exhibited among the genotypes studied. The [(*Z. japonica* × *Z. pacifica*) × *Z. japonica*] experimental progeny in this study may have improved shade tolerance over the other *Zoysia* cultivars evaluated.

References

Anderson, S. 2000. Taxonomy of *Zoysia* (Poaceae): Morphological and molecular variation. Ph.D. diss. Texas A&M University, College Station, TX.

Atkinson, J.L., L.B. McCarty, H. Liu, J. Faust, and J.E. Toler. 2012. Diamond zoysiagrass golf green response to reduced light environments with the use of trinexapac-ethyl. Agron. J. 104(4):847-852.

Beard, J.B. 1973. Turfgrass: science and culture. Prentice Hall, Englewood Cliffs, NJ.

Beard, J.B. 1997. Shade stress and adaptation mechanisms of turfgrasses. Int. Turfgrass Soc. Res. J. 8:1186-1195.

Bell, G.E. and T.K. Danneberger. 1999. Temporal shade on creeping bentgrass turf. Crop Sci. 39(4):1142-1146.

Bell, G.E., T.K. Danneberger, and M.J. McMahon. 2000. Spectral irradiance available for turfgrass growth in sun and shade. Crop Sci. 40(1):189-195.

Bremer, D.J. and J.M. Ham. 2005. Measurement and partitioning of in situ carbon dioxide fluxes in turfgrasses using a pressurized chamber. Agron. J. 97(2):627-632 [errata: 98(5):1375].

Burton, G.W., J.E. Jackson, and F.E. Knox. 1959. The influence of light reduction upon the production, persistence and chemical composition of Coastal bermudagrass, *Cynodon dactylon*. Agron. J. 51(9):537-542.

Dudeck, A.E. and C.H. Peacock. 1992. Shade and turfgrass culture. *In.* D.V. Waddington et al. (eds.) Turfgrass. ASA Monogr. 32. ASA,CSSA, SSSA, Madison, WI.

Dunn, J.H., D.D. Minner, B.F. Fresenburg, and S.S. Bughrara. 1993. Fall fertilization of zoysiagrass. Int. Turfgrass Soc. Res. J. 7:565-571.

Engelke, M.C. and S. Anderson. 2003. Zoysiagrasses (*Zoysia* spp.). p. 271-285. *In* M.D. Casler and R.R. Duncan (eds). Turfgrass biology, genetics, and breeding. John Wiley & Sons, Hoboken, NJ.

Ervin, E.H., C.H. Ok, B.S. Fresenburg, and J.H. Dunn. 2002. Trinexapac-ethyl restricts shoot growth and prolongs stand density of 'Meyer' zoysiagrass fairway under shade. HortScience. 37(3):502-505.

Frigge, M., D.C. Hoaglin, and B. Iglewicz. 1989. Some implementations of the boxplot. Am. Stat. 43(1):50-54.

Fry, J.D. and B. Huang. 2004. Applied Turfgrass Science and Physiology. John Wiley & Sons. Hoboken, NJ.

Fry, J.D., Q. Zhang, D. Okeyo, M. Engelke, and D. Genovesi. 2008. Improved Zoysia cultivar could have use in transition zone. TurfGrass Trends, Golfdom, Cleveland, OH. p. 58,60-61.

Grau, F.V. and A.M. Radko. 1951. Meyer (Z-52) Zoysia. USGA J. Turf Manage. 4:30-31.

Karcher, D.E. and M.D. Richardson. 2005. Batch analysis of digital images to evaluate turfgrass characteristics. Crop Sci. 45:1536-1539.

Lewis, J.D. 2010. Carbon, nitrogen, and water fluxes from turfgrass ecosystems. Ph.D. diss. Kansas State Univ., Manhattan, KS.

Okeyo, D.O., J.D. Fry, D.J. Bremer, A. Chandra, A.D. Genovesi, and M.C. Engelke. 2011a. Stolon growth and tillering of experimental zoysiagrasses in shade. HortScience. 46(10):1418-1422.

Okeyo, D.O., J.D. Fry, D. Bremer, C.B. Rajashekar, M. Kennelly, A. Chandra, D.A. Genovesi, and M.C. Engelke. 2011b. Freezing tolerance and seasonal color of experimental zoysiagrasses. Crop Sci. 51(6):2858-2863.

Ögren, E. and U. Sundin. 1996. Photosynthetic responses to variable light: a comparison of species from contrasting habitats. Oecologia. 106(1):18-27.

Peacock, C.H. and A.E. Dudeck. 1993. Response of St. Augustinegrass cultivars [*Stenotaphrum secundatum* (Walt.) Kuntze] to shade. Int. Turfgrass Soc. Res. J. 7:657-663.

Qian, Y.L. and M.C. Engelke. 1997. Evaluation of zoysiagrass genotypes for shade tolerance. Texas Turfgrass Res. Rep. 97-24:1-11.

Qian, Y.L., M.C. Engelke, M.J.V. Foster, and S. Reynolds. 1998. Trinexapac-ethyl restricts shoot growth and improves quality of 'Diamond' zoysiagrass under shade. HortScience. 33(6):1019-1022.

Richardson, M.D., D.E. Karcher, and L.C. Purcell. 2001. Quantifying turfgrass cover using digital image analysis. Crop Sci. 41:1884-1888.

Riffell, S.K., M.C. Engelke, and S.J. Morton. 1995. Performance of three warm-season turfgrasses cultured in shade: Zoysiagrass. Texas Turfgrass Res. Rep. 95-11:60-65.

Sladek, B.S., G.M. Henry, and D.L. Auld. 2009. Evaluation of zoysiagrass genotypes for shade tolerance. HortScience. 44(5):1447-1451.

Trappe, J.M., D.E. Karcher, M.D. Richardson, and A.J. Patton. 2011. Shade and traffic tolerance varies for bermudagrass and zoysiagrass cultivars. Crop Sci. 51(2):870-877.

Turgeon, A.J. 2005. Turfgrass management. 7th ed. Pearson Prentice Hall, Upper Saddle River, NJ.

Wherley, B.G., P. Skulkaew, A. Chandra, A.D. Genovesi, and M.C. Engelke. 2011. Low-input performance of zoysiagrass (*Zoysia* spp.) cultivars maintained under dense tree shade. HortScience. 46(7):1033-1037.

Wilkinson, J.F. and J.B. Beard. 1974. Morphological responses of *Poa pratensis* and *Festuca rubra* to reduced light intensity. Int. Turfgrass Soc. Res. J. 2:231-240.

Winstead, C.W. and C.Y. Ward. 1974. Persistence of southern turfgrasses in a shade environment. Int. Turfgrass Soc. Res. J. 2:221-230.

Table 3.1. Mean turfgrass quality ratings of zoysiagrass genotypes for 2010, 2011, and 2012.

	2010				2011				2012			
Genotype[†]	June	July	Aug	Sept	June	July	Aug	Sept	June	July	Aug	Sept
	Quality Rating (1-9)[‡]											
Chinese Common	7.0 d[§]	6.8 c	6.8 d	6.6 b	6.6 b	6.0 bcd	6.6 bc	5.8 cd	4.0 d	3.4 d	4.0 c	3.2 c
Emerald	8.4 ab	7.2 bc	7.6 abc	8.0 a	4.0 cd	5.2 de	6.4 bc	5.8 cd	7.2 abc	7.4 ab	8.0 a	7.0 a
Meyer	7.8 bc	7.4 ab	7.8 ab	7.2 b	7.0 ab	6.6 abc	7.0 abc	6.8 abc	6.4 bc	5.6 c	5.4 bc	4.4 bc
Zorro	8.8 a	7.8 ab	8.0 a	8.0 a	3.4 d	4.6 e	5.8 c	5.6 d	6.2 bc	6.4 bc	7.4 a	7.2 a
Exp1	8.2 abc	7.2 bc	7.2 cd	6.8 b	4.8 c	5.6 cde	6.0 c	6.2 bcd	5.8 c	5.6 c	6.6 ab	5.8 ab
Exp2	8.6 a	8.0 a	8.0 a	8.2 a	8.2 a	7.8 a	8.2 a	7.8 a	8.2 a	8.0 a	7.4 a	6.4 a
Exp3	7.6 cd	6.8 c	7.4 bc	7.2 b	6.2 b	7.0 ab	7.6 ab	7.0 ab	7.6 ab	7.4 ab	7.6 a	7.2 a
Overall Mean	8.1	7.3	7.5	7.4	5.7	6.1	6.8	6.4	6.5	6.3	6.6	5.9

[†]Meyer and Chinese Common (*Z. japonica*), Zorro (*Z. matrella*), Emerald (*Z. japonica* × *Z. pacifica*), Exp1 (*Z. matrella* × *Z. japonica*), Exp2 and Exp3 [(*Z. japonica* × *Z. pacifica*) × *Z. japonica*]
[‡]Visual zoysiagrass quality was rated on a 1-9 scale (1 = poor, 6 = minimally acceptable, 9 = superior).
[§]Genotype means in the same column followed by a different letter are significantly different based on Fisher's least significant difference at $P < 0.05$. Means represent ratings from five replications on one rating date during the month.

Table 3.2. Tiller density percentage of June 2010 for zoysiagrass genotypes in 2010, 2011, and 2012.

	2010			2011				2012			
Genotype†	July	Aug	Sept	June	July	Aug	Sept	June	July	Aug	Sept
	---------- Tiller Density Percentage of June 2010 (%)‡ ----------										
Chinese Common	87^NS	86^NS	80^NS	63 a§	44 b	56 bc	39^NS	40 c	43 d	27 c	19 c
Emerald	89	96	80	18 c	35 b	58 bc	40	72 ab	78 a	64 ab	45 ab
Meyer	109	109	78	45 b	48 ab	76 ab	46	53 bc	44 cd	44 bc	32 abc
Zorro	78	94	78	21 c	31 b	40 c	40	41 c	51 bcd	66 ab	47 a
Exp1	92	88	71	28 c	36 b	43 c	27	46 bc	40 d	46 bc	30 bc
Exp2	109	105	78	70 a	69 a	90 a	65	99 a	68 abc	58 ab	34 abc
Exp3	90	85	76	47 b	45 b	61 bc	49	73 ab	75 ab	70 a	44 ab
Overall Mean	93	95	77	42	44	60	43	61	57	54	36

†Meyer and Chinese Common (*Z. japonica*), Zorro (*Z. matrella*), Emerald (*Z. japonica* × *Z. pacifica*), Exp1 (*Z. matrella* × *Z. japonica*), Exp2 and Exp3 [(*Z. japonica* × *Z. pacifica*) × *Z. japonica*]

‡Tiller density was adjusted to represent the percentage of June 2010 as: $\text{Tiller Density}\,(\%) = \frac{\text{Monthly Tiller Count}}{\text{June 2010 Tiller Count}} \times 100$

§Genotype means in the same column followed by a different letter are significantly different based on Fisher's least significant difference at $P < 0.05$. Means represent ratings from five replications on one rating date during the month.

NS Indicates that means were not statistically different.

Table 3.3. Leaf extension rates for zoysiagrass genotypes in 2010, 2011, and 2012.

	2010			2011				2012		
Genotype†	July	Aug	Sept	June	July	Aug	Sept	June	July	Aug
	Leaf extension rate (mm d^{-1})§									
Chinese Common	11.5 a‡	6.5 a	1.8NS	7.4 a	5.0 a	2.3NS	2.9 a	8.1NS	6.0NS	2.7NS
Emerald	2.5 d	1.5 c	0.5	2.0 c	1.5 b	1.2	1.1 b	3.7	4.5	2.0
Meyer	9.2 b	4.3 abc	1.4	2.8 bc	3.0 ab	1.7	0.9 b	4.7	3.8	2.6
Zorro	6.3 c	3.3 bc	2.0	3.0 bc	1.3 b	2.2	1.4 ab	5.3	5.8	2.0
Exp1	8.7 b	3.8 abc	0.9	5.2 ab	5.3 a	3.5	1.7 ab	6.6	7.0	2.6
Exp2	7.3 bc	5.8 ab	1.8	4.2 bc	5.3 a	2.0	2.7 a	7.3	6.0	2.8
Exp3	6.5 c	4.0 abc	0.9	5.2 ab	4.3 a	3.0	2.7 a	6.9	5.8	2.6
Overall Mean	7.4	4.1	1.3	4.3	3.7	2.3	1.9	6.1	5.5	2.4

†Meyer and Chinese Common (*Z. japonica*), Zorro (*Z. matrella*), Emerald (*Z. japonica* × *Z. pacifica*), Exp1 (*Z. matrella* × *Z. japonica*), Exp2 and Exp3 [(*Z. japonica* × *Z. pacifica*) × *Z. japonica*]

‡Leaf extension rate was determined by measuring leaf length immediately after mowing and 5-7 days later.

§Genotype means in the same column followed by a different letter are significantly different based on Fisher's least significant difference at $P < 0.05$. Means represent ratings from five replications on one rating date during the month.

NS Indicates that means were not statistically different.

Table 3.4. Leaf width for zoysiagrass genotypes in 2010, 2011, and 2012.

	2010			2011				2012		
Genotype[†]	July	Aug	Sept	June	July	Aug	Sept	June	July	Aug
	Leaf Width (mm)[‡]									
Chinese Common	3.3 a[§]	3.5 a	3.0 a	4.4 a	4.2 a	3.8 a	4.0 a	3.6 a	3.6 a	3.2 a
Emerald	1.8 de	1.8 c	1.7 c	2.0 d	1.8 d	1.9 cd	1.9 e	2.1 cd	2.1 cd	1.9 cd
Meyer	2.6 b	2.4 b	2.5 b	3.2 b	3.0 b	3.0 b	2.9 b	3.3 a	3.1 b	2.8 ab
Zorro	1.7 e	1.7 c	1.6 c	2.0 d	1.9 d	1.7 d	1.8 e	1.9 d	1.7 e	1.7 d
Exp1	2.2 bcd	2.2 bc	2.4 b	3.0 bc	2.5 c	2.2 cd	2.6 bc	2.5 bc	2.4 cd	2.5 b
Exp2	2.3 bc	2.0 bc	2.2 b	2.7 c	2.5 c	2.0 cd	2.2 de	2.5 bc	2.4 cd	2.3 bc
Exp3	2.2 cd	2.2 bc	2.2 b	2.8 bc	2.6 c	2.4 c	2.5 cd	2.6 b	2.4 cd	2.4 b
Overall Mean	2.3	2.3	2.2	2.8	2.7	2.4	2.5	2.6	2.5	2.4

[†]Meyer and Chinese Common (*Z. japonica*), Zorro (*Z. matrella*), Emerald (*Z. japonica* × *Z. pacifica*), Exp1 (*Z. matrella* × *Z. japonica*), Exp2 and Exp3 [(*Z. japonica* × *Z. pacifica*) × *Z. japonica*]

[‡]Leaf width was determined by measuring the width of fully developed leaves at its midpoint.

[§]Genotype means in the same column followed by a different letter are significantly different based on Fisher's least significant difference at $P < 0.05$. Means represent ratings from five replications on one rating date during the month.

Table 3.5. Percentage green cover for zoysiagrass genotypes in 2011 and 2012.

	2011						2012					
Genotype[†]	May	June	July	Aug	Sept	Oct	April	June	July	Aug	Sept	Nov
	Green Cover (%)[‡]											
Chinese Common	53 a[§]	69 b	64 bcd	61 c	36 d	4 d	20 bcd	50 b	42 c	47 c	46 b	7 c
Emerald	7 d	37 c	50 de	57 c	49 bc	20 b	16 cd	87 a	83 a	81 a	71 a	32 a
Meyer	47 a	69 b	72 bc	76 ab	45 cd	6 d	27 ab	75 a	64 b	60 b	47 b	5 c
Zorro	4 d	35 c	48 e	64 bc	59 ab	30 a	12 d	85 a	82 a	82 a	77 a	37 a
Exp1	18 c	47 c	57 cde	63 bc	46 cd	15 bc	15 cd	78 a	68 ab	65 b	58 b	14 b
Exp2	52 a	87 a	89 a	85 a	71 a	14 bc	33 a	93 a	81 a	66 b	53 b	9 bc
Exp3	36 b	66 b	74 ab	78 ab	54 bc	9 cd	23 bc	86 a	81 a	72 ab	56 b	6 c
Overall Mean	31	58	65	69	51	14	21	79	72	68	58	16

[†]Meyer and Chinese Common (*Z. japonica*), Zorro (*Z. matrella*), Emerald (*Z. japonica* × *Z. pacifica*), Exp1 (*Z. matrella* × *Z. japonica*), Exp2 and Exp3 [(*Z. japonica* × *Z. pacifica*) × *Z. japonica*]

[‡]Percent green cover was obtained from digital image analysis (Richardson et al., 2001).

[§]Genotype means in the same column followed by a different letter are significantly different based on Fisher's least significant difference at $P < 0.05$. Means represent ratings from five replications on one rating date during the month.

Table 3.6. Fall color for zoysiagrass genotypes in 2011, and 2012.

Genotype[†]	15 Nov. 2010	31 Oct. 2011	4 Nov. 2012
	---------------- Fall Color Rating (1-9)[‡] ----------------		
Chinese Common	3.2 e[§]	1.2 d	1.2 d
Emerald	6.4 a	5.6 a	6.0 a
Meyer	3.6 de	2.4 cd	2.0 bcd
Zorro	7.2 a	6.4 a	6.6 a
Exp1	5.0 bc	3.4 bc	2.8 b
Exp2	5.4 b	4.0 b	2.4 bc
Exp3	4.2 cd	4.0 b	1.6 cd
Overall Mean	5.0	3.9	3.2

[†]Meyer and Chinese Common (*Z. japonica*), Zorro (*Z. matrella*), Emerald (*Z. japonica* × *Z. pacifica*), Exp1 (*Z. matrella* × *Z. japonica*), Exp2 and Exp3 [(*Z. japonica* × *Z. pacifica*) × *Z. japonica*]

[‡]Fall color was rated on a 1-9 scale (1 = straw brown, 6 = minimally acceptable color, and 9 = dark green).

[§]Genotype means in the same column followed by a different letter are significantly different based on Fisher's least significant difference at $P < 0.05$. Means represent ratings from five replications on one rating date during the month.

Table 3.7. Spring green-up for zoysiagrass genotypes in 2011, and 2012.

Genotype†	23 May 2011	2 April 2012
	---- Spring Green-up Rating (1-9)‡ ----	
Chinese Common	8.0 a§	5.6 ab
Emerald	2.6 cd	3.4 c
Meyer	7.2 ab	6.4 a
Zorro	1.2 d	1.8 d
Exp1	3.6 c	2.8 cd
Exp2	7.2 ab	5.8 a
Exp3	5.8 b	4.2 bc
Overall Mean	5.1	4.3

†Meyer and Chinese Common (*Z. japonica*), Zorro (*Z. matrella*), Emerald (*Z. japonica* × *Z. pacifica*), Exp1 (*Z. matrella* × *Z. japonica*), Exp2 and Exp3 [(*Z. japonica* × *Z. pacifica*) × *Z. japonica*]

‡Spring green-up was rated on a 1-9 scale (1 = straw brown, 6 = minimally acceptable color, and 9 = dark green).

§Genotype means in the same column followed by a different letter are significantly different based on Fisher's least significant difference at $P < 0.05$. Means represent ratings from five replications on one rating date during the month.

Table 3.8. Carbon dioxide flux measurements conducted in July of 2010, 2011, and 2012.

	Net Ecosystem Exchange[†]			Respiration[‡]			Gross Photosynthesis[§]		
Genotype[¶]	2010[#]	2011[#]	2012[#]	2010	2011	2012	2010	2011	2012
	---------- μmol CO_2 m^{-2} turf s^{-1} ----------								
Chinese Common	5.8[††]	3.5	5.9	9.5	4.2	7.1	3.4	0.8	1.8
Emerald	4.5	1.6	7.3	9.2	2.4	10.6	5.2	1.1	0.9
Meyer	7.8	3.2	4.6	10.6	4.6	5.3	0.1	1.7	1.0
Zorro	5.9	2.5	4.1	8.2	3.6	5.6	2.1	1.6	1.3
Exp1	7.7	3.5	4.2	7.3	4.7	6.2	0.1	1.1	2.0
Exp2	5.0	3.6	8.1	6.0	6.5	9.5	3.8	3.1	2.1
Exp3	4.2	2.6	6.2	7.9	3.2	7.3	4.2	1.3	1.2

[†]Net ecosystem exchange was measured with a sunlit chamber. This measurement contains gross photosynthesis and canopy and soil respiration ($P_g - R_c - R_s$).
[‡]Respiration represents were made by covering the chamber to eliminate light entering the chamber. This measurement represents canopy and soil respiration ($R_c + R_s$).
[§]P_g is gross photosynthesis and is calculated from the sunlit and shaded measurements (|sunlit-shaded|).
[¶]Meyer and Chinese Common (*Z. japonica*), Zorro (*Z. matrella*), Emerald (*Z. japonica* × *Z. pacifica*), Exp1 (*Z. matrella* × *Z. japonica*), Exp2 and Exp3 [(*Z. japonica* × *Z. pacifica*) × *Z. japonica*]
[#]Carbon dioxide exchange measurement dates were 22 July 2010, 14 July 2011, 27 July 2012
[††]Means are the least squares means.

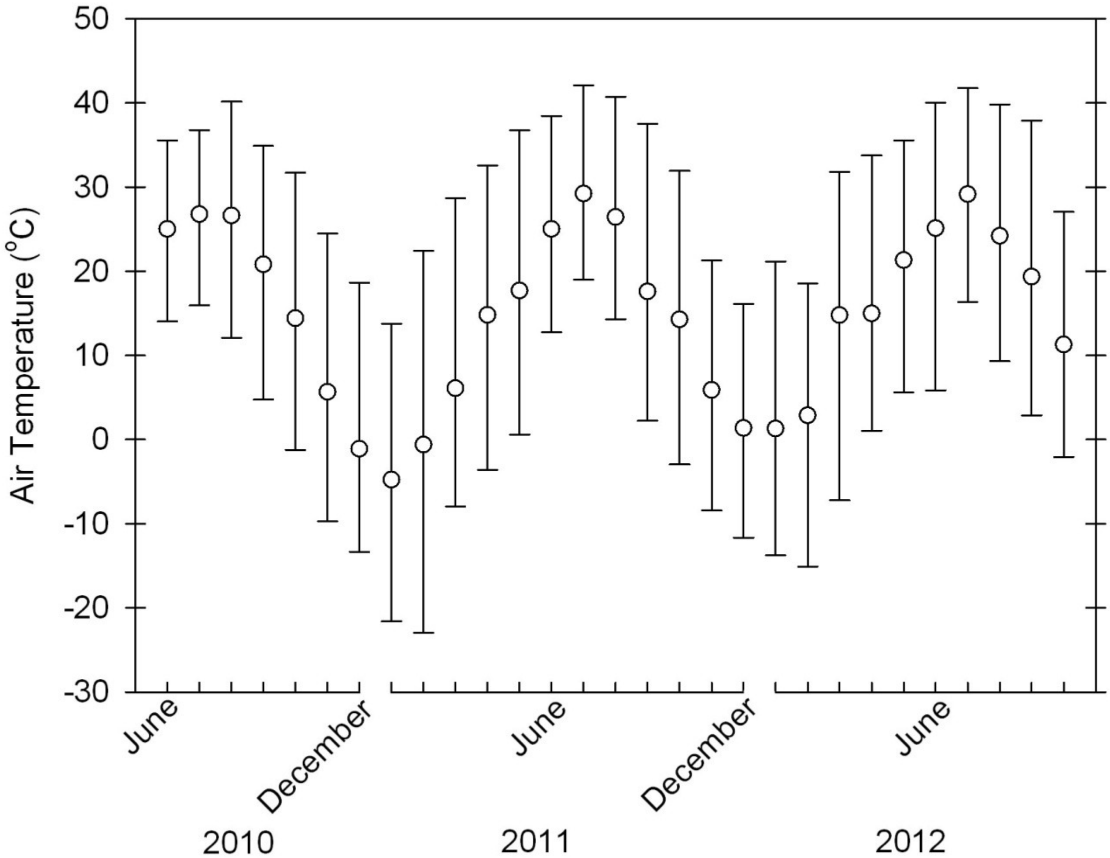

Figure 3.1. Monthly mean, maximum, and minimum air temperatures at the study site from June 2010 through October 2012. Circles represent the mean monthly air temperature. Bars represent the maximum and minimum temperatures for each month.

Appendix A - Using Infrared Thermometry to Calculate Canopy Stomatal Conductance to Water Vapor from Tall Fescue (*Festuca arundinacea* Schreb.) Turfgrass

Introduction

Leaf or plant canopy temperature can be an indicator of plant water status. Stomata control the conductance of water from the leaf to atmosphere. When a plant is not stressed, water evaporates from the leaf's interior and exits through stomata, cooling the plant in a process called transpirational cooling. Measuring the temperature of a plant can help researchers understand and quantify the transport of energy from leaf to atmosphere.

Obtaining a temperature of the canopy, or leaf, can be done with thermocouples. However, this technique requires the thermocouple to be in direct contact with the leaf and does not provide an accurate representation of the entire leaf or canopy (Tanner, 1963). An infrared thermometer (IRT) can measure the temperature of multiple leaves in a canopy, eliminating the problems associated with thermocouple measurements. Infrared thermometers measure the canopy temperature based upon received thermal radiation in the 8 to 14 μm range (Jackson et al., 1980). Advantages of using infrared thermometers are their ease of use to collect rapid temperature measurements, they are nondestructive, and they can integrate the temperature over a large area (Kirkham, 2005).

The thermal radiation observed by the IRT has two components: radiation emitted from the canopy and reflected radiation (Blonquist et al., 2009). Observation of a temperature without correcting for these two components will result in an erroneous temperature observation. Correction of the brightness temperature, measured directly by the IRT, for surface thermal emissivity (ε) and reflected radiation ($1-\varepsilon$) is necessary (Fuchs and Tanner, 1966). Thermal emissivity is calculated as the actual radiation emitted by an object divided by the theoretical maximum radiation emitted (blackbody radiation) and is typically 0.95 to 0.97 for green plants (Tanner, 1963). Therefore, the thermal radiation detected by the IRT is:

$$E_{IRT} = \varepsilon E_{canopy} + (1\text{-}\varepsilon)E_{sky} \qquad [1]$$

where E_{IRT} is the thermal radiation detected by the IRT, E_{canopy} is the emitted energy from the canopy, and E_{sky} is the emitted energy from the sky. Stefan's Law , $E = \varepsilon\sigma T^4$, is used to convert the measured energy, E, from the IRT to a temperature, T. Rewriting Eq. 1 to include the Stefan-Boltzman constant (σ), 5.67 x 10^{-8} W m^{-2} K^{-4}, yields:

$$\sigma E_{IRT} = \sigma\varepsilon E_{canopy} + \sigma(1\text{-}\varepsilon)E_{sky} \qquad [2]$$

which can then be solved for canopy temperature:

$$T_c = \sqrt[4]{\frac{T_{IRT}^4 - (1-\varepsilon)T_{sky}^4}{\varepsilon}} \qquad [3]$$

where T_c, T_{IRT}, and Tsky are canopy, IRT, and sky temperature, respectively, all in K. For a thorough review and explanation of Eqs. 1-3 and associated terminologies, see Norman and Becker (1995), Campbell and Norman (1998), or Blonquist et al. (2009).

Plant temperature is an indicator of plant water status. In theory, water-stressed plants stomata will close; transpirational cooling will slow or cease, and plant temperature will rise. Infrared thermometers can be used to measure the plant canopy's temperature accurately, and with additional meteorological data, plant response, such as stomatal conductance, can be calculated. Pinter et al. (1979) used infrared thermometry to detect plant stress due to root-rotting fungi. Others have used the IRT measured canopy temperature to create a stress-degree-day index, canopy minus air temperature, or canopy to air vapor pressure deficit (Idso et al., 1980; Idso et al., 1981; Idso et al., 1982; Jackson et al., 1981; Kirkham et al., 1983). The most common index that has been developed using infrared canopy temperature is the crop water stress index (Jackson et al., 1981; Idso et al., 1982; Wang et al., 2005) which is often used to create more efficient irrigation scheduling (Pinter and Reginato, 1982; Alves and Pereira, 2000; Irmak et al., 2000).

Infrared thermometry may also be used to estimate energy fluxes, which is an important component for determination of stomatal conductance. Norman et al. (1995) proposed a two-source model to estimate latent and sensible heat fluxes using surface temperature. This model has predicted heat fluxes very well (Zhan et al., 1996) and has gone through refinement over the years for partial canopy cover (Kustas and Norman, 1999; Kustas and Norman , 2000) and use for satellite remote sensing (Kustas and Norman, 1997).

Recently, Blonquist et al. (2009) developed a canopy stomatal conductance model using infrared temperature obtained with an IRT. In addition to canopy temperature, their model utilized commonly measured meteorological variables, air temperature, barometric pressure, relative humidity, net radiation, and wind speed along with a measurement of plant canopy height. Their canopy stomatal conductance equation is:

$$g_c = \frac{g_v P_B\left[\left(R_{nc} - A_n\right) - g_h C_p\left(T_c - T_a\right)\right]}{g_v \lambda\left(e_{sc} - e_a\right) - P_B\left[\left(R_{nc} - A_n\right) - g_h C_p\left(T_c - T_a\right)\right]} \qquad [4]$$

where g_v is boundary layer water vapor conductance (mol m^{-2} s^{-1}), g_h is boundary layer heat conductance (mol m^{-2} s^{-1}), C_p is the heat capacity of air (29.17 J mol^{-1} C^{-1}), T_c is aerodynamic canopy temperature (C), T_a is air temperature (C), P is atmospheric pressure (kPa), e_a is vapor pressure (kPa), e_{sc} is saturation vapor pressure at T_c (kPa), A_n is net assimilation (W m^{-2}), R_{nc} is net radiation divergence in the canopy (W m^{-2}), and λ is latent heat of vaporization (J mol^{-1}). This approach treats the canopy as a "big-leaf" (Baldocchi et al., 1991; Blonquist et al., 2009). The commonly used Penman-Monteith equation is an example of a big-leaf approach. There has been concern that big-leaf models may not provide physiological values of canopy conductance (Monteith, 1981). However, Furon et al., (2007) examined the Penman-Monteith equation and found big-leaf resistance to be similar to canopy resistance from scaled-up leaf resistance.

If one assumes the IRT is observing only plant canopy and no underlying soil or non-green vegetation, canopy temperature, T_c, in Eq. 4, the radiometric temperature, can be considered equal to the aerodynamic temperature of the canopy. The definition of aerodynamic and radiometric temperatures should be clarified. Aerodynamic temperature cannot be measured directly and must be calculated using knowledge of sensible heat flux as it is influenced by soil and underlying leaves. The radiometric temperature is the measured temperature of the surface. Aerodynamic and radiometric temperatures may be different values, especially under sparse canopies. If underlying soil or non-green vegetation is in the field-of-view of the IRT, T_c should be corrected using a dual angle correction (Kustas and Norman, 1997).

Sensitivity analysis of Eq. 4 showed that g_c was highly sensitive to small changes in canopy and air temperature (Blonquist et al., 2009). This highlights the importance of making accurate canopy and air temperature measurements. Stomatal conductance measurements were also sensitive when conducted under cloudy, cool, and humid conditions. The stomatal conductance model will likely not function properly in environments or climates with predominate cloudy, cool, and humid conditions. Blonquist et al. (2009) compared g_c calculated from Eq. 4 to potential stomatal conductance (g_{cp}) in alfalfa (*Medicago sativa* L.) and turfgrass (*Poa pratensis* L.) and found g_c:g_{cp} to range from 0.5 to 1. After irrigation or rainfall the ratio was at or near 1. They were able to observe stomatal response to drydown and precipitation, giving support for the ability of this model to be used for continuous calculation of g_c (Blonquist et al., 2009).

Objective

The objective of this study was to adapt the model presented by Blonquist et al. (2009) to a turfgrass setting for calculation of stomatal conductance and transpiration.

Model Procedure

The canopy stomatal conductance model is very sensitive to accurate measurement of canopy temperature (Blonquist et al., 2009). Radiometric canopy temperature was calculated from Eq. 3 using the T_{sky} model from Blonquist et al. (2009). Emissivity of the grass was assumed to be 0.97. This calculated canopy temperature assumes that the IRT sees only green vegetation and no underlying soil. In most turfgrass settings, this assumption should be met. However, the presence of senesced leaves in the IRT viewing area could contribute to canopy temperature deviation between aerodynamic and radiometric temperature, much like soil. To overcome this issue, radiometric temperature calculated from Eq. 3 can be corrected by using the dual-angle, 0° and 50°, radiometric temperature formulation described by Kustas and Norman (1997). Assuming that the turfgrass canopy is random and has a spherical leaf angle distribution, the turfgrass canopy fraction in the field of view of the IRT, f(θ), and fraction of vegetative cover, f_c, are calculated as:

$$f(\theta) = 1 - \exp\left(\frac{-0.5\mathrm{LAI}}{\cos\theta}\right), \text{ and} \qquad [5]$$

$$f_c = 1 - \exp(-0.5\mathrm{LAI}), \qquad [6]$$

where θ is IRT zenith angle, 50°, and LAI is leaf area index, assumed to be 4 m^{-2} leaf m^{-2} soil. Soil temperature, e.g. non-green vegetation, can then be calculated as:

$$T_s = \left[\frac{f(\theta_{50^\circ})T_{IRT}^4(\theta_{0^\circ}) - f(\theta_{0^\circ})T_{IRT}^4(\theta_{50^\circ})}{f(\theta_{50^\circ})\left[(1 - f(\theta_{0^\circ}) - f(\theta_{0^\circ})(1 - f(\theta_{50^\circ}))\right]}\right]^{0.25}, \qquad [7]$$

and a corrected canopy temperature can be calculated as:

$$T_c = \left[\frac{T_{IRT}^4(\theta_{0^\circ}) - (1 - f(\theta_{0^\circ}))T_s^4}{f(\theta_{0^\circ})} \right]^{0.25}, \quad [8]$$

where T_{IRT}, $T_{s,}$ and T_c are in K.

Net radiation divergence between the canopy and soil can be calculated using Beer's Law:

$$R_{nc} = R_n \times 1 - \exp\left(\frac{-kLAI}{\sqrt{2\cos\theta}}\right), \text{ and} \quad [9]$$

$$R_{ns} = R_n \times \exp\left(\frac{-kLAI}{\sqrt{2\cos\theta}}\right) \quad [10]$$

where θ is the solar zenith angle, R_n is net radiation, and k is an extinction coefficient based on solar zenith angle. The value of the extinction coefficient is k = 0.60 where θ < 30°, and k = 0.45 where θ > 30° (Kustas and Norman, 1999).

The canopy stomatal conductance equation requires knowledge of soil heat flux and net assimilation. Soil heat flux can be estimated according to Friedl (1996) as:

$$G = 0.35R_{ns} \times \cos\theta \quad [11]$$

where G is soil heat flux in W m^{-2}. Net assimilation is:

$$A_n = 0.01R_s \quad [12]$$

where A_n is net assimilation, W m^{-2}, and the coefficient 0.01 is the estimated quantity of shortwave radiation used for photosynthesis (Campbell and Norman, 1998; Blonquist et al., 2009).

The boundary layer conductance terms, g_h and g_v, are based upon the wind speed, humidity, and temperature profile curves described by the Monin-Obukhov Similarity Theory

(Monin and Obukhov, 1954). Boundary layer conductance to heat and water vapor are often considered equal. Therefore, g_h and g_v are calculated as:

$$g_v = g_h = \frac{u\rho_{mol}k^2}{\left[\ln\left(\frac{z_u - d}{z_m}\right) - \Psi_m\right]\left[\ln\left(\frac{z_{ta} - d}{z_h}\right) - \Psi_h\right]} \quad [13]$$

where z_u and z_{ta} are heights of wind speed and air temperature measurements, k is von Karman's constant, assumed to be 0.40, and Ψ_m and Ψ_h are stability parameters for momentum and heat transfer. The displacement height, d, is calculated as 0.65 × h (Shaw and Pereira, 1982), where h is the canopy height in m (i.e. mowing height, 0.10 m in this study). The roughness lengths for momentum, z_m, is $z_m = 0.125 \times h$ (Shaw and Pereira, 1982), and heat transfer, z_h, is $z_h = 0.2 \times z_m$ (Campbell and Norman, 1998). The g_h and g_v terms calculated form Eq. 13 do not include the leaf boundary layer (Blonquist et al., 2009). Therefore, leaf boundary layer conductance for heat and water vapor were calculated from Campbell and Norman (1999) as:

$$g_h = 0.135\sqrt{\frac{u}{d}}\text{, and} \quad [14]$$

$$g_v = 0.147\sqrt{\frac{u}{d}}, \quad [15]$$

where u is wind speed and d = 0.75 × average leaf width (m), and added to g_h and g_v calculated from Eq. 13 before inclusion in Eq. 4.

The stability parameters require knowledge of the Obukhov length (L), friction velocity (u*), and virtual heat flux (H_v). Therefore, an iterative approach is necessary to solve for the stability parameters and boundary layer conductance terms. The equations used to solve L, u*, and H_v are:

$$L = \frac{-u*^3 T}{kg \frac{H_v}{\rho_{mol} C_p}}, \quad [16]$$

$$u* = \frac{uk}{\ln\left(\frac{z-d}{z_m}\right) - \Psi_m}, \text{ and} \quad [17]$$

$$H_v = H + 0.61 T_a C_p E, \quad [18]$$

where T is air temperature (K), k is the acceleration due to gravity (9.81 m s^{-1}), H is sensible heat flux (W m^{-2}), and E is evaporation (mol m^{-2} s^{-1}). Evaporation is calculated by dividing latent heat flux, LE in W m^{-2}, by the latent heat of vaporization.

Sensible and latent heat fluxes may be calculated using a single-source or two-source approach (Norman et al., 1995; Kustas and Norman, 1999). Using the single-source approach assumes that the radiometric temperature of the canopy is equal to the aerodynamic temperature. Using this approach, sensible heat flux is calculated as:

$$H = \rho C_p (T_c - T_a) g_a, \quad [19]$$

$$g_a = u\rho_{mol} k^2 \left[\ln\left(\frac{z_u - d}{z_m}\right) - \Psi_m\right]^{-1} \left[\ln\left(\frac{z_{ta} - d}{z_h}\right) - \Psi_h\right]^{-1}, \quad [20]$$

where g_a is the aerodynamic conductance. Latent heat flux can then be calculated as the residual of the energy balance equation:

$$LE = R_n - G - H - A_n, \quad [21]$$

forcing closure of the energy balance equation.

Calculation of sensible and latent heat fluxes using the two-source approach, sensible heat flux of the canopy (H_c) and soil (H_s) are calculated as:

$$H_c = \rho C_p (T_c - T_a) g_a \text{, and} \quad [22]$$

$$H_s = \rho C_p (T_s - T_a)(g_a \times g_s), \quad [23]$$

where g_s is the soil-surface conductance calculated using the method described in Appendix B of Norman et al., (1995). Latent heat flux of the soil (LE_s) is calculated as the soil energy residual:

$$LE_s = R_{ns} - G - H_s . \quad [24]$$

Latent heat flux of the canopy (LE_c)can be calculated as the canopy energy residual:

$$LE_c = R_{nc} - H_c , \quad [25]$$

or by using the Priestley-Taylor approximation (Norman et al., 1995):

$$LE_c = \alpha F_g \frac{\Delta}{\Delta + \gamma} R_{nc} \quad [26]$$

where α is the Priestley-Taylor parameter, F_g is the fraction of LAI that is "green", Δ is the slope of the saturation vapor pressure curve at T_c, and γ is the psychrometric constant.

The stability parameters for stable ($L > 0$) and unstable ($L < 0$) conditions can now be calculated. Under stable conditions, the stability parameters are calculated according to (Holtslag and De Bruin, 1988; Beljaars and Holtslag, 1991) as:

$$\Psi_m = -X + B\left(X - \frac{C}{D}\right)\exp(-DX) + \left(\frac{BC}{D}\right), \quad [27]$$

$$\Psi_v = \Psi_h = -\left(1 + \frac{2}{3}AX\right)^{3/2} + B\left(X - \frac{C}{D}\right)\exp(-DX) + \left(\frac{BC}{D}\right) + 1 \text{, and} \quad [28]$$

$$X = \frac{z - d}{L}, \quad [29]$$

where the constants used are A = 1, B = 0.667, C = 5, and D = 0.35. The stability parameters for unstable conditions are calculated according to (Businger et al., 1971; Dyer, 1974; Hogstrom, 1988) as:

$$\Psi_m = 2\ln\left(\frac{1+\chi_m}{2}\right) + \ln\left(\frac{1+\chi_m^2}{2}\right) - 2\arctan \times \chi_m + \frac{\pi}{2}, \quad [30]$$

$$\Psi_v = \Psi_h = 2\ln\left(\frac{1+\chi_h^2}{2}\right), \quad [31]$$

$$\chi_m = \left[1 - 16\left(\frac{z-d}{L}\right)\right]^{0.25}, \text{ and} \quad [32]$$

$$\chi_h = \left[1 - 16\left(\frac{z-d}{L}\right)\right]^{0.5}. \quad [33]$$

Under neutral conditions, $|L| > 100$, the stability parameters can be considered negligible (Ham, 2005). Equations 13 through 33 can be solved iteratively beginning by assuming some instability (e.g. L = -10) and continuing the iteration until L converges (Blonquist et al., 2009).

Transpiration water loss, $COND_T$, can be calculated using g_c and g_v to calculate g_t, total water vapor conductance. See Example 6.1 in Campbell and Norman (1998) and McDermitt (1990). Using these examples for a 30-minute time step, g_t and $COND_T$ can be calculated as:

$$g_t = \frac{1}{\left(\frac{1}{g_v}\right) + \left(\frac{1}{g_c}\right)}, \text{ and} \quad [34]$$

$$COND_T = a1800g_t\left(\frac{e_{sc} - e}{P}\right), \quad [35]$$

where a is 0.018 kg H_2O mol^{-1} H_2O and 1800 is the number of seconds in a 30-minute period.

Field Data Collection

Data were collected on 42 precipitation-free days within a sward of tall fescue (*Festuca arundinacea* Schreb.) turfgrass, beginning in June 2012 at the Rocky Ford Turfgrass Research Center at Manhattan, KS. Soil type was a Chase silt loam (fine, montmorillonitic, mesic, Aquic, Argiudoll). The turfgrass was maintained at 10 cm mowing height. Irrigation was applied to prevent drought stress and to ensure that measurements were made under non water-limiting conditions.

A weather station at the site recorded meteorological variables necessary for model input. Air temperature and relative humidity were obtained using a platinum resistance thermometer and capacitive chip, respectively, (HMP50, Vaisala, Inc., Helsinki, Finland). Wind speed and direction were obtained with a two-dimensional sonic anemometer (WindSonic1, Gill Instruments Ltd., Hampshire, England). Incoming shortwave radiation was measured with a pyranometer (SP110, Apogee Instruments, Inc., Logan, UT).Net radiation, was measured using a net radiometer (NR-Lite, Kipp & Zonen, Inc., The Netherlands). All meteorological data were recorded at 1 Hz on a CR1000 (Campbell Scientific, Inc., Logan, UT) datalogger and stored at 30-minute intervals. Three infrared radiometers (SI-111, Apogee Instruments, Inc., Logan, UT) were used to measure canopy temperature. Radiometers were installed at 1.5 m height, aimed in the compass directions, east, west, and south, with a view angle of 50° from nadir. A fourth radiometer was installed vertically, 0° from nadir, over the turf surface.

Model Output

Comparison of Single-Source and Two-Source Approach

There are two approaches, single-source or two-source, to solve the energy balance for the canopy stomatal conductance model. To compare these two approaches for estimating sensible and latent heat fluxes, Eq. 19-21 were used for the single-source approach and Eqs. 22-25 were used for the two-source approach. Both approaches close the energy balance equation. In either approach, LE or LE_c could be calculated using the Priestley-Taylor approximation (Eq. 26). Using the single-source approach and the Priestley-Taylor approximation, one would assume that LE_s is negligible. Under most turfgrass situations this may be an acceptable assumption, however, under well watered conditions, LE from the soil may be a significant contributor to total LE.

Analysis of these two approaches shows that sensible and latent heat flux values produced are nearly identical. Mean sensible and latent heat fluxes were 24 and 280 W m^{-2}, respectively, for the single-source approach and 26 and 284 W m^{-2}, respectively for the two-source approach. Correlation of the single-source and two-source approach using daytime ($R_n > 0$) only data resulted in a Pearson correlation coefficient of approximately 1.0 for both sensible ($y = 1.04x + 0.98$) and latent ($y = 1.01x + 1.70$) heat flux. The high correlation coefficient is surprising. However, in a healthy turfgrass stand the canopy is completely closed and should consist almost entirely of green leaves. The two-source approach may be slightly more precise in accounting for senesced leaves, however, the difference between the two approaches should be considered negligible.

Canopy Stomatal Conductance Results

Canopy stomatal conductance and meteorological variables, air and canopy temperature, wind speed, and vapor pressure deficit of the canopy to air, are presented for 28 June 2012 (Fig. A.1) and 5 Sept. 2012 (Fig. A.2). On 28 June maximum g_c was 0.63 mol m^{-2} s^{-1} at 1430 h. Blonquist et al. (2009) reported similar values at mid-day during mid August at Logan, UT. However, they observed much greater mid-day values, ~1.3 - 1.4 mol m^{-2} s^{-1}, on days where the turfgrass was irrigated the previous night. The greater availability of water in the soil may have resulted in greater conductance observed after the irrigation. Our study site was irrigated on 24 June and 3 Sept. On 5 Sept. canopy and air temperatures were lower than on 28 June (Figs. A.1, A.2). Interestingly, canopy temperature was well above air temperature most of the day. Canopy stomatal conductance was much lower on 5 Sept. than on 28 June. Maximum g_c on 5 Sept. was only 0.29 mol m^{-2} s^{-1} at 1000 h. Lower stomatal conductance and a lower drying power of the atmosphere may prevent canopy temperature from cooling as effectively as it did on 28 June, causing the larger canopy to air temperature difference observed on 5 Sept. than on 28 June.

The g_c model performs well but there are areas where much improvement or validation is needed. The model is most sensitive to measures of air and canopy temperature. Validation of the T_c calculation is needed, most notably a valid T_{sky} model for Manhattan, KS. Additionally, assumptions for the use of Beer's Law spherical leaf angle distribution should be investigated further.

Observations of the output indicate that during the hours near sunrise and sunset, g_c determination can be difficult to calculate. This is likely due in part to rapid changes in meteorological variables, such as temperature and solar radiation, which occur at sunrise and sunset. Also during these hours, it is very possible for dew formation to occur on the turfgrass. This would result in the IRT observations to be incorrect, likely an uncorrectable situation.

Conclusions

Overall, this model, with further validation, should perform well in turfgrass settings and provide researchers a valuable tool. The capabilities of this model could be used to:

- decouple evaporation and transpiration from ET measurements,
- identify and quantify turfgrass stress (due to stomatal closure) among treatments,
- study drought tolerance or water use efficiency of turfgrasses,
- model photosynthesis (CO_2 conductance is related to H_2O conductance), or
- aid irrigation management.

References

Alves, I., and L.S. Pereira. 2000. Non-water-stressed baselines for irrigation scheduling with infrared thermometers: a new approach. Irrig. Sci. 19:101-106.

Baldocchi, D.D., R.J. Luxmoore, and J.L. Hatfield. 1991. Discerning the forest from the treesL an essay on scaling canopy stomatal conductance. Agric. Forest Meteorol. 54:197-226.

Beljaars, A.C.M. and A.A.M. Holtslag. 1991. Flux parameterization over land surfaces for atmospheric models. J. Appl. Meteorol. 30:327-341.

Blonquist Jr., J.M., J.M. Norman, and B. Bugbee. 2009. Automated measurement of canopy stomatal conductance based on infrared temperature. Agric. Forest Meteorol. 149:1931-1945.

Businger, J.A., J.C. Wyngaard, Y. Izumi, and E.F. Bradley. 1971. Flux: profile relationships in the atmospheric surface layer. L. Atmo. Sci. 28:181-189.

Campbell, G.S. and J.M. Norman. 1998. An Introduction to Environmental Biophysics. 2nd ed. Springer-Verlag, New York.

Dyer, A.J. 1974. A review of flux-profile relationships. Boundary Layer Meteorol. 7:363-372.

Friedl, M.A. 1996. Relationships among remotely sensed data, surface energy balance, and area-averaged fluxes over partially vegetated land surfaces. J. Appl. Meteorol. 35:2091-2103.

Fuchs, M. and C.B. Tanner. 1966. Infrared thermometry of vegetation. Agron. J. 58:597-601.

Furon, A.C., J.S. Warland, and C. Wagner-Riddle. 2007. Analysis of scaling-up resistances from leaf to canopy using numerical solutions. Agron. J. 99:1483-1491.

Ham, J.M. 2005. Useful equations and tables in micrometeorology. p. 533-560. *In*. J.L. Hatfield and J.M. Baker (eds.), Micrometeorology in Agricultural Systems. American Society of Agronomy, Madison, WI.

Hogstrom, U. 1988. Non-dimensional wind and temperature profiles in the atmospheric surface layer: a re-evaluation. Boundary Layer Meteorol. 42:55-78.

Holtslag, A.A.M. and H.A.R. De Bruin. 1988. Applied modeling of the nighttime surface energy balance over land. J. Appl. Meteorol. 27:689-704.

Idso, S.B., R.D. Jackson, P.J. Pinter, Jr., R.J. Reginato, and J.L. Hatfield. 1981. Normalizing the stress-degree-day parameter for environmental variability. Agric. Meteorol. 24:45-55.

Idso, S.B., R.J. Reginato, J.L. Hatfield, G.K. Walker, R.D. Jackson, and P.J. Pinter Jr. 1980. A generalization of the stress-degree-day concept of yield prediction to accommodate a diversity of crops. Agric. Meteorol. 21:205-211.

Idso, S.B., R.J. Reginato, and J.W. Radin. 1982. Leaf diffusion resistance and photosynthesis in cotton as related to a foliage temperature based plant water stress index. Agric. Meteorol. 27:27-34.

Irmak, S., D.Z. Haman, and R. Bastug. 2000. Determination of crop water stress index for irrigation timing and yield estimation of corn. Agron. J. 92:1221-1227.

Jackson, R.D., S.B. Idso, R.J. Reginato, and P.J. Pinter, Jr. 1981. Canopy temperature as a crop water stress indicator. Water Resour. Res. 17(4):1133-1138.

Jackson, R.D., P.J. Pinter, Jr., R.J. Reginato, and S.B. Idso. 1980. Hand-held radiometry. Agric. Rev. Manuals, ARM-W-19, United States Department of Agriculture, Science and Education Administration, Western Region, Oakland, CA.

Kirkham, M.B. 2005. Principles of Soil and Plant Water Relations. Elsevier Academic Press, Burlington, MA.

Kirkham, M.B., D.E. Johnson Jr., E.T. Kanemasu, and L.R. Stone. 1983. Canopy temperature and growth of differentially irrigated alfalfa. Agric. Meteorol. 29:235-246.

Kustas, W.P. and J.M. Norman. 1997. A two-source approach for estimating turbulent fluxes using multiple angle thermal infrared observations. Water Resour. Res. 33(6):1495-1508.

Kustas, W.P. and J.M. Norman. 1999. Evaluation of soil and vegetation heat flux predictions using a simple two-source model with radiometric temperatures for partial canopy cover. Agric. Forest Meteorol. 94:13-29.

Kustas, W.P. and J.M. Norman. 2000. A two-source energy balance approach using directional radiometric temperature observations for sparse canopy covered surfaces. Agron. J. 92:847-854.

McDermitt, D.K. 1990. Sources of error in the estimation of stomatal conductance and transpiration from porometer data. HortSci. 25(12):1538-1548.

Monin, A.S. and A.M. Obukhov. 1954. Basic laws of turbulent mixing in the surface layer of the atmosphere. Tr. Akad. Nauk SSSR Geophiz. Inst. 24(151):163-187.

Monteith, J.L. 1981. Evaporation and surface temperature. Q. J. Royal Meteorol. Soc. 107:1-27.

Norman, J.M. and F. Becker. 1995. Terminology in thermal infrared remote sensing of natural surfaces. Agric. Forest Meteorol. 77:153-166.

Norman, J.M., W.P. Kustas, and K.S. Humes. 1995. A two-source approach for estimating soil and vegetation energy fluxes in observations of directional radiometric surface temperature. Agric. Forest Meteorol. 77:263-293.

Pinter, Jr., P.J. and R.J. Reginato. 1982. A thermal infrared technique for monitoring cotton water stress and scheduling irrigation. Trans. ASAE. 25(6):1651-1655.

Pinter, Jr., P.J. M.E. Stanghellini, R.J. Reginato, S.B. Idso, A.D. Jenkins, and R.D. Jackson. 1979. Remote detection of biological stresses in plants with infrared thermometry. Science, New Series. 205(4406):585-587.

Shaw, R.H. and A.R. Pereira. 1982. Aerodynamic roughness of a plant canopy: a numerical experiment. Agric. Meteorol. 26:51-65.

Tanner, C.B. 1963. Plant temperatures. Agron. J. 55:210-211.

Wang, L., G.Y. Qui, X. Zhang, and S. Chen. 2005. Application of a new method to evaluate crop water stress index. Irrig. Sci. 24:49-54.

Zhan, X., W.P. Kustas, and K.S. Humes. 1996. An intercomparison study on models of sensible heat flux over partial canopy surfaces with remotely sensed surface temperature. Remote Sensing Environ. 58:242-256.

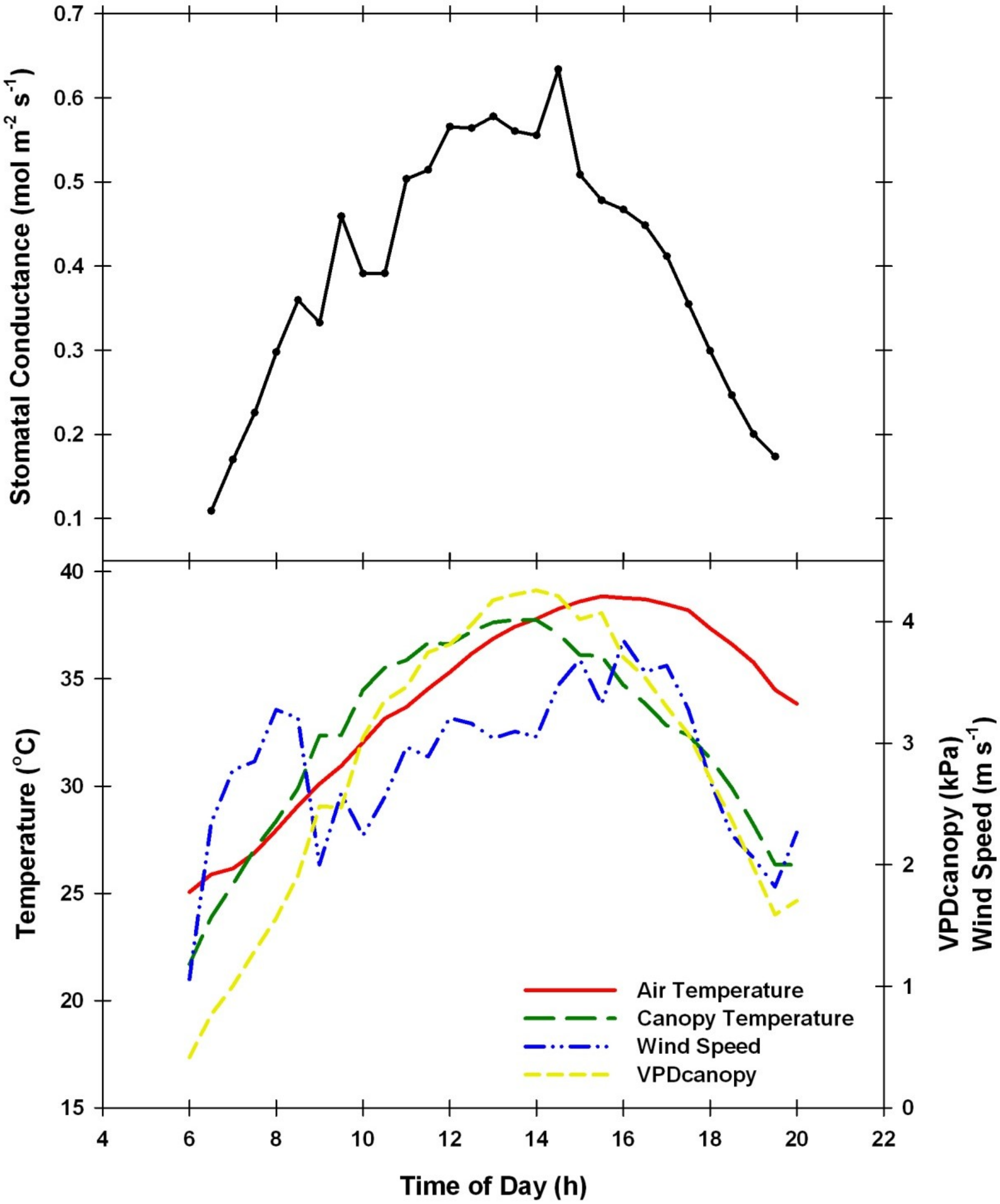

Figure A.1. Hourly canopy stomatal conductance, air temperature, canopy temperature, wind speed, and vapor pressure deficit of canopy temperature on 28 June 2012.

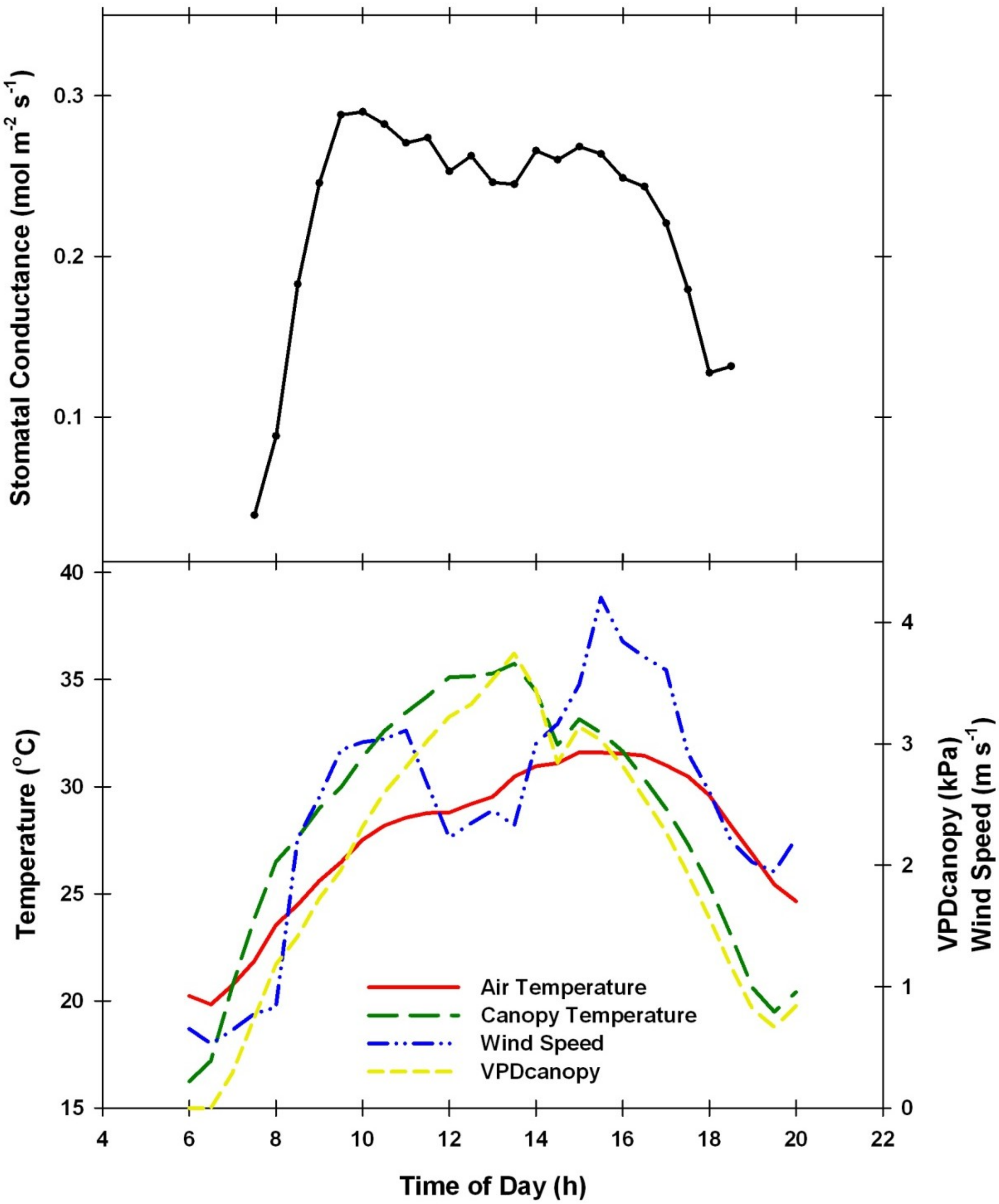

Figure A.2. Hourly canopy stomatal conductance, air temperature, canopy temperature, wind speed, and vapor pressure deficit of canopy temperature on 5 September 2012.

Appendix B - Summary of Environmental Variables

Table B.1. Average Daytime ($R_n > 0$) Net Radiation, Air Temperature, Wind Speed, Relative Humidity, and Vapor Pressure Deficit from Evapotranspiration Comparison Study

Year	DOY	Net Radiation	Air Temperature	Wind Speed	Relative Humidity	Vapor Pressure Deficit
		W m^{-2}	°C	m s^{-1}	%	kPa
2010	188	93	24.7	1.3	81	0.6
2010	189	164	24.6	2.2	74	0.8
2010	190	339	25.4	1.5	61	1.4
2010	191	358	28.3	2.6	58	1.7
2010	192	360	29.0	2.2	64	1.6
2010	193	160	25.0	2.4	77	0.8
2010	194	417	31.1	4.3	66	1.6
2010	224	373	35.2	2.7	41	3.6
2010	226	324	29.9	1.7	60	1.8
2010	227	262	26.8	1.8	46	2.0
2010	228	300	27.3	2.2	50	1.9
2010	260	314	26.6	2.4	61	1.5
2010	261	268	26.3	2.1	66	1.3
2010	262	258	20.9	1.3	71	0.8
2010	263	361	30.9	5.1	43	2.6
2010	264	233	28.1	3.8	59	1.6
2010	287	232	18.7	3.1	44	1.5
2010	288	250	19.8	2.0	38	1.6
2010	289	225	22.5	2.0	40	1.7
2010	290	254	19.7	2.6	36	1.5
2010	291	187	17.1	3.3	40	1.3
2010	292	176	15.1	1.4	45	1.0
2011	136	412	17.8	1.8	38	1.4
2011	142	367	24.4	3.4	46	1.7
2011	143	325	23.8	1.9	56	1.4
2011	179	404	25.7	2.6	47	1.8
2011	180	397	31.1	3.6	53	2.3
2011	181	419	35.0	4.2	36	3.7
2011	182	387	33.3	3.9	39	3.4
2011	183	334	29.1	2.9	59	1.7
2011	185	373	28.3	1.9	64	1.5
2011	235	359	33.6	2.3	44	3.1
2011	236	341	31.7	3.7	49	2.5
2011	237	336	26.8	1.7	43	2.1
2011	238	347	29.3	1.9	42	2.7
2011	239	326	39.6	2.3	51	2.2

Year	DOY	Net Radiation	Air Temperature	Wind Speed	Relative Humidity	Vapor Pressure Deficit
		W m^{-2}	°C	m s^{-1}	%	kPa
2012	177	371	30.5	2.3	59	1.9
2012	178	385	31.3	3.6	55	2.2
2012	179	405	35.1	4.4	41	3.5
2012	180	400	34.5	3.0	38	3.6
2012	181	391	34.0	3.1	34	3.6
2012	191	140	25.1	2.6	63	1.2
2012	192	381	27.9	2.9	46	2.2
2012	193	399	29.6	1.5	44	2.5
2012	194	383	32.4	1.7	37	3.2
2012	201	378	33.2	1.7	43	3.2
2012	202	388	31.6	2.1	45	2.8
2012	203	413	32.6	2.1	40	3.1
2012	204	336	34.1	2.1	33	4.0
2012	205	377	35.0	3.0	32	4.0
2012	213	327	32.9	2.1	40	3.2
2012	217	203	25.7	2.8	61	1.3
2012	218	383	27.5	2.0	42	2.3
2012	219	316	30.7	1.9	34	3.2
2012	220	194	31.1	1.5	39	2.9
2012	222	349	26.7	3.8	48	1.9
2012	223	350	24.6	2.8	42	2.0
2012	233	328	26.4	1.4	32	2.6
2012	234	355	29.9	1.6	27	3.3
2012	235	331	29.9	3.9	31	3.1
2012	240	365	29.5	1.6	51	2.1
2012	241	296	27.6	1.8	50	2.2
2012	242	346	30.7	2.2	41	2.8
2012	243	304	30.4	1.5	40	3.0
2012	248	340	31.5	1.5	49	2.6
2012	249	370	29.3	3.0	47	2.2
2012	253	309	20.9	2.0	46	1.5
2012	254	338	25.6	3.6	37	2.2
2012	255	342	29.6	5.1	28	3.1
2012	265	329	23.6	3.2	30	2.1
2012	266	276	15.8	3.3	36	1.2
2012	267	290	18.0	2.6	33	1.5
2012	268	218	21.4	1.9	50	1.3
2012	269	230	23.2	1.4	57	1.3
2012	273	272	20.3	1.7	45	1.4
2012	274	182	20.7	0.9	52	1.3
2012	275	217	18.7	3.9	53	1.1
2012	276	284	17.9	1.8	39	1.4

Appendix C - Summary of Daily Evapotranspiration Values

Table C.1. Summary of Daily Evapotranspiration Values from Evapotranspiration Comparison Study

Year	DOY	Lysimeter	FAO56-PM	Priestley-Taylor	Atmometer	Eddy Covariance	Conductance Model
		---------------------------------- mm ET d^{-1} ----------------------------------					
2010	188	0.91	1.58	1.87	1.27	2.76	-
2010	189	2.86	2.11	2.59	2.12	2.70	-
2010	190	6.63	5.75	7.61	4.74	8.16	-
2010	191	6.10	5.60	6.44	4.83	6.31	-
2010	192	6.50	5.70	7.14	4.91	7.10	-
2010	193	4.55	2.55	3.09	2.20	3.40	-
2010	194	8.55	5.54	6.47	4.23	6.64	-
2010	224	8.34	7.71	7.22	8.38	6.52	-
2010	226	2.95	5.03	5.97	5.25	5.96	-
2010	227	5.45	3.94	4.47	4.32	4.81	-
2010	228	2.54	4.46	4.92	4.06	5.23	-
2010	260	3.74	4.17	4.87	3.56	4.78	-
2010	261	3.96	3.58	4.24	4.06	4.08	-
2010	262	3.48	2.95	4.02	2.54	4.27	-
2010	263	6.69	5.70	4.53	5.21	3.84	-
2010	264	3.74	3.83	3.18	3.81	3.02	-
2010	287	2.87	3.45	3.18	1.40	3.53	-
2010	288	2.97	3.16	3.07	2.67	2.87	-
2010	289	3.30	3.50	3.21	3.68	2.20	-
2010	290	3.24	2.78	2.72	2.54	2.81	-
2010	291	2.54	2.90	2.22	2.29	1.72	-
2010	292	2.01	2.30	2.44	2.03	1.36	-
2011	136	4.72	4.72	5.89	3.68	6.90	-
2011	142	6.25	6.61	7.37	4.70	8.24	-
2011	143	4.56	4.84	6.06	4.74	6.25	-
2011	179	6.99	6.05	7.05	4.49	7.35	-
2011	180	8.19	7.93	7.95	6.52	7.81	-
2011	181	9.62	8.96	7.75	7.70	7.17	-
2011	182	10.29	9.58	8.55	8.13	8.26	-
2011	183	6.39	5.49	6.12	4.40	6.37	-
2011	185	4.63	5.72	7.31	4.32	7.45	-
2011	235	6.34	5.85	6.57	5.42	6.26	-
2011	236	7.82	6.13	6.17	4.74	8.50	-
2011	237	6.06	4.63	5.49	4.06	5.35	-
2011	238	6.52	5.32	5.88	4.83	5.61	-
2011	239	7.32	5.39	6.07	4.66	6.20	-
2012	177	5.74	6.40	7.46	5.67	-	5.14
2012	178	6.45	7.41	7.42	6.10	-	5.43

Year	DOY	Lysimeter	FAO56-PM	Priestley-Taylor	Atmometer	Eddy Covariance	Conductance Model
				mm ET d^{-1}			
2012	179	8.07	9.43	8.13	8.21	-	7.02
2012	180	7.74	8.81	7.99	8.64	-	6.51
2012	181	5.95	8.59	7.46	8.30	-	6.28
2012	191	3.21	2.73	2.42	2.54	-	1.98
2012	192	7.76	6.98	7.45	5.67	-	5.52
2012	193	6.64	6.19	7.32	6.01	-	5.20
2012	194	6.73	6.04	6.93	6.18	4.82	5.27
2012	201	7.69	7.05	7.80	7.11	7.52	5.93
2012	202	7.29	6.57	7.58	6.18	7.66	5.62
2012	203	6.89	6.23	7.14	5.93	6.58	5.40
2012	204	8.60	7.70	7.80	7.79	7.42	6.55
2012	205	9.89	8.98	7.87	8.81	7.44	6.56
2012	213	6.78	5.88	6.20	5.84	6.10	4.90
2012	217	3.88	3.11	3.26	2.96	3.90	2.47
2012	218	6.59	5.50	6.58	4.91	7.22	4.81
2012	219	7.29	6.08	6.36	5.93	6.45	5.13
2012	220	4.77	3.69	3.61	4.23	3.26	3.17
2012	222	7.19	5.98	6.20	4.49	6.97	4.67
2012	223	7.23	5.88	6.35	4.66	6.33	4.66
2012	233	5.12	5.04	5.83	4.74	6.32	3.81
2012	234	5.53	5.41	6.02	5.59	5.63	4.11
2012	235	6.60	7.15	5.84	5.93	5.60	4.01
2012	240	4.75	4.38	5.57	3.98	5.90	3.58
2012	241	5.37	5.02	5.63	4.23	5.34	4.90
2012	242	6.08	5.07	5.64	4.49	5.13	4.11
2012	243	6.50	5.42	6.13	5.25	6.31	4.53
2012	248	5.78	5.39	5.57	5.50	5.54	3.36
2012	249	5.85	5.22	5.36	4.57	4.96	3.49
2012	253	4.53	3.56	4.27	3.05	5.11	2.55
2012	254	5.75	5.79	5.17	4.40	4.86	3.67
2012	255	7.92	7.50	5.26	6.10	4.78	4.04
2012	265	5.57	4.41	4.24	3.30	3.60	2.97
2012	266	4.86	3.97	4.02	3.64	4.72	2.64
2012	267	4.22	3.56	3.62	2.46	4.62	2.42
2012	268	2.96	2.54	2.68	2.03	3.37	1.81
2012	269	1.56	2.28	2.65	2.03	2.65	1.77
2012	273	3.93	2.86	3.37	2.46	3.94	2.22
2012	274	2.34	2.10	2.51	2.12	2.78	1.58
2012	275	4.48	3.35	2.92	2.46	2.71	1.97
2012	276	3.44	2.88	3.39	2.71	4.01	1.92